Title
Application of fractal analysis on hand-wrist radiographs to assess growth of caucasian females ages 7-15

Author
Chen, Robert Shi-Sen

Publication Date
2000

Peer reviewed|Thesis/dissertation

APPLICATION OF FRACTAL ANALYSIS ON HAND-WRIST RADIOGRAPHS TO ASSESS GROWTH OF CAUCASIAN FEMALES AGES 7-15

by

ROBERT SHI-SEN CHEN, D.M.D.

THESIS

Submitted in partial satisfaction of the requirements for the degree of

MASTER OF SCIENCE

in

ORAL BIOLOGY

in the

GRADUATE DIVISION

of the

UNIVERSITY OF CALIFORNIA

San Francisco

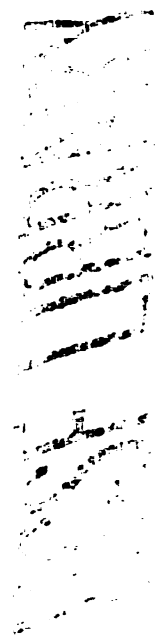

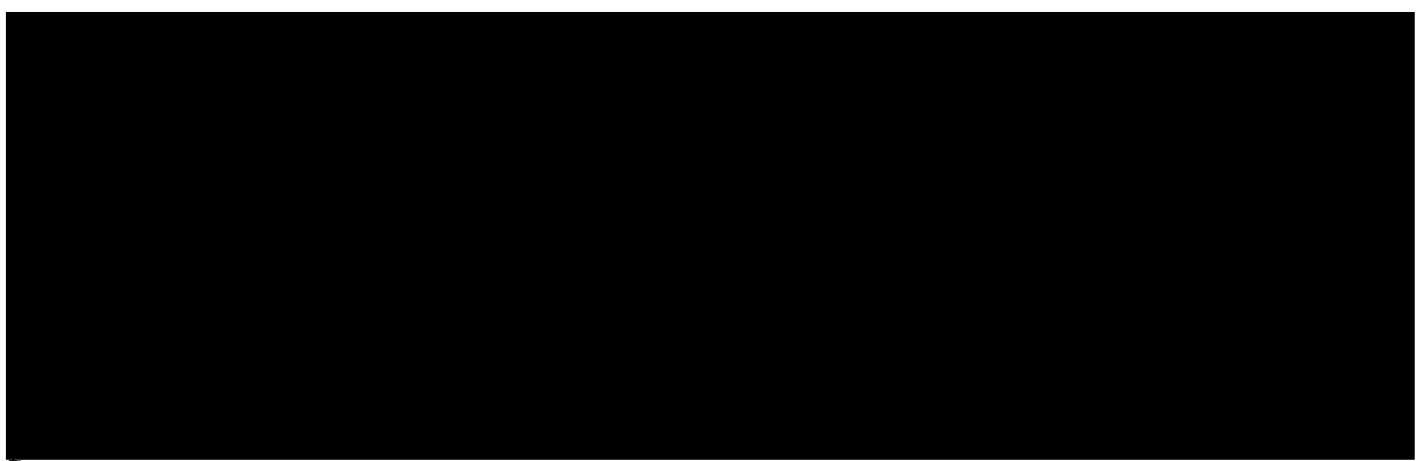

Date

University Librarian

Acknewledgements

I would like to express my sincere gratitude to Dr. Sharmila Majumdar for mentoring me on this project. She allowed me the freedom to think, explore, and create. At the same time, she provided me very supportive guidance.

I would like to thank Dr. Catherine Klifa for give me very good technical guidance. Her support of this project was greatly appreciated. She was still worrying about my progress when she was on her maternity leave.

Thanks also go out to Dr. David Newitt for his help and technical guidance.

I also would like to thank Dr. Art Miller and Dr. Karin Vargervik for serving on the committee and providing guidance.

Dr. Vincente Gilsanz's willingness to share his radiographs was appreciated.

Special thanks to Dr. Stuart Gansky's invaluable help on statistics.

I also want to thank my parents, Rex, and Alice for their love and support. Without them, I would never make it.

Lastly, but not the least, I want to say a very special thanks to Grace who have accompanied me through seven years of dental school and orthodontic residency. And I can never thank her enough for her enduring support and love.

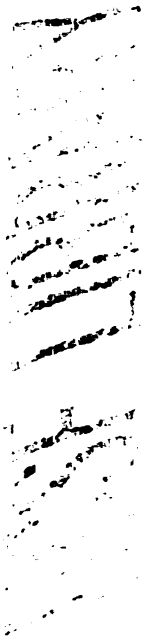

ABSTRACT

Hand-wrist films were first utilized by the pediatricians to estimate if a child's weight and height were within normal limits for the child's particular age. Hand-wrist films have also used to monitor treatments to correct growth-related problems. Growth prediction is important to orthodontists who want to utilize growth modification to correct malocclusions due to skeletal dysplasia. A young patient's growth status has an impact on how the patient is to be treated to correct the orthodontic problem. A significant sagittal skeletal discrepancy due to a retrusive mandible can be treated by growth modification or combined orthodontics-orthognathic surgery approaches. The treatment decision is based on where the patient is located on his/her growth curve. The ability to predict the amount of growth remaining is important.

Orthodontists disagree on the usefulness of current methods of using hand-wrist films in orthodontic treatment planning[2,3,4,6]. All the known methods of using hand-wrist films assess the degree of ossification of certain bones to determine the patient's growth status. This project is a pilot study applying fractal analysis to trabecular bone of the hand-wrist area to determine patient's growth status. Trabecular bone is more sensitive to metabolic changes than cortical bone [12]. Trabecular bone may be a better indicator to assess the amount of growth remaining or growth intensity present.

The goal of this study was to determine if fractal dimension correlates with the maturation process in Caucasian females from age 7 to 15. The results show that fractal dimension correlates strongly with maturation in Caucasian females. However, the correlation coefficients are sensitive to the anatomic sites and the frequency ranges selected.

TABLT OF CONTENTS

INTRODUCTION

In 1929, Dr. Todd of Western Reserve University School of Medicine (Cleveland, Ohio), started an ambitious project of investigating human growth. A few three-month-old infants were taken into this research program. In 1937, he published the first hand/wrist skeletal atlas [16]. It was the first practical guide for health care practitioners who were interested in growth. Following Dr. Todd's effort, Greulich and Pyle published another hand atlas [17]. This atlas was popular among pediatricians who used the atlas to monitor the growth of their patients and the treatment effect of growth-related disorders.

While the pediatricians were primarily concerned whether their adolescent patient's growth was within normal limit at the particular age, the orthodontist faced a greater challenge of determining the growth spurt of the adolescent patient who needed growth modification to correct a skeletal discrepancy. If a young girl presents with a severe Class II, division 1 malocclusion due to a retrusive mandible, the orthodontic practitioner must assess the girl's maturation to plan the best treatment. If modification of growth is attempted, it is assumed that the patient still has some growth available to achieve the desired correction. The correction could be achieved within a short period of time during the facial growth spurt. This maximizes treatment efficiency and minimizes the chance of a patient's "burning out" of orthodontic treatment. Orthodontists must have the tools to assess the growth status of the adolescent patients. Ideally, orthodontists desire to know the amount of growth remaining and the growth rate. This information is not provided by the contemporary hand-wrist techniques. Traditionally, orthodontists use the hand-wrist radiographs to assess the skeletal age and to estimate the amount of growth remaining. In some cases, an orthodontist also uses hand-wrist radiographs to predict the growth spurt, attempting to time the delivery

of treatment. However, the orthodontic community questions the usefulness of the current technique of interpreting hand-wrist films in orthodontics [2,3,4,6].

There is much variability in adolescent growth. The assessment made by the current methods of using the hand-wrist radiographs are often deficient in predicting when the growth spurt will occur and how much more growth will occur. By using the longitudinal sample from the Child Research Council in Denver, Co., Bambha and Van Natta[3] and Hunter[4] found that skeletal age was not a better indicator than chronological age for predicting the adolescent facial growth spurt in the female. In the male, assessment of skeletal age using hand-wrist radiograph was of some use. Skeletal age was determined by using the presence of certain bony outlines of the hand-wrist bones. Thompson et al.,[5] using the subjects from Burlington Growth Center, found that skeletal age offered "no additional value (beyond chronological age) in predicting maximum facial growth velocities in the female." Pileski et al.,[6] found that the relationship between ossification of the metacarpophalangeal sesamoid and facial growth is quite variable. Bjork and Helm[7] found that sesamoid ossification and peak growth in body height did not demonstrate a clinically significant correlation. This information did not offer much improvement in the prediction of the age at which the peak height velocity (PHV) occurred. Houston et al.,[9] found a few ossification events in the hand-wrist region could predict the PHV, but only to a limited extent. Houston [10] showed that skeletal age estimated by using hand-wrist radiographs was useful to predict adult stature, but there was a poor correlation between the estimated skeletal age and the timing of the growth spurt[10]. Assessing the bony outline of the hand-wrist bones to determine the patient's growth status could be problematic, especially for the female adolescent patient. Orthodontics needs new or additional indicators to forecast the

occurrence of facial growth spurt. Instead of using the bony outlines of the hand-wrist bones, one possibility is to measure the trabecular bone pattern to assess maturation status.

Recently, researchers have shown that fractal analysis is useful in differentiating between osteoporotic and non-osteoporotic women. Majumdar et al.,[1] showed that fractal analysis is potentially capable of differentiating osteoporotic bone from normal bone structures. Ruttiman et al., [27] using dental periapical films, demonstrated that the osseous fractal dimension can distinguish the premenopausal (age 32.8$\pm$3.9) from postmenopausal (age 62.5$\pm$4.1) women. These results suggest that fractal analysis is promising in detecting the changes in trabecular pattern due to osteoporosis.

How about applying fractal analysis to growth? When humans grow, the weight and height increase. The human skeleton must also increase in size and strength to accommodate increased metabolic and physical demand of the maturing body. When the human bones are maturing, the trabecular structure inside the bones is also changing, probably in the opposite direction of the osteoporotic trabecular changes. It is reasonable and logical to suggest that if fractal analysis can be used to detect trabecular changes due to osteoporosis, fractal analysis could also be useful in detecting trabecular changes due to growth and maturation of the skeleton.

Change in trabecular bone deserves serious consideration as an indicator of growth, because trabecular bone has a calculated remodeling (turnover) rate approximately eight times that of cortical bone due to its high surface to volume ratio and its greater sensitivity to metabolic changes [11,12]. Allison and Brooks [36] found that if bone was not in use, the earliest change in bone occurred in the trabecular portion. The result was absorption of

LITERATURE REVIEW

Fractal Analysis

Fractal analysis, popularized by Mendelbrot[18] in the early 1980's, has been applied to many areas of scientific research. In the study of geography, researchers have used fractal analysis to study the coast lines. In medical and biological research, fractal analysis has been used to study objects, structures or images that are too complex to describe sufficiently with the Euclidean measurements [20-25]. In early 1980's, Mandelbrot [18] showed how to measure complex structures in nature and mathemathical objects with the fractal technique. He pointed to the similarity between the complex structures and certain types of mathematical objects, that he called natural and ideal fractals, respectively. An example of an ideal fractal is the Sierpinski carpet [18]. An important characteristics of fractal objects are self-similarity. This means that whether the fractal objects are viewed up close or far away, the fractal objects look the same. A natural fractal also has this property of self-similarity, but it is only good for a limited range of scale.

There are many types of fractal analysis. The divider method (ruler method)[26] is the oldest technique. The ruler method is used to measure the length of curve, with different sizes of resolution, or "ruler." The result of the measurement of the curve would then be a certain number of the "ruler." The length of the "ruler" is a unit of measurement, which is just like the units in the metric system. Then a Richardson plot of the log of the curve versus the log of the ruler length is constructed. If the resulting plot is a straight line, it is said that the curve has fractal geometry. The slope of the line is used to compute the fractal dimension. The box-counting method could be used to measure the length of a curve or the density of lines or points over an area [26]. The Fourier transform power spectrum-based

fractal analysis is used in this study, and the details of this technique will be discussed in the **Method** section.

Development of Trabecular Bone

In a growing child, the skeleton needs to grow or mature in order to meet the physical demand of the child's daily activities. The trabecular architecture changes with the growth process. Through complicated biochemical pathways, osteoblasts and osteoclasts add and remove bone matrix to establish the bone architecture. There are two types of trabeculae: coarse trajectory and fine trabeculae. Both are related to the same basic supporting function. Dynamic remodeling of trabeculae is constantly occurring, in response to mechanical and metabolic demand[29]. The broad trajectory trabeculae are formed along major lines of force and stress, with the intention to support physical demand [30-35]. There are also intervening fine trabeculae which contribute to the strength of the broad trabeculae. At places where forces of stress and loads are constantly changing, there is an abundance of fine trabeculae and a low concentration of broad trajectory trabeculae. These areas include joint surfaces, bone ends, ilium, ribs and wrists [29].

Hand-Wrist Radiographs Studies

From Grave's 1976 study of children for pure aboriginal ancestry in Australia, fourteen hand-wrist ossification events were used to approximately estimate subjects' maturation status [15]. In this article, Grave stated "because of wide variation between children in developmental timing, ossification events should be used only as guides to growth activity and supplemented by a more complete knowledge of the child's developmental history if this is available." It was obvious that Grave did not feel the development of the

bony outline in the hand-wrist bones was a sufficient indicator to reveal a patient's maturation status.

By examining the data provided by Grave in his study [15], Grave's lack of confidence in using the different stages of formation of bony outline to predict future growth was evident. The only two ossification stages that preceded peak growth rate were PP2= and MP3=. The average age of PP2= and MP3= for girls was about 9.8 years old. The average age of PP2= for boys was about 10.6 years old. The average age of MP3= was about 11.2 years old. In H-1 stage, some girls and boys are at their peak growth rate, even though the female H-1 stage is about 1.5 years earlier than the average peak growth rate. The male H-1 stage is approximately 1.8 years earlier than the average peak growth rate. The more disturbing inference drawn from Grave's study was by the R= stage, which signifies the starting point of the acceleration phase of growth in both males and females, 20-25% of the subjects were either at or past the peak growth rates. With these data, it was not surprising that Grave was not comfortable in using the formation of hand-wrist bony outlines to locate patient's maturation on the growth velocity curve.

In his 1966 study, Hunter [17] expressed doubt about the usefulness of skeletal age determined from the Greulich-Pyle method in orthodontics. Hunter's data on the female subjects showed that the maximum facial growth could occur at skeletal age 8.79-13.13; the corresponding chronological age range 8.75-13.75. Hunter stated in this article that "there was little difference between the chronological and skeletal age range at the onset [of maximum facial growth] in females."

To the best of our knowledge, no researchers have used fractal analysis on radiographic trabecular bone pattern of hand-wrist bones to assess growth or maturation

status of growing children. However, fractal analysis of dental radiographs has been used to study periodontitis and osteoporosis. Shrout el al.,[8] demonstrated that fractal analysis could potentially be useful in distinguishing gingivitis and periodontitis by using non-standardized dental periapical radiographs. Ruttiman and his co-workers [27] completed fractal analysis on the maxillary periapical films of dentolalveolar bone of pre-menopausal and post-menopausal patients. The difference of the fractal dimensions between the two groups was statistically significant. Ruttiman's result suggested fractal dimension measured from the maxillary periapical radiographs can reflect changes in trabecular bone structure that occur with the onset of post-menopausal osteoporosis. Khosrovi[28] showed that fractal analysis on dental periapical radiographs could distinguish periodontitis from the healthy periodontal condition. The difference was statistically significant ($p<0.001$).

Researchers have used other radiographic films to demonstrate that fractal analysis is a potentially useful technique in detecting osteoporosis. Using photomicrographs of iliac crest biopsies, Majumdar et al.,[1] showed that fractal dimension changes with the fractional trabecular bone content. These results suggest that fractal analysis may be useful in distinguishing osteoporotic bone structure from normal. Khosrovi[28] demonstrated that fractal analysis on wrist radiographs can differentiate pre-menopausal from postmenopausal osteoporotic wrist radiographs. The difference was statistically significant ($p=0.0042$). Majumdar et al.,[37] performed fractal analysis on the distal of the radius of a hip fracture group vs an age-matched non-hip fracture group. The difference in fractal dimensions of the fracture and non-fracture groups was statistically significant ($p<0.03$).

SIGNIFICANCE OF THE STUDY

This new approach of assessing growth using fractal analysis of the hand wrist radiograph may offer information that the traditional methods do not render. Additional information may be obtained on the amount of growth remaining or the growth intensity. This study should yield information on the usefulness of the fractal technique to assess growth status.

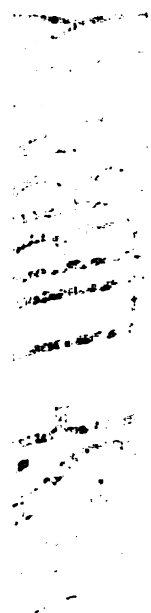

AIM

The aim of this study was to examine if the Fourier-transform-based fractal analysis on the trabecular pattern in the hand-wrist radiograph is potentially useful in assessing human growth status. In order to evaluate its usefulness, we examined if fractal dimensions obtained from the Fourier transform power spectrum-based fractal analysis had any correlation with maturation of Caucasian females from ages 7 to 15.

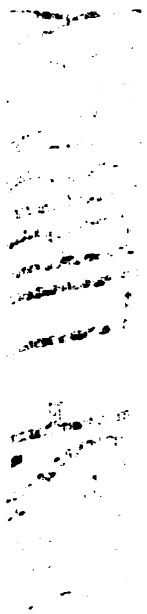

HYPOTHESIS

The fractal dimension from the Fourier-transform-based fractal analysis of the hand-wrist radiograph detecting trabecular structural correlates with human maturation from chronologic ages 7 to 15. Human maturation was determined by the following parameters: the chronologic age, the skeletal age, and the breast development.

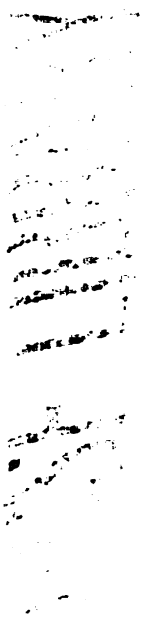

METHODS AND MATERIALS

Subjects

A cross-sectional sample of 51 Caucasian females hand-wrist films was used. Subjects' ages ranged from 7-15. These female subjects were originally recruited for a study to develop a digitized hand atlas. The inclusion criteria were the following:

1. Normal Caucasian girl, age range between ages 7-15.
2. Height and weight within normal limits for their respective ages as determined by Hamill et al., [42].
3. No history of chronic illness.
4. No hospitalization or no illness for more than two weeks during the six months prior to obtaining the hand-wrist films.
5. No regular intake of medications, vitamin preparations or calcium supplements during the six months prior to the study.

All 51 subjects' films were used for the study on the proximal phalange of the middle finger. Fifty of the 51 subjects' films were used for the study on the distal of the radius. The reason that one subject was excluded was the distal radius for this particular film was covered by an X-ray lable.

The radiographic technique was a 2 mA- 60kV x-ray source that was 40 inches away from the hand. The film was Lannex detail film. The films were digitized with a Lumiscan Digitizer (Lumisys, Sunnyvale, CA). The digitation was performed at 100 micron per pixel. Each pixel size was 100um x 100um. The digitized images were analyzed on the SunMicrosystem's Sparc WorkStation platform (Palo Alto, CA).

Fourier Transform Power Spectrum-based Fractal Analysis

The Fourier transform power spectrum establishes the frequency spectrum of the trabecular patterns. The Fourier transform measures the rate at which textural variations occur. Rapid changes in texture are reflected as high frequency components in the power spectrum. The frequency-power graph is generated with the X-axis representing the log of frequency and the y-axis representing the log of the average power at each particular frequency. To obtain the Fractal Dimension (FD), the slope of the linear portion of the logarithmic plot of the power spectrum vs the logarithmic plot of frequency is obtained. From the Fourier analysis, a two-dimensional power spectrum S(u,v) of the Fourier transform [F(u,v)] is defined as the following:

$$S^2(u,v)=|F(u,v)\ F^*(u,v)|$$

where F*(u,v) is the complex conjugate of F(u,v), and u and v are the spatial frequencies in the x- and y- directions, respectively. In the polar coordinate system, the average angular power spectrum S(f) from a given spatial frequency f is related to the fractal dimension (Dfft) as

$$S(f) \text{ [proportional to] } f^{-Dfft}$$

The Fourier based fractal dimension (Dfft) is calculated from slopes of the log-power-and-log-spatial frequency plot:

$$Dfft=(7-|slope|)/2$$

The lowest and highest spatial frequency data points of the log-log plot are discarded to minimize noise due to variations in X-ray quanta, film grain, etc. From the logarithmic plot, several spatial frequency regions are selected arbitrarily to determine the different fractal dimensions. The slopes are calculated from the following log-spatial frequency regions for

the middle finger: 1-1.2, 1.2-1.4, and 1.3-1.4; for the distal of the radius: 0.6-1.0, 1.0-1.2, 1.0-1.4, and 1.2-1.4. **Figure 1** graphically demonstrates the frequency ranges selected from the entire frequency spectrum generated for each anatomic site. The unit for the spatial frequency is 1/pixel.

Anatomic Sites of the Fractal Analysis and Determination of Region of Interest (ROI)

The distal of the radius and the medial diaphysis of the proximal phalanx of the middle finger are the sites of analyses. The shape of region of interest (ROI) is a circle. To determine the location and the proper size of the circular ROI, the size and location of the first circle needs to be established. The size of the first circle will be the largest achievable, but not so large that the circle includes any cortical bone. As the first circle is obtained, the size and the coordinate of the center of the large circle are recorded. Then the size of the ROI circle is 80% of the size of the first larger circle. The coordinate of the center of the ROI circle will be the same as the initial larger circle. Fourier transform power spectrum-based fractal analysis was performed on the ROI selected by the aforementioned method.

Marshall-Tanner Maturation Staging System

The Marshall-Tanner Maturation Staging System was used in this study as an indicator of the subject's maturational status [14]. The system consists of 5 stages that define the development of the breast. The following describes how each stage is defined:

Stage 1: Pre-adolescent; elevation of papilla only

Stage 2: Breast Bud stage; elevation of breast and papilla as a small mound, with enlargement of areola diameter.

Stage 3: Further enlargement of breast and areola with no separation of their

contours.

Stage 4: Projection of areola and papilla to form a secondary mound above the level of the breast.

Stage 5: Mature stage; projection of papilla only, due to recession of the areola to the general contour of the breast.

Photographs were taken of the nude subjects at each examination. Then the appropriate stage was determined from examining the photographs.

Tanner/Whitehouse Skeletal Age (TW2 Method)

The skeletal age of each subject was determined by the Tanner/Whitehouse RUS scoring system [37]. This scoring system uses 13 bones:

1. radius
2. ulna
3. first metacarpal
4. third metacarpal
5. fifth metacarpal
6. proximal phalanx of the thumb
7. proximal phalanges of third finger
8. proximal phalanges of fifth finger
9. middle phalanges of third finger
10. middle phalanges of fifth finger
11. distal phalanx of the thumb
12. distal phalanx of third finger
13. distal phalanx of fifth finger

After each bone is scored, the sum of all the individual scores is used to determine the skeletal age. The radiographs were read, and the maturation stage of each bone was determined.

Interoperator Reliability

A second-year orthodontic resident was recruited to perform the same fractal analysis as completed by third-year orthodontic resident to examine the interoperator reliability of the fractal analysis technique. Three training sessions were provided to make sure the determination of the size and location of ROI was understood. Each session was approximately two hours. The second-year orthodontic resident independently performed the fractal analysis described previously.

To assess the reproducibility of ROI, 16 of the 51 hand-wrist films were chosen for the interoperator study of the proximal phalange of the middle finger. Fifteen of the 50 hand-wrist films were chosen for the interoperator study of the distal of the radius. Fractal dimension was calculated from each of the measurements.

The sizes of the circles, the coordinate locations of the circles' centers, and the fractal dimension were compared between both investigators. The sizes of the ROI circles are represented by the radii.

The "location difference" is the absolute distance between the centers of circles that is calculated by using the Pathagryn Theorem. The following formula was applied:

Location Difference $=[(\text{Difference of X})^2)+(\text{Difference of Y})^2]^{1/2}$.

"Percentage of the location difference" was calculated by the location difference (the unit is pixel) divided by the size of the first circle (obtained by the author) that is represented by its radius. The result was multiplied by 100.

"Size difference" was calculated by the difference between the radii of the two circles. "Percentage of the size difference" was determined by taking the size difference divided by the size of the first circle. The size of the first circle was represented by the radius of the circle.

Intraoperator Reliability

To assess the reproducibility of ROI, 16 of the 51 hand-wrist films were chosen for the intraoperator study of the proximal phalange of the middle finger. Fifteen of the 50 hand-wrist films were chosen to be in the intraoperator study of the distal of the radius. The intraoperator reliability studies were done about 4 months after the initial acquisition of the data.

The sizes of the circles, the coordinate locations of the circles' centers, and the fractal dimension were compared to the first set of results obtained by the author. The sizes of the ROI circles were represented by the radii.

STATISTICAL ANALYSES

Scattergrams of the fractal dimensions were generated for each of the two sites and for each of the frequency ranges. Pearson correlation analyses were generated for fractal dimensions (FD) vs the chronologic age and the fractal dimensions (FD) vs. the skeletal age (TW2). The Spearman rank correlation was used to quantify the correlation strength between the fractal dimension (FD) and the Tanner Maturation Index for breast development.

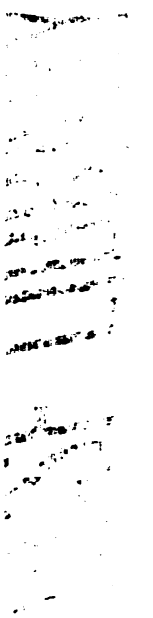

RESULTS

The distribution of the subjects by chronologic age was normal (**Figure 2a**). **Figure 2b** graphically demonstrated the subjects' distribution according to the skeletal age determined by the TW2 method. It demonstrated a reasonably normal distribution. The subject pool's distribution by the Tanner Maturation Index (e.g. breast development) showed a very high percentage (41%) of our pool of subjects is in Stage 1 (**Figure 2c**).

Our pool of subjects' skeletal age, determined by the TW2 method, correlated strongly with the chronologic age (**Figure 3a**). **Figure 3b** showed that for chronologic age 7-11, the Tanner Maturation Index was either Stage 1 or 2. After chronologic age 12, the Tanner Maturation Index rose quickly. This phenomenon was also demonstrated in **Figure 3c**, which illustrated the relationship between Tanner Maturation Index and the Skeletal Age (TW2). After skeletal age 12 or 13, the maturation of breasts advanced quickly. This should not be too surprising, because the chronologic and the skeletal ages were strongly correlated.

As discussed in the **Methods** section, the following frequency ranges were analyzed for the middle finger: 1-1.2, 1.2-1.4, and 1.3-1.4. The data were tabulated in **Table 1.** The results of correlation strengths were summarized in **Table 2**. The figures were presented in **Figures 4-6**. The results from **Table 2** showed that the correlation strength between the chronologic age and the fractal dimension for the middle finger was moderately strong for the frequency range of 1.0-1.2 (R=0.636); moderate for the frequency range of 1.2-1.4 (R=0.476); and weak for the frequency of 1.3-1.4 (R=0.360). For the correlation strength between the skeletal age and the fractal dimension, the frequency range of 1.0-1.2 demonstrated a moderately strong correlation (R=0.605); the frequency range of 1.2-1.4 had moderate correlation (R=0.397); and in the frequency range of 1.3-1.4, the FD and the

skeletal age were weakly correlated (R=0.305). For the same frequency ranges, the correlations between fractal dimensions and the Tanner Maturation Index for breast development were weaker than the chronologic age and the skeletal age **(Table 2)**. The results indicated that fractal dimension of trabecular bone pattern in the middle finger had various correlation strengths with the human maturation process in different frequency range.

As discussed in the **Method** section, the following frequency ranges were analyzed for the distal of the radius: 0.6-1.0, 1.0-1.2, 1.0-1.4, and 1.2-1.4. The data were presented in **Table 3**. The results of correlation studies were summarized in **Table 4**. The figures were presented in **Figures 7-9**.

In the frequency ranges of 0.6-1.0 and 1.0-1.2, the correlation for the FD vs the chronologic age (R=0.782 and R=0.798, respectively) and the correlation for the FD vs the skeletal age (R=0.757 and 0.758) were strong. For the frequency ranges of 1.0-1.4 and 1.2-1.4, the FD and the chronologic age had moderately strong correlation (R=0.624 and R=0.669). For the frequency ranges of 1.2-1.4, the FD and the skeletal age also demonstrated a moderately strong correlation (R=0.640). The FD and the skeletal age had a moderate correlation for the frequency range of 1.0-1.4 (R=0.555). Interestingly, in the ranges of frequencies we studied, the 1.0-1.2 was the frequency range that demonstrated the strongest correlation between the FD and the chronologic age and the FD and the skeletal age in both the proximal phalange of the middle finger and the distal of the radius. **These data supported our hypothesis that the fractal analysis correlates strongly with the human maturation process, but only in certain frequency ranges.** The correlation was weaker in the proximal phalange of the middle finger than in the distal of the radius. For the same frequency ranges, the correlations between fractal dimensions and the Tanner Maturation

Index for breast development were weaker than the chronologic age and the skeletal age **(Table 4)**.

In **Table 5-6**, the average fractal dimension (FD) for each Tanner Stage and for each frequency range was tabulated for the middle finger and the distal of the radius. No relationship could be determined between the average fractal dimension and the Tanner Maturation Index for breast development.

Interoperator Reliability

The data for the interoperator reliability study for the proximal phalange of the middle finger were shown in **Table 7 and 9**. The results were shown graphically in **Figure 10.** These results suggested that the location difference between the two operators was not related to the average size of the two circles when the sizes were determined by two independent operators (**Figures 10a-b**). Large location discrepancies had come from ROI's of both small and large average sizes. The largest percent location difference was about 13%, with the majority (81.3%) being below 10%. The results from this interoperator reliability study of the middle finger suggested the size difference between the ROI circles was not due to the sizes of circle **(Figures 10c-d)**. Again, large size discrepancies have come from ROI's of both small and large average sizes. The largest percent size difference was about 6%, with the majority (87.5%) below 4%. **Figures 10e-j** graphically illustrated the interoperator difference of FD for the three frequency ranges for the middle finger. In this particular sample for the interoperator reliability study of the middle finger, all discrepancies of FD in terms of percentage to the FD obtained by the author were all under 6%.

The data for the interoperator reliability study for the distal of the radius were presented in **Table 8 and 10**. The graphic results were shown in **Figure 11**. In **Figures 11a-**

b, the discrepancy in locations increases as the sizes of the ROI circles increase. The reproducibility of the location was more difficult in Subjects 12-16. Subjects 12-16 were from the older group of the entire pool. However, Subjects 12-16's ROI sizes did not appear to be more difficult to be reproduced, even though their sizes were larger than that of the younger subjects. The largest percent location difference was about 13%, with the majority of the subjects (93.3%) below the 10% mark. The magnitude of the differences in sizes between the two operators was not related to the sizes of the ROI circles, which was shown in **Figures 11c-d**. The largest percent size difference was about 9%, with the majority (86.7%) below 6%. **Figures 11e-l** represented the interoperator difference of FD for the four frequency ranges for the distal of the radius. In this sample for the interoperator reliability study for the distal of the radius, all discrepancies of FD in terms of percentage to the FD obtained by the author were all under 5%. The correlations between interoperator discrepancies between FD and the average sizes of ROI circles were weak or almost none.

Intraoperator Reliability

The data for the intraoperator reliability study of the proximal phalange of the middle finger were shown in **Tables 11 and 13** and graphically summarized in **Figure 12**. Like the results in the interoperator reliability study, the discrepancies in the determinations of location and size were not related to the size of the ROI circle. The largest percent location difference was slighly larger than 8%, with the majority (93.8%) at or under 8%. This was a smaller discrepancy than the interoperator reliability results. The largest percent size difference was about 3.6%, with all the differences below 4%. This represented a smaller disagreement than the results of the interoperator reliability study. **Figures 12e-j** summarized the intraoperator difference of FD. In our sample for the intraoperator reliability study for

the middle finger, all discrepancies of FD in terms of percentage to the first set of FD obtained by the author were under 8%.

The data for the intraoperator reliability study for the distal of the radius were shown in **Tables 12 and 14 and Figure 13**. The results showed the intraoperator reliability of the determinations of the locations and the sizes of the ROI circles on the distal of the radius was not related to the size of the ROI circles. The largest percent location difference was about 13.5%, with 73.3% of the subjects below 10%. The largest percent size difference was 7%; the majority (86.7%) being below 4%. **Figures 13e-l** illustrated the intraoperator difference of FD for the four frequency ranges for the distal of the radius. In this sample for the intraoperator reliability study of the distal of the radius, all discrepancies of FD in terms of percentage to the first set of FD obtained by the author were under 5%. The correlations between intraoperator discrepancies between FD and the average sizes of ROI circles were weak or almost none. The results from the interoperator reliability study have shown that this particular fractal analysis technique could be easily learned after just a few hours of training. The repeated measurements between different two different operators were very close. The results from the intraoperator reliability study demonstrated that repeated measurements of the fractal dimension could be done very accurately by the same operator

DISCUSSION

When we requested a sample of 50 subjects from Dr. Vincente Gilsanz (Los Angeles, CA) who had collected a pool of subjects for a hand-wrist radiograph atlas, the only criterion we specified was normal and healthy Caucasian female subjects in ages from 7-15. Dr. Gilsanz randomly selected the subjects based on the selection criteria we gave him. A large percentage of subjects were in the Stage 1 of the Tanner Maturation Index (e.g. breast development). However, the distributions of the subjects by the chronologic and skeletal ages are fairly normal. It was determined that the sample was a good cross-sectional representation that would allow us to study whether fractal dimension correlates with the maturation process of Caucasian females between ages 7-15.

It is important to keep in mind that the hand-wrist radiographs are a 2-dimensional representation of 3-dimensional cortical and trabecular structures. Therefore, the hand-wrist films do not record exact anatomical details. Rather, an x-ray film is an image of overlaying anatomical structures. This means that two hand-wrist radiographs taken on the same person's hand could be slightly different. This could be due to a slightly vertical turning or angulation of the hand when the films are taken. We assume when the hand-wrist radiographs were taken, the hand was lying flat on a flat surface, and the x-ray tube was aimed perpendicular to the flat surface. One of the weaknesses of this project was that we did not independently evaluate the effect of turning the hand/wrist 5-10 degrees on the image. The x-ray source could also be aimed at a slight angulation to the hand. We do not know any study which has examined this potential problem.

As discussed in the Literature Review section, at anatomical sites experiencing much physical activity, there is a high concentration of fine trabeculae and a low concentration of

broad trajectory trabeculae. The wrist is one of these sites [29]. Siffert [29] postulated that in bone atrophy, the fine mesh and cross-bracing trabeculae are the first to disappear on the roentgenogram. This is solely due to their relatively smaller size than the broader and thicker main weight bearing trajectory trabeculae. The result is the evolution of patterns of fine trabeculae becomes thin, demonstrates discontinuity, and eventually absorbs. This makes the main supporting trabeculae more prominent. If the wrist has a high concentration of fine trabeculae, and the fine trabeculae are very sensitive to physical demands and enviromental changes, the wrist is a good anatomic site to apply fractal analysis of the trabecular pattern. In the anatomical locations where there is a high concentration of fine trabeculae [29], the wrist is the most accessible to take radiographs. It is logical that the wrist has higher concentration of fine trabeculae than the middle finger, since the wrist experiences more physical demand than the middle finger. If this concept is correct, it may explain why our data demonstrate fractal analysis on the distal of the radius with stronger correlation to the maturation process than the fractal analysis on the proximal phalange of the middle finger.

In this study, we selected a circle as the shape of the region of interest (ROI). To define an ROI circle, we first found the largest possible circle that could be fitted into the distal radius or the proximal phalange of the middle finger, with the circle just touching the inner edge of the cortical bone. The ROI circle's size is 80% of the larger circle. A circle's location is represented by the coordinate of its center. By making the centers of both circle identical, it was ensured that the ROI did not cover any cortical bone that was all radiopaque. This was not possible in using the rectangle or square in the current version of our fractal analysis program, because the location of a rectangular or a square is defined by the coordinate of the upper left corner. If a command is issued to reduce the size of the rectangle

or the square by 20% with the same coordinate location, the upper left corner will still be on the same point while the rest of the area is shrunken by 20%. This cannot assure the boundary is entirely in trabecular bone, because the upper left corner is probably still touching radiopaque cortical bone in the radiographs.

Hunter's 1966 study [4] showed that the skeletal age determined by using the Greulich-Pyle method [17] was useless to orthodontists. Hunter's data on the female subjects showed that the maximum facial growth could occur at skeletal ages 8.79-13.13; the corresponding chronological ages 8.75-13.75[4]. The problem could be the way the skeletal age was first established by Greulich and Pyle. Greulich and Pyle took 100 films that had the same chronological age, plus/minus 21 days. The 100 films were then ranked in order of their skeletal maturation, from the least mature to the most mature. The standard film for that particular skeletal age was the median film[17], that was either the 50^{th} or the 51^{st} film. This way of establishing the skeletal age may be useful to pediatricians, because the skeletal age was established by the statistical median. Pediatricians are assessing if their growing patients are statistically within the normal limits of their height and weight. This information could not be useful to the orthodontist, however, who wants to know if the mandible can be expected to grow to mitigate the skeletal sagittal discrepancy, because maximal facial growth can occur at any time between skeletal ages 8.79-13.13[4]. Therefore, to make hand-wrist films useful to orthodontists, it is necessary to have different approaches of establishing skeletal age, in which fractal dimensions can be expected to play a role.

The traditional methods (TW2 and Greulich-Pyle, for example) do not offer information on the growth rate or the amount of growth remaining. This is more useful information than knowing where the patient is on his/her growth curve. The fractal analysis

can potentially be useful in gaining information on growth rate and the amount of growth remaining. Further longitudinal studies are necessary to determine if fractal analysis can reveal the growth intensity or the amount of growth still available. Other indicators, such as menarche or the information from the current methods of interpreting hand-wrist films, could be combined with information from fractal analysis to make better assessment of patient's growth status.

For the selection of anatomic sites, we chose the proximal phalange of the middle finger and the distal of the radius, because these two sites were used quite extensively in hand-wrist studies [13, 17, 37, 40]. The distal of the radius was also a site used in many osteoporosis studies that applied fractal analysis on the hand-wrist radiographs [1, 28, 38]. It is possible that other sites offer better correlation between the fractal dimension and the maturation process than our data. The frequency ranges were chosen arbitrarily because we could not find any published data indicating the appropriate frequency ranges to be used. It is possible that the fractal dimension and the maturation process correlate better in other frequency ranges than the frequency ranges we arbitrarily selected. Further research in this area will be necessary to understand how the correlations between fractal dimension and maturation can vary according to certain anatomic sites and frequency ranges. Stevenson[41] found that in bone atrophy due to disuse, different changes in trabecular patterns may be observed in different locations and bones. Some bone region demonstrate more pronounced change, and some experience less. Although we have focused on using the hand-wrist radiographs, it's entirely possible that better sites can be found elsewhere. We do not understand why the correlation is positive in certain frequency regions and negative in other

frequency regions. We also do not understand the biological meanings of positive or negative correlation, which needs further research to clarify.

Data from Marshall et al.,[14] suggested that breast development correlated poorly with menarche. Menarche normally occurs during breast development Stages 3 or 4. However, Marshall et al.,[14] showed that some normal females did not menstruate until their development was mature. Our data suggest fractal measurements correlate weakly with breast development.

For the same frequency ranges, the correlations between fractal dimensions and the Tanner Maturation Index for breast development are weaker than the chronologic age and the skeletal age. As we have noted earlier, the breast development did not correlate with human maturation as linearly as the chronologic and skeletal ages. This results in the weak correlation between the fractal dimensions and the Tanner Maturation Index

No interoperator or intraoperator reliability study could be done on the Marshall-Tanner Maturation results, which were given to the authors when the radiographs were requested. Marshall et al.,[14] did note that girls with large breasts at Stage 3 could be mistaken to be at Stage 5. Girls with small breasts at Stage 5 could be erroneously rated to be at Stage 3. However, re-rating by Marshall et al [14] showed that mistakes made in this manner were rare. They also presented data showing that more than 25% of their female subjects, whose breast development was just in the earliest stage, reached the peak of their adolescent height spurts, and their growth began to slow down. This indicated that breast development correlates poorly with growth spurts in statural height.

Marshall et al.,[14] also reported that all girls in the study had passed the peak of their growth spurt in height before menstruation started. Deming [39] presented similar results, in

which 20 out of 24 girls had menarche within 6 months of the time that their growth was decelerating most rapidly. In agreement with Marshall et al.,[14] and Deming [39], Hagg and Taranger [40] found that menstruation did not start before peak height velocity, and menarche always occurred before the end of the growth spurt. Unfortunately, the information on our subjects' menarche occurrences was not available. Otherwise, it would be valuable to correlate fractal dimension with the occurrences of the subject's menarche to obtain information about the patient's growth status.

CONCLUSION

1. Our data could not reject the hypothesis that the fractal dimensions from the Fourier-transform-based fractal analysis of the hand-wrist radiographs detecting trabecular structural changes correlates with human maturation from chronologic ages 7 to 15.
2. The strengths of correlations between fractal dimensions and the chronologic age, the Tanner Maturation Index of breast development, and the skeletal age depend on the anatomic site and the frequency range selected.

Table 1: FD (The Middle Finger)

Subj	Chronologic Age	Tanner Maturation Index	Skeletal Age (TW2)	1.0-1.2	1.2-1.4	1.3-1.4
1	8.59	1	10.90	2.645	2.940	2.950
2	8.63	1	11.04	2.688	2.954	3.164
3	8.85	1	10.04	2.662	3.038	3.122
4	8.90	1	10.03	2.667	2.996	3.135
5	10.28	1	11.09	2.619	2.960	3.029
6	10.35	1	13.08	2.668	2.982	2.923
7	10.43	2	14.00	2.659	2.838	2.928
8	10.49	1	11.03	2.857	2.981	3.178
9	12.05	3.5	14.00	2.633	2.954	2.843
10	12.21	3	13.10	2.665	2.958	2.943
11	12.34	2	14.02	2.617	2926	2.686
12	12.37	2.5	13.01	2.872	2.807	2.928
13	14.20	4	14.03	2.963	2.833	2.850
14	14.37	5	15.05	2.882	2.819	2.914
15	14.59	3.5	15.02	2.967	2.806	2.779
16	14.70	5	16.00	2.944	2.832	2.878
17	7.09	1	7.01	2.511	2.877	2.750
18	7.09	1	6.01	2.642	2.980	3.165
19	7.27	1	9.01	2.661	2.978	3.022
20	7.44	1	9.08	2.691	2.985	3.215
21	7.76	1	9.01	2.647	2.932	3.007
22	7.93	1	9.11	2.639	2.857	2.922
23	7.98	1	10.01	2.594	2.936	2.657
24	8.17	1	9.08	2.583	2.917	2.979
25	8.90	2	10.10	2.663	2.931	2.943
26	9.77	1	11.02	2.683	2.936	2.972
27	9.89	1.5	11.02	2.637	2.975	2.943
28	9.94	1	10.10	2.611	2.918	2.907
29	10.00	1	13.07	2.765	2.941	2.993
30	10.24	1	13.08	2.708	2.955	3.043
31	10.43	1.5	14.00	2.695	2.967	3.157
32	Subject excluded from the study					
33	10.55	1	10.09	2.647	2.946	2.922
34	10.97	1.5	12.00	2.665	2.855	2.615
35	11.97	2	14.00	2.862	2.878	2.693
36	11.97	2	14.05	2.701	2.920	2.850
37	11.97	1	14.09	2.860	2.883	2.986
38	12.26	1.5	14.00	2.630	3.017	3.007
39	12.26	2	11.08	2.641	2.866	2.907
40	12.64	3.5	14.03	2.697	2.908	2.929
41	12.75	3	13.11	2.755	2.893	2.822
42	12.81	3	14.07	2.658	2.942	2.900
43	12.90	2	14.03	2.671	3.007	2.957
44	13.51	3	14.09	2.739	2.908	2.907
45	13.56	4.5	16.00	2.827	2.891	2.957
46	13.58	2.5	14.03	2.721	2.943	2.865
47	13.72	3	13.08	2.704	2.925	2.936
48	13.83	5	16.00	2.651	2.929	2.836
49	14.33	5	16.00	2.999	2.748	2.779
50	14.74	5	16.00	2.955	2.787	3.036
51	14.79	5	16.00	2.747	2.941	2.922
52	15.03	5	16.00	2.750	2.892	2.879

Table 2: Correlation Strengths for FD and Commonly Used Aging Indicator (The Middle Finger)

Freq Range	Chronologic Age (r)	Tanner Maturation Stage (r_s)	Skeletal Age (TW2) (r)
1.0-1.2	0.636	0.422	0.605
1.2-1.4	0.476	0.510	0.397
1.3-1.4	0.360	0.497	0.305

Table 3: FD (The Distal of the Radius)

Subj	Chronologic Age	Tanner Maturation Index	Skeletal Age (TW2)	0.6-1.0	1.0-1.2	1.0-1.4	1.2-1.4
1	8.59	1	10.90	2.601	2.697	2.815	2.801
2	8.63	1	11.04	2.614	2.866	2.945	2.893
3	8.85	1	10.40	2.666	2.705	2.820	2.865
4	8.90	1	10.03	2.639	2.627	2.879	2.899
5	10.28	1	11.09	2.675	2.681	2.993	3.094
6	10.35	1	13.08	2.679	2.575	2.799	2.840
7	10.43	2	14.00	2.649	2.674	2.813	2.866
8	10.49	1	11.03	2.651	2.618	2.843	2.923
9	12.05	3.5	14.00	2.712	2.473	2.785	2.976
10	12.21	3	13.10	2.726	2.471	2.834	3.088
11	12.34	2	14.02	2.666	2.523	2.794	2.877
12	12.37	2.5	13.01	2.713	2.604	2.820	3.046
13	Subject excluded from the study						
14	14.37	5	15.05	2.695	2.583	2.790	2.942
15	14.59	3.5	15.02	2.706	2.445	2.741	2.981
16	14.70	5	16.00	2.723	2.479	2.680	2.909
17	7.09	1	7.01	2.531	2.984	2.828	2.647
18	7.09	1	6.01	2.571	2.791	2.786	2.647
19	7.27	1	9.01	2.595	2.730	2.835	2.729
20	7.44	1	9.08	2.633	2.658	2.829	2.814
21	7.76	1	9.01	2.639	2.607	2.793	2.823
22	7.93	1	9.11	2.616	2.709	2.827	2.767
23	7.98	1	10.01	2.588	2.783	2.830	2.717
24	8.17	1	9.08	2.600	2.747	2.830	2.731
25	8.90	2	10.10	2.607	2.721	2.808	2.730
26	9.77	1	11.02	2.640	2.609	2.789	2.841
27	9.89	1.5	11.02	2.565	2.770	2.777	2.637
28	9.94	1	10.10	2.629	2.671	2.827	2.761
29	10.00	1	13.07	2.668	2.502	2.777	2.877
30	10.24	1	13.08	2.611	2.661	2.802	2.810
31	10.43	1.5	14.00	2.585	2.776	2.821	2.741
32	Subject excluded from the study						
33	10.55	1	10.09	2.666	2.494	2.775	2.925
34	10.97	1.5	12.00	2.603	2.723	2.818	2.754
35	11.97	2	14.00	2.690	2.454	2.752	2.945
36	11.97	2	14.05	2.694	2.449	2.744	2.931
37	11.97	1	14.09	2.712	2.406	2.710	3.002
38	12.26	1.5	14.00	2.668	2.490	2.771	2.942
39	12.26	2	11.08	2.615	2.652	2.799	2.829
40	12.64	3.5	14.03	2.661	2.533	2.787	2.891
41	12.75	3	13.11	2.688	2.476	2.732	2.919
42	12.81	3	14.07	2.690	2.469	2.765	2.957
43	12.90	2	14.03	2.632	2.613	2.797	2.824
44	13.51	3	14.09	2.704	2.431	2.728	2.988
45	13.56	4.5	16.00	2.690	2.452	2.766	2.932
46	13.58	2.5	14.03	2.668	2.509	2.779	2.888
47	13.72	3	13.08	2.702	2.433	2.708	2.964
48	13.83	5	16.00	2.712	2.502	2.792	2.993
49	14.33	5	16.00	2.704	2.431	2.723	2.967
50	14.74	5	16.00	2.706	2.458	2.661	2.883
51	14.79	5	16.00	2.700	2.440	2.733	2.929
52	15.03	5	16.00	2.697	2.433	2.717	2.996

Table 4: Correlation Strengths (R) for FD and Commonly Used Aging Indicators (The Distal of Radius)

	Chronologic Age (r)	Tanner Maturation Stage (r_s)	Skeletal Age (TW2) (r)
0.6-1.0	0.782	0.562	0.757
1.0-1.2	0.798	0.646	0.758
1.0-1.4	0.624	0.648	0.555
1.2-1.4	0.669	0.448	0.640

Table 5: Average FD for Each of the Tanner Maturation Indices (The Middle Finger)

	Freq 1.0-1.2	Freq 1.2-1.4	Freq 1.3-1.4
Tanner Stage 1 (n=21)	2.659±0.068	2.949±0.048	2.988 ±0.161
Tanner Stage 2 (n=7)	2.705 ±0.079	2.902 ±0.032	2.890 ±0.099
Tanner Stage 3 (n=5)	2.694 ±0.074	2.945 ±0.042	2.919 ±0.052
Tanner Stage 4 (n=1)	2.963	2.833	2.850
Tanner Stage 5 (n=7)	2.879±0.108	2.836 ±0.070	2.901 ±0.083

Table 6: Average FD for Each of the Tanner Maturation Indices (The Distal of the Radius)

	Freq 0.6-1.0	Freq 1.0-1.2	Freq 1.0-1.4	Freq 1.2-1.4
Tanner Stage 1 (n=21)	2.629 ±0.034	2.672 ±0.128	2.825 ±0.059	2.829 ±0.109
Tanner Stage 2 (n=7)	2.650 ±0.162	2.583 ±0.109	2.786 ±0.027	2.857 ±0.073
Tanner Stage 3 (n=5)	2.702 ±0.015	2.456 ±0.022	2.753 ±0.049	2.983 ±0.064
Tanner Stage 4 (n=0)	NA	NA	NA	NA
Tanner Stage 5 (n=7)	2.705 ±0.010	2.475 ±0.054	2.728 ±0.050	2.945 ±0.043

Table 7: Interoperator Reliability Study for Proximal Phalange of the Middle Finger.

Subj	1X	1Y	1-size	2X	2Y	2-size	Loc Diff (pixels)	Size Diff (pixels)	% Loc Diff	% Size Diff
1	582	689	32	582	689	30	0.00	2	0.0000%	6.2500%
2	380	342	30	382	339	29	3.61	1	12.019%	3.3333%
3	402	380	33	403	379	33	1.41	0	4.2855%	0.0000%
4	403	336	30	403	336	30	0.00	0	00000%	0.0000%
5	403	402	32	403	404	33	2.00	1	6.2500%	3.1250%
6	382	456	33	382	456	32	0.00	1	0.0000%	3.0303%
7	420	448	31	420	450	31	2.00	0	6.4516%	0.0000%
8	309	463	32	310	463	32	1.00	0	3.1250%	0.0000%
9	721	769	32	722	768	31	1.41	1	4.4194%	3.1250%
10	539	429	35	535	427	34	4.47	1	12.7780%	2.8571%
11	554	695	28	555	694	27	1.41	1	5.0508%	3.5714%
12	389	709	35	388	708	35	1.41	0	4.0406%	0.0000%
13	534	841	37	534	845	36	4.00	1	10.811%	2.7027%
14	762	864	38	763	866	36	2.24	2	5.8844%	5.2632%
15	777	858	39	778	855	40	3.16	1	8.1084%	2.5641%
16	628	841	38	628	840	38	1.00	0	2.6316%	0.0000%

Table 8: Interroperator Reliability Study of the Distal of Radius.

Subj	1-X	1-Y	1-size	2-X	2-Y	2-size	Loc Diff (pixel)	Size Diff (pixel)	% Loc Diff	% Size Diff
1	385	446	65	385	445	64	1.00	1	1.5385%	1.5385%
2	294	205	62	295	205	61	1.00	1	1.6129%	1.6129%
3	266	204	66	266	201	65	3.00	1	4.5455%	1.5152%
4	389	342	68	390	343	62	1.41	6	2.0797%	8.8235%
5	236	330	70	238	325	66	5.39	4	7.6931%	5.7143%
6	376	180	70	374	180	67	2.00	3	2.8571%	4.2857%
7	240	161	68	238	160	65	2.24	3	3.2883%	4.4118%
8	372	298	68	371	301	67	3.16	1	4.6504%	1.4706%
9	383	197	75	384	196	73	1.41	2	1.8856%	2.6667%
10	238	126	80	240	126	74	2.00	6	2.500%	7.5000%
11	397	443	71	397	443	69	0.00	2	0.0000%	2.8169%
12	256	304	82	257	297	79	7.07	3	8.6233%	3.6585%
13	Subject excluded from the study									
14	379	277	77	374	276	77	5.10	0	6.6221%	0.0000%
15	401	280	78	400	278	78	2.24	0	2.8668%	0.0000%
16	410	257	86	403	260	88	7.62	2	8.8555%	2.3256%

Table 9: FD from Interoperator Reliability Study of the Proximal Phalange of the Middle Finger.

Subj	1-1.2 (1)	1-1.2 (2)	1.0-1.2 FD Diff	1.0-1.2 Diff (%)	1.2-1.4 (1)	1.2-1.4 (2)	1.2-1.4 FD Diff	1.2-1.4 Diff (%)	1.3-1.4 (1)	1.3-1.4 (2)	1.3-1.4 FD Diff	1.3-1.4 Diff (%)
1	2.645	2.703	0.0580	2.1932%	2.940	2.999	0.0590	2.0071%	2.950	3.122	0.1715	5.8136%
2	2.688	2.639	0.0490	1.8415%	2.954	2.963	0.0090	0.3047%	3.165	3.043	0.1215	3.8395%
3	2.662	2.654	0.0080	0.3005%	3.038	3.025	0.0130	0.4280%	3.122	3.095	0.0270	0.8650%
4	2.667	2.670	0.0030	0.1125%	2.996	3.022	0.0265	0.8847%	3.136	3.115	0.0210	0.6698%
5	2.619	2.625	0.0060	0.2291%	2.960	2.988	0.0285	0.9630%	3.029	2.979	0.0500	1.6510%
6	2.668	2.612	0.0560	2.0993%	2.982	2.973	0.0090	0.3018%	2.923	2.979	0.0555	1.8987%
7	2.659	2.683	0.0245	0.9216%	2.838	2.839	0.0010	0.0352%	2.929	2.936	0.0070	0.2390%
8	2.857	2.883	0.0260	0.9101%	2.981	2.997	0.0165	0.5536%	3.179	3.150	0.0285	0.8966%
9	2.633	2.619	0.0140	0.5318%	2.954	2.928	0.0265	0.8971%	2.843	2.943	0.1000	3.5174%
10	2.665	2.669	0.0045	0.1689%	2.958	2.923	0.0350	1.1832%	2.943	2.950	0.0070	0.2379%
11	2.617	2.618	0.0015	0.0573%	2926	2.895	0.0315	1.0766%	2.686	2.793	0.1075	4.0030%
12	2.872	2.879	0.0075	0.2612%	2.807	2.837	0.0300	1.0689%	2.929	2.972	0.0430	1.4683%
13	2.963	2.849	0.1135	3.8312%	2.833	2.879	0.0460	1.6061%	2.850	2.886	0.0355	1.2456%
14	2.882	2.778	0.1045	3.6260%	2.819	2.888	0.0685	2.4399%	2.915	2.943	0.0285	0.9779%
15	2.967	2.940	0.0265	0.8933%	2.806	2.832	0.0260	0.9266%	2.779	2.936	0.1570	5.6505%
16	2.944	2.964	0.0205	0.6965%	2.832	2.881	0.0490	1.7305%	2.879	2.986	0.1070	3.7172%

Table 10: FD from Interoperator Reliability Study of the Distal of the Radius.

Subj	0.6-1 (1)	0.6-1 (2)	0.6-1.0 FD Diff	0.6-1 Diff (%)	1.0-1.2 (1)	1.0-1.2 (2)	1.0-1.2 FD Diff	1.0-1.2 Diff (%)	1-1.4 (1)	1-1.4 (2)	1-1.4 FD Diff	1-1.4 Diff (%)	1.2-1.4 (1)	1.2-1.4 (2)	1.2-1.4 FD Diff	1.2-1.4 Diff (%)
1	2.601	2.618	0.017	0.6536	2.697	2.698	0.001	0.0371	2.815	2.823	0.0080	0.2842%	2.801	2.831	0.0305	1.0891%
2	2.614	2.597	0.017	0.6503	2.866	2.871	0.005	0.1745	2.945	2.959	0.0145	0.4925%	2.893	2.878	0.0145	0.5013%
3	2.666	2.652	0.014	0.5251	2.705	2.756	0.051	1.8854	2.820	2.831	0.0105	0.3724%	2.865	2.920	0.0545	1.9023%
4	2.639	2.618	0.021	0.7958	2.627	2.786	0.159	6.0525	2.879	2.865	0.0145	0.5036%	2.899	2.945	0.0455	1.5695%
5	2.675	2.634	0.041	1.5327	2.681	2.864	0.183	6.8258	2.993	3.011	0.0175	0.5847%	3.094	3.067	0.0265	0.8566%
6	2.679	2.634	0.045	1.6797	2.575	2.635	0.060	2.3301	2.799	2.816	0.0165	0.5895%	2.840	2.858	0.0185	0.6515%
7	2.649	2.617	0.032	1.2080	2.674	2.750	0.076	2.8422	2.813	2.843	0.0305	1.0844%	2.866	2.783	0.0825	2.8791%
8	2.651	2.637	0.014	0.5281	2.618	2.613	0.005	0.1910	2.843	2.828	0.0150	0.5276%	2.923	2.939	0.0160	0.5474%
9	2.712	2.682	0.030	1.1062	2.473	2.521	0.048	1.9410	2.785	2.797	0.0125	0.4489%	2.976	2.989	0.0130	0.4369%
10	2.726	2.681	0.045	1.6508	2.471	2.603	0.132	5.3420	2.834	2.878	0.0445	1.5705%	3.088	3.106	0.0180	0.5829%
11	2.666	2.635	0.031	1.1628	2.523	2.556	0.033	1.3080	2.794	2.821	0.0270	0.9665%	2.877	2.954	0.0770	2.6769%
12	2.713	2.735	0.022	0.8109	2.604	2.461	0.143	5.4916	2.820	2.842	0.0225	0.7980%	3.046	3.055	0.0090	0.2955%
13	Subject excluded from the study															
14	2.695	2.691	0.004	0.1484	2.583	2.522	0.061	2.3616	2.790	2.799	0.0085	0.3047%	2.942	2.998	0.0565	1.9208%
15	2.706	2.702	0.004	0.1478	2.445	2.477	0.031	1.2674	2.741	2.757	0.0155	0.5655%	2.981	3.016	0.0355	1.1911%
16	2.723	2.709	0.014	0.5141	2.479	2.432	0.047	1.8959	2.680	2.664	0.0160	0.5970%	2.909	2.888	0.0200	0.6876%

Table 11: Intraoperator Reliability Study of the Proximal Phalange of the Middle Finger.

Subj	1-X	1-Y	1-size	2-X	2-Y	2-size	Loc Diff	Size Diff	% Loc Diff	% Size Diff
1	582	689	32	582	691	31	2.00	1	6.2500%	3.1250%
2	380	342	30	381	344	30	2.24	0	7.4536%	0.0000%
3	402	380	33	402	380	34	0.00	1	0.0000%	3.0303%
4	403	336	30	403	337	30	1.00	0	3.3333%	0.0000%
5	403	402	32	404	401	33	1.41	1	4.4194%	3.125%
6	382	456	33	383	456	33	1.00	0	3.0303%	0.0000%
7	420	448	31	419	448	31	1.00	0	3.2258%	0.0000%
8	309	463	32	310	462	33	1.41	1	4.4194%	3.1250%
9	721	769	32	723	769	32	2.00	0	6.2500%	0.0000%
10	539	429	35	537	427	36	2.83	1	8.0812%	2.8571%
11	554	695	28	555	693	29	2.24	1	7.9860%	3.5714%
12	389	709	35	389	710	36	1.00	1	2.8571%	2.8571%
13	534	841	37	534	842	37	1.00	0	2.7027%	0.0000%
14	762	864	38	761	863	38	1.41	0	3.7216%	0.0000%
15	777	858	39	776	857	39	1.41	0	3.6262%	0.0000%
16	628	841	38	628	839	38	2.00	0	5.2632%	0.0000%

Table 12: Intraoperator Reliability Study of the Distal of Radius.

Subj	1-X	1-Y	1-size	2-X	2-Y	2-size	Loc Diff	Size Diff	% Loc Diff	% Size Diff
1	385	446	65	384	446	66	1.00	1	1.5385%	1.5385%
2	294	205	62	294	206	62	1.00	0	1.6129%	0.0000%
3	266	204	66	267	203	68	1.41	2	2.1427%	3.0303%
4	389	342	68	390	342	66	1.00	2	1.4706%	2.9412%
5	236	330	70	243	329	65	7.07	5	10.102%	7.1429%
6	376	180	70	375	173	69	7.07	1	10.102%	1.4286%
7	240	161	68	237	155	66	6.71	2	9.8650%	2.9412%
8	372	298	68	370	289	69	9.22	1	13.558%	1.4706%
9	383	197	75	383	194	74	3.00	1	4.0000%	1.3333%
10	238	126	80	238	124	79	2.00	1	2.5000%	1.2500%
11	397	443	71	396	440	70	3.16	1	4.4539%	1.4085%
12	256	304	82	262	302	82	6.32	0	7.7129%	0.0000%
13	Subject excluded from the study									
14	379	277	77	377	276	74	2.24	3	2.9040%	3.8961%
15	401	280	78	401	281	81	1.00	3	1.2821%	3.8462%
16	410	257	86	406	265	90	8.94	4	10.400%	4.6512%

Table 13: FD from Intraoperator Reliability Study of the Proximal Phalange of the Middle Finger.

Subj	1-1.2 (1)	1-1.2 (2)	1-1.2 FD Diff	1.0-1.2 Diff (%)	1.2-1.4 (1)	1.2-1.4 (2)	1.2-1.4 FD Diff	1.2-1.4 Diff (%)	1.3-1.4 (1)	1.3-1.4 (2)	1.3-1.4 FD Diff	1.3-1.4 Diff (%)
1	2.645	2.654	0.0095	0.358%	2.940	2.888	0.0510	1.766%	2.950	3.036	0.0855	2.817%
2	2.688	2.707	0.0195	0.720%	2.954	2.999	0.0360	1.204%	3.165	3.057	0.1080	3.517%
3	2.662	2.704	0.0420	1.553%	3.038	2.928	0.1100	3.758%	3.122	2.900	0.2210	7.638%
4	2.667	2.701	0.0345	1.277%	2.996	2.980	0.0150	0.503%	3.136	3.128	0.0070	0.224%
5	2.619	2.662	0.0435	1.634%	2.960	2.952	0.0070	0.237%	3.029	2.857	0.1720	6.003%
6	2.668	2.714	0.0460	1.695%	2.982	2.884	0.0985	3.416%	2.923	2.872	0.0515	1.794%
7	2.659	2.673	0.0140	0.524%	2.838	2.836	0.0015	0.053%	2.929	2.964	0.0360	1.214%
8	2.857	2.898	0.0415	1.432%	2.981	3.024	0.0440	1.455%	3.179	3.079	0.1000	3.248%
9	2.633	2.622	0.0105	0.400%	2.954	2.943	0.0115	0.391%	2.843	2.936	0.0925	3.151%
10	2.665	2.751	0.0865	3.144%	2.958	2.872	0.0860	2.994%	2.943	2.878	0.0645	2.241%
11	2.617	2.728	0.112	4.087%	2926	2.817	0.1090	3.869%	2.686	2.593	0.0925	3.567%
12	2.872	2.874	0.0025	0.070%	2.807	2.908	0.1020	3.507%	2.929	2.971	0.0430	1.447%
13	2.963	2.961	0.0015	0.051%	2.833	2.840	0.0070	0.246%	2.850	2.885	0.0355	1.230%
14	2.882	2.851	0.0310	1.087%	2.819	2.861	0.0420	1.468%	2.915	2.829	0.0860	3.041%
15	2.967	2.989	0.0225	0.753%	2.806	2.791	0.0150	0.537%	2.779	2.793	0.0145	0.519%
16	2.944	2.936	0.0075	0.255%	2.832	2.885	0.0540	1.871%	2.879	3.000	0.122	4.050

Table 14: FD from Intraoperator Reliability Study of the Distal of the Radius.

Subj	0.6-1 (1)	0.6-1 (2)	0.6-1 FD Diff	0.6-1 Diff (%)	1.0-1.2 (1)	1.0-1.2 (2)	1.0-1.2 FD Diff	1.0-1.2 Diff (%)	1-1.4 (1)	1-1.4 (2)	1-1.4 FD Diff	1-1.4 Diff (%)	1.2-1.4 (1)	1.2-1.4 (2)	1.2-1.4 FD Diff	1.2-1.4 Diff (%)
1	2.601	2.639	0.0380	1.4613%	2.697	2.645	0.0525	1.9466%	2.815	2.812	0.0035	0.1245%	2.801	2.831	0.0305	1.0774%
2	2.614	2.614	0.0000	0.0000%	2.866	2.855	0.0110	0.3839%	2.945	2.947	0.0020	0.0679%	2.893	2.878	0.0145	0.5038%
3	2.666	2.671	0.0050	0.1876%	2.705	2.736	0.0310	1.1460%	2.820	2.819	0.0014	0.0532%	2.865	2.920	0.0545	1.8668%
4	2.639	2.619	0.0195	0.7391%	2.627	2.661	0.0340	1.2943%	2.879	2.894	0.0145	0.5011%	2.899	2.945	0.0455	1.5453%
5	2.675	2.615	0.0595	2.2247%	2.681	2.814	0.1330	4.9618%	2.993	3.002	0.0090	0.2998%	3.094	3.067	0.0265	0.8640%
6	2.679	2.675	0.0045	0.1680%	2.575	2.580	0.0050	0.1942%	2.799	2.802	0.0030	0.1071%	2.840	2.858	0.0185	0.6473%
7	2.649	2.656	0.0065	0.2454%	2.674	2.682	0.0080	0.2992%	2.813	2.811	0.0015	0.0534%	2.866	2.783	0.0825	2.9644%
8	2.651	2.647	0.0040	0.1509%	2.618	2.550	0.0685	2.6165%	2.843	2.825	0.0180	0.6372%	2.923	2.939	0.0160	0.5444%
9	2.712	2.690	0.0225	0.8297%	2.473	2.486	0.0135	0.5460%	2.785	2.793	0.0085	0.3043%	2.976	2.989	0.0130	0.4350%
10	2.726	2.712	0.0135	0.4953%	2.471	2.507	0.0360	1.4569%	2.834	2.833	0.0010	0.0353%	3.088	3.106	0.0180	0.5795%
11	2.666	2.657	0.0090	0.3377%	2.523	2.525	0.0025	0.0991%	2.794	2.825	0.0315	1.1150%	2.877	2.954	0.0770	2.6071%
12	2.713	2.726	0.0130	0.4792%	2.604	2.554	0.0505	1.9393%	2.820	2.811	0.0085	0.3024%	3.046	3.055	0.0090	0.2946%
13	Subject excluded from the study															
14	2.695	2.682	0.0125	0.4639%	2.583	2.581	0.0020	0.0774%	2.790	2.828	0.0375	1.3263%	2.942	2.998	0.0565	1.8846%
15	2.706	2.705	0.0010	0.0370%	2.445	2.461	0.0155	0.6338%	2.741	2.734	0.0075	0.2744%	2.981	3.016	0.0355	1.1771%
16	2.723	2.699	0.0245	0.8998%	2.479	2.506	0.0270	1.0891%	2.680	2.690	0.0100	0.3718%	2.909	2.888	0.0200	0.6924%

Figure 1a: Frequency Ranges Used for the Middle Finger

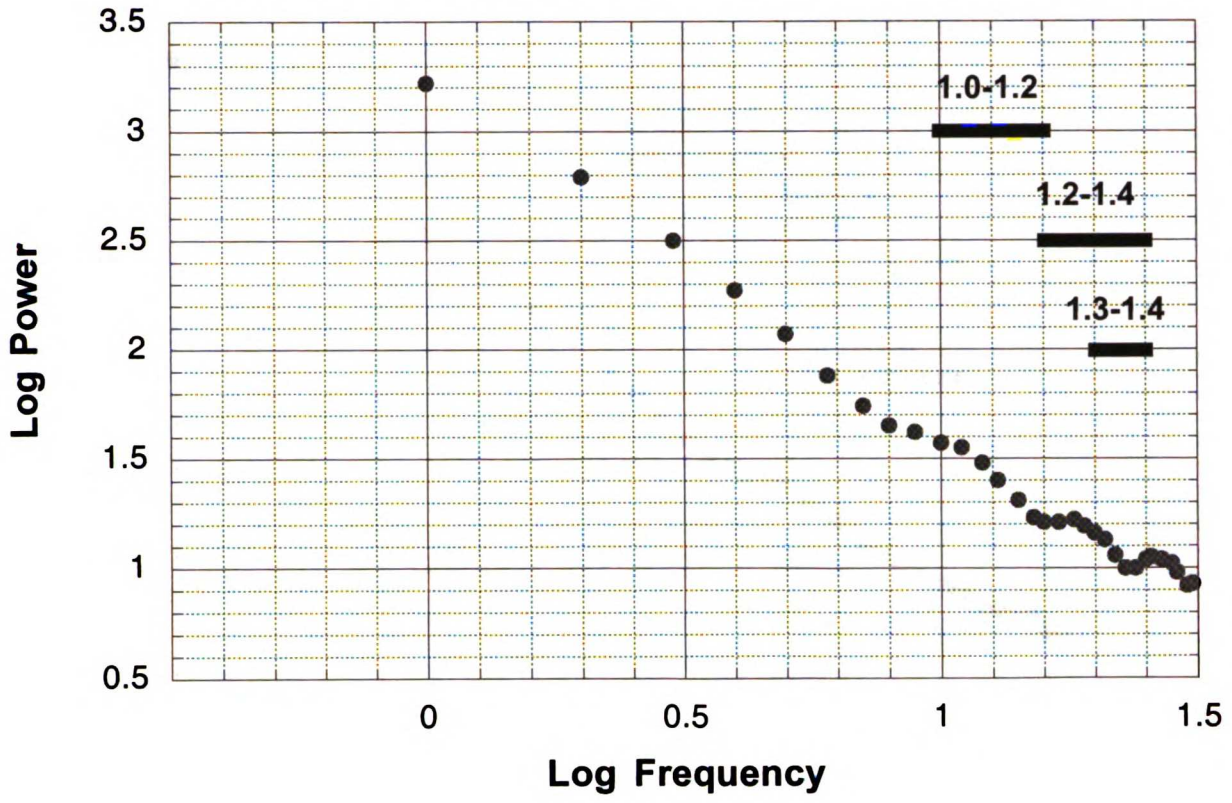

Figure 1b:Frequency Ranged Used for the Distal of Radius

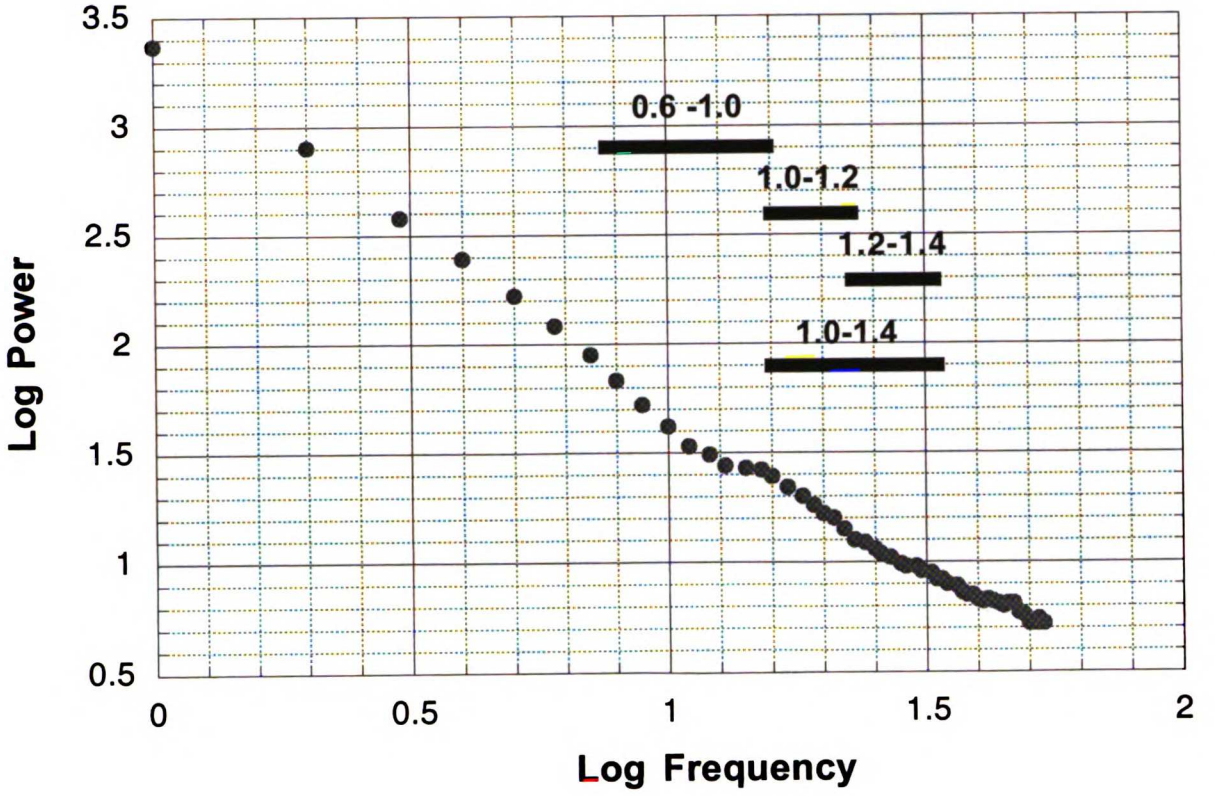

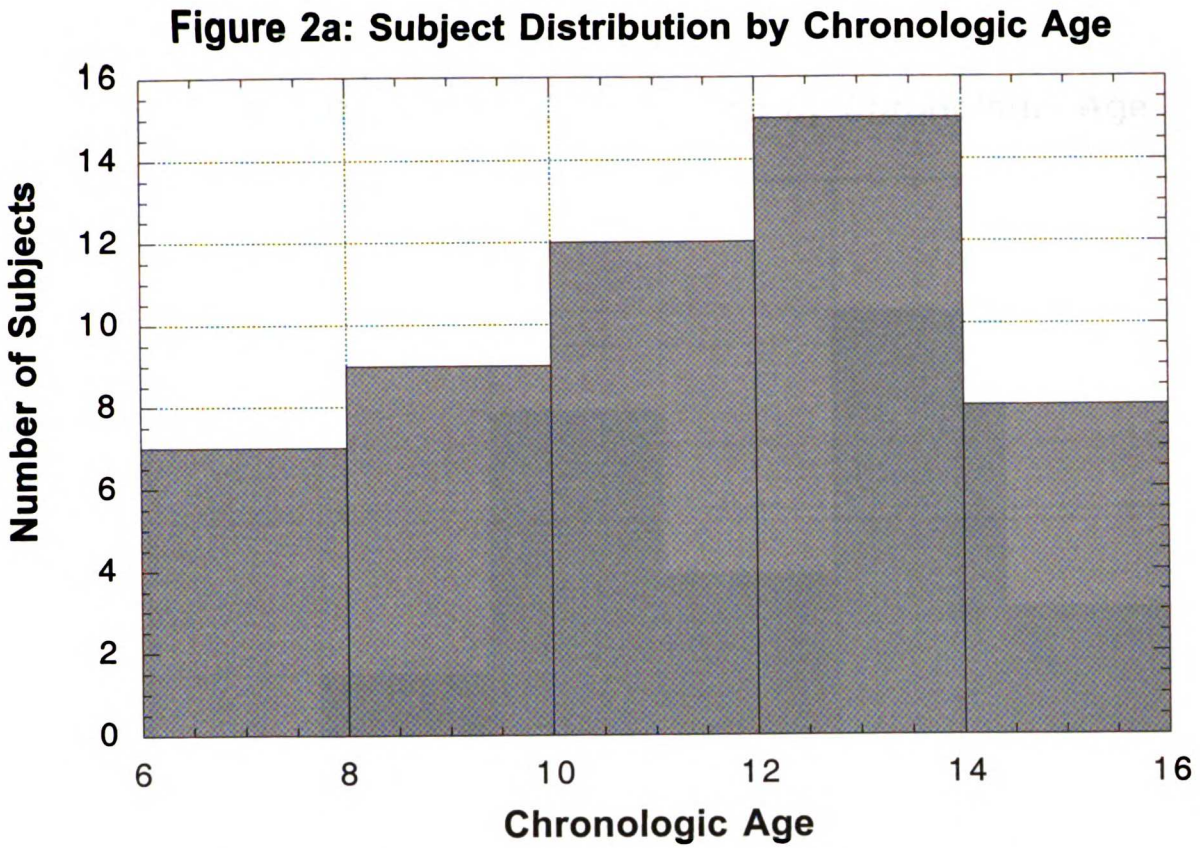

Figure 1: Subject distribution by chronologic age, skeletal age, and Tanner maturation index (breast development)

Figure 2b: Subject Composition by Chronologic Age

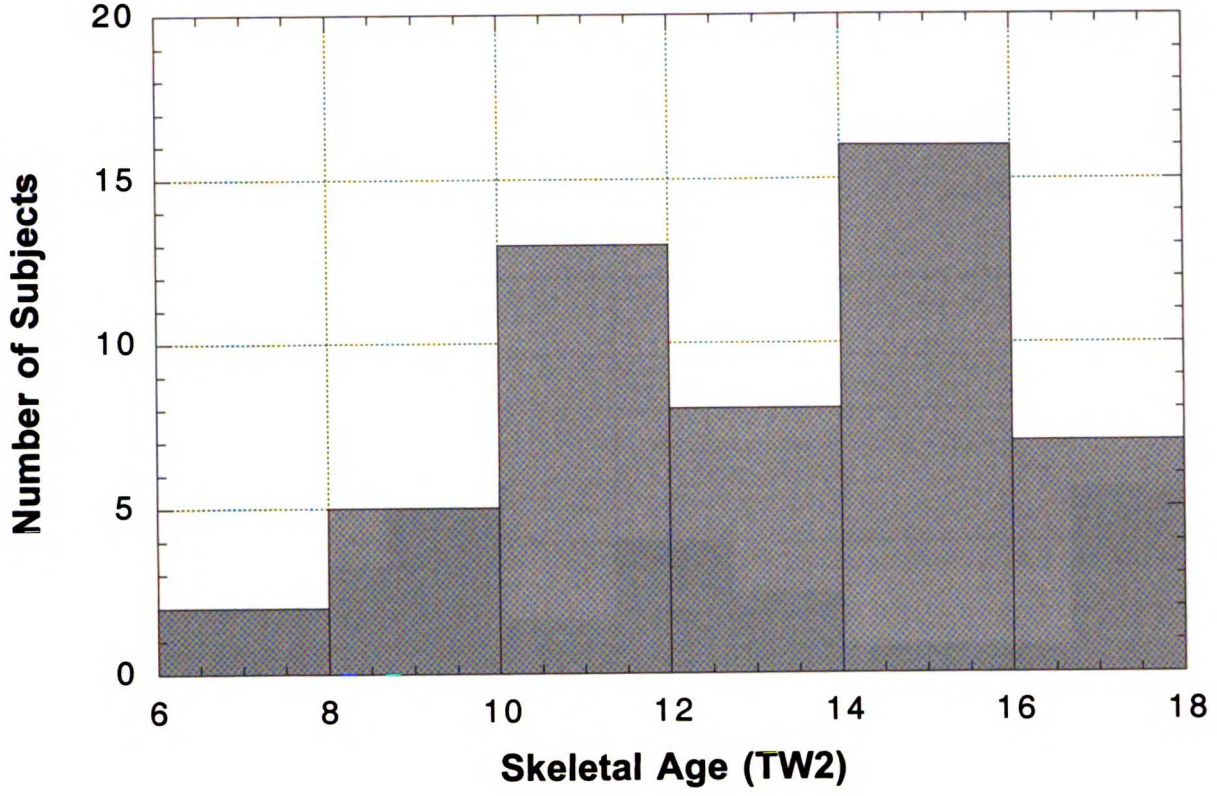

Figure 2c: Subject Composition by Tanner Stage

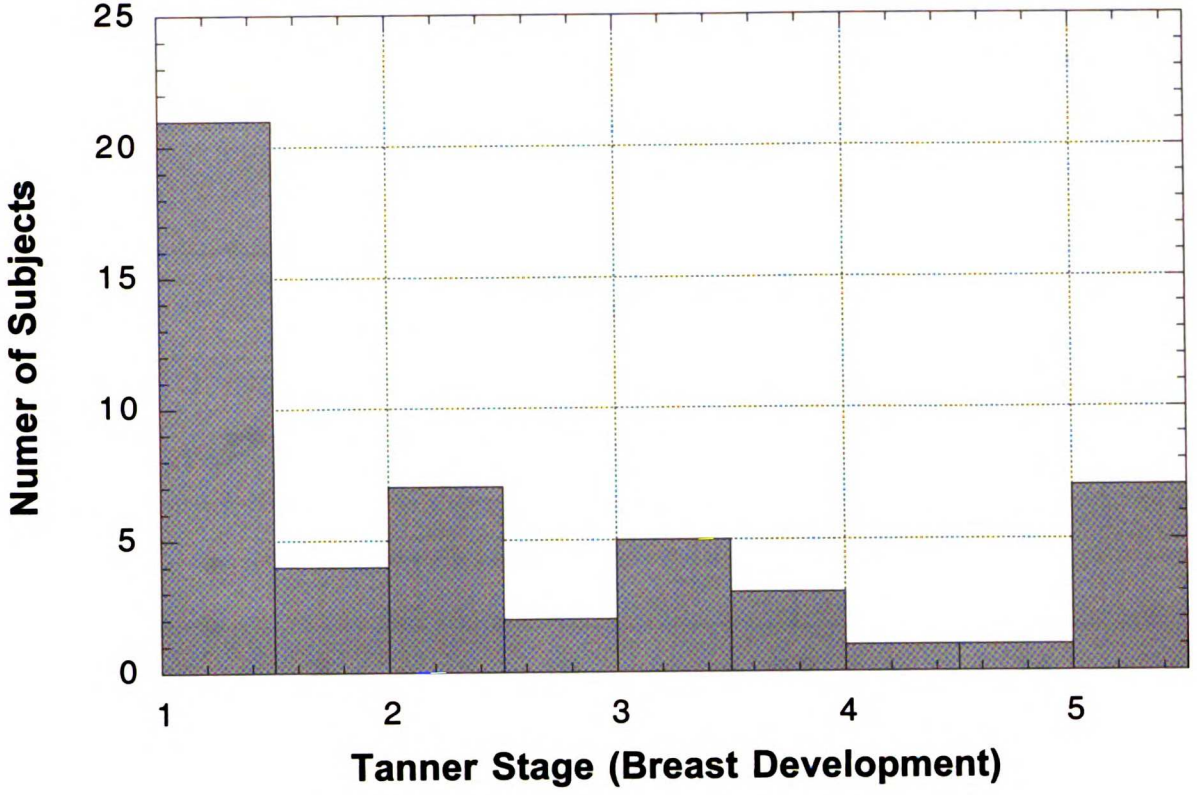

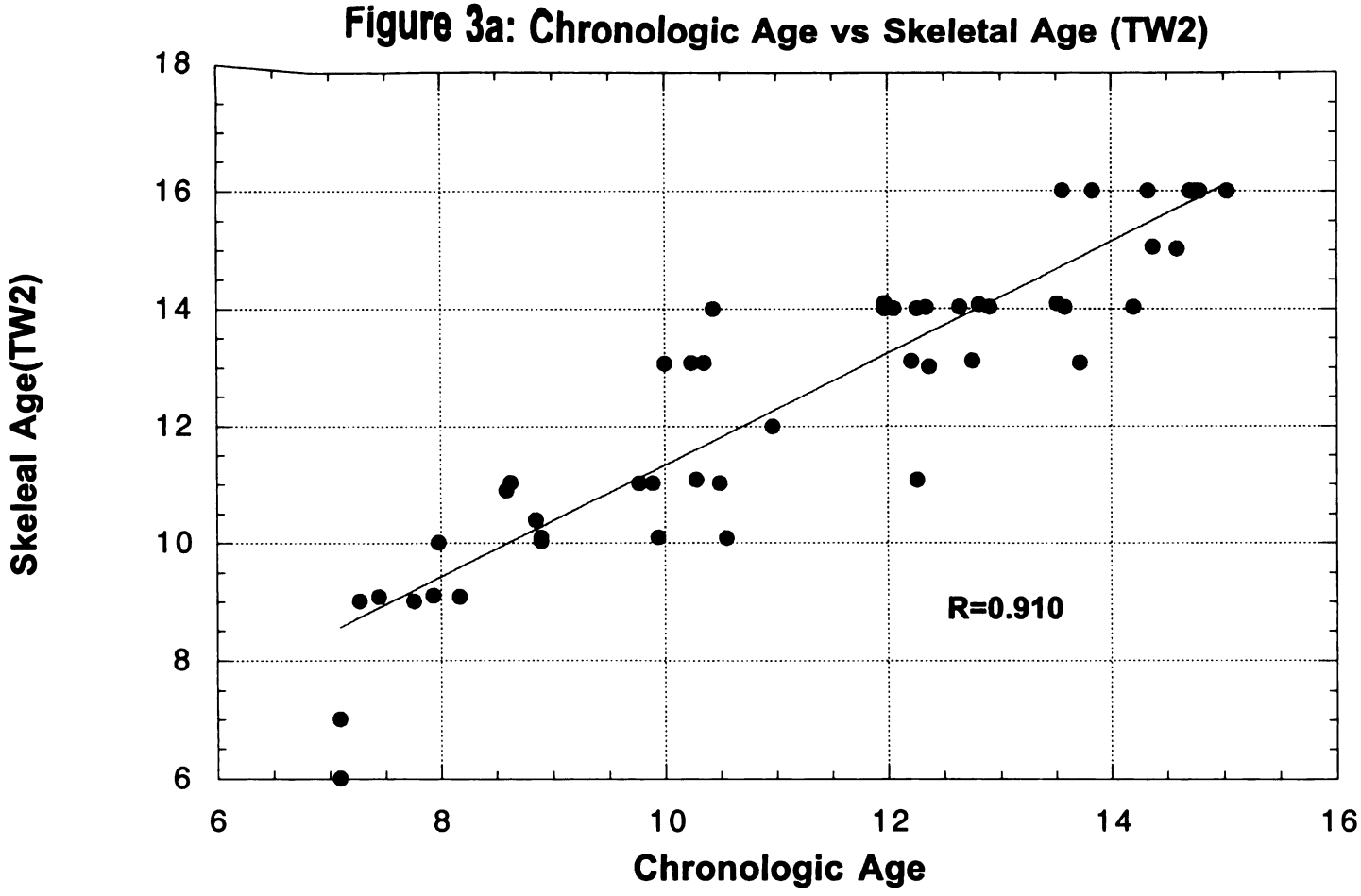

Figure 3: Correlations between chronologic age, skeletal age (TW2), and Tanner maturation index (breast development)

Figure 3b: Chronologic Age vs Tanner Maturation Index (Breast)

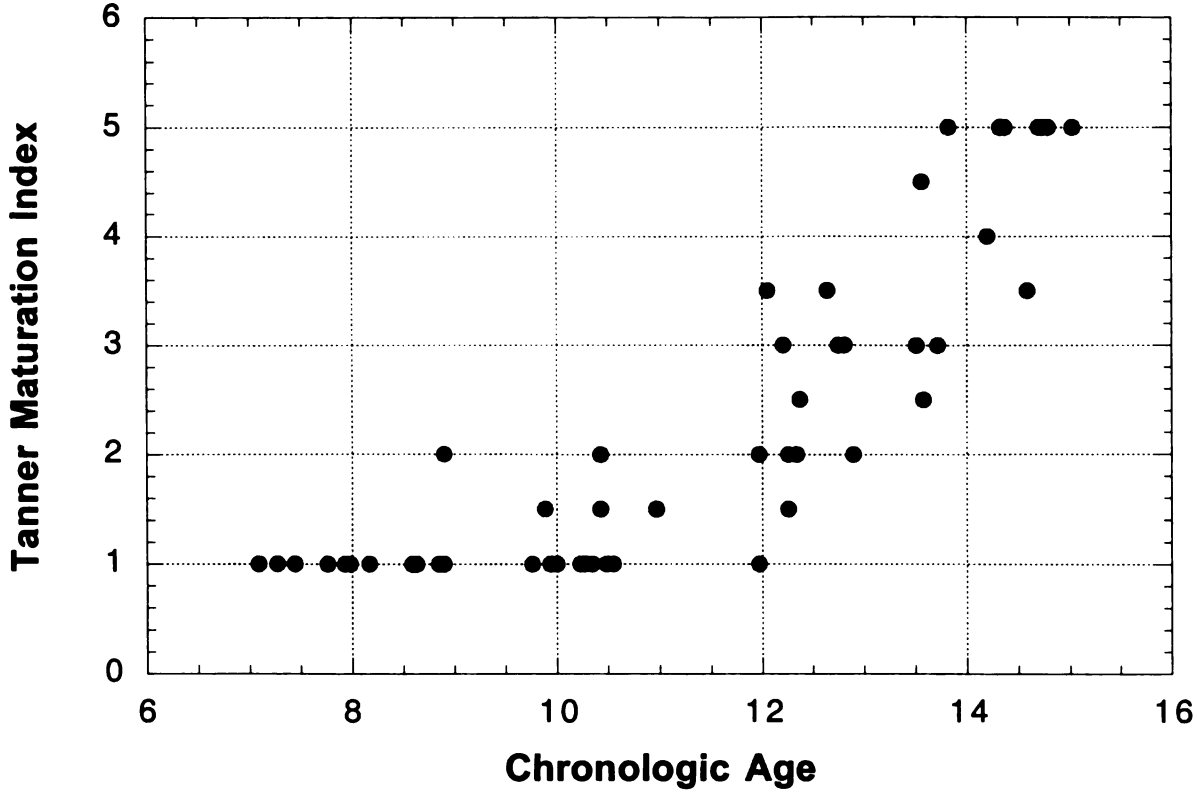

Figure 3c: Skeletal Age (TW2) vs Tanner Maturation Index (Breast)

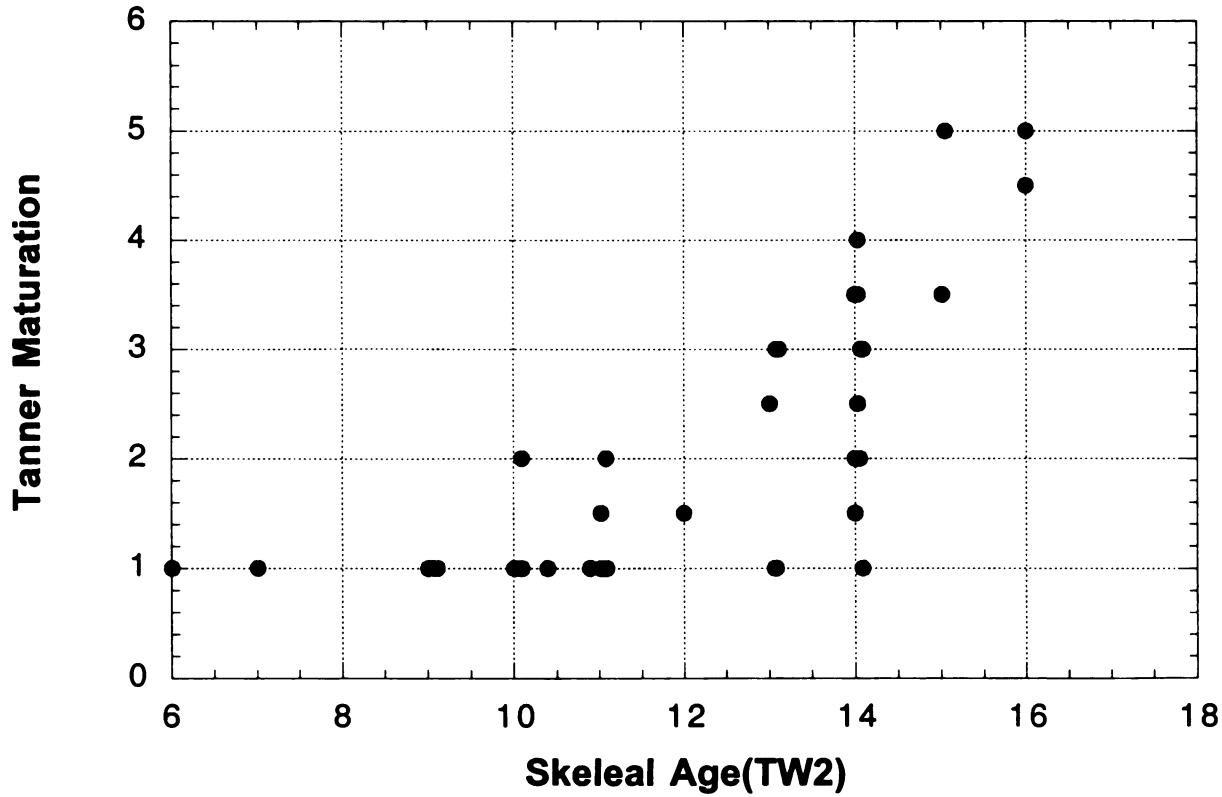

Figure 4a: Chronologic Age vs FD (Freq 1.0-1.2) - Middle Finger

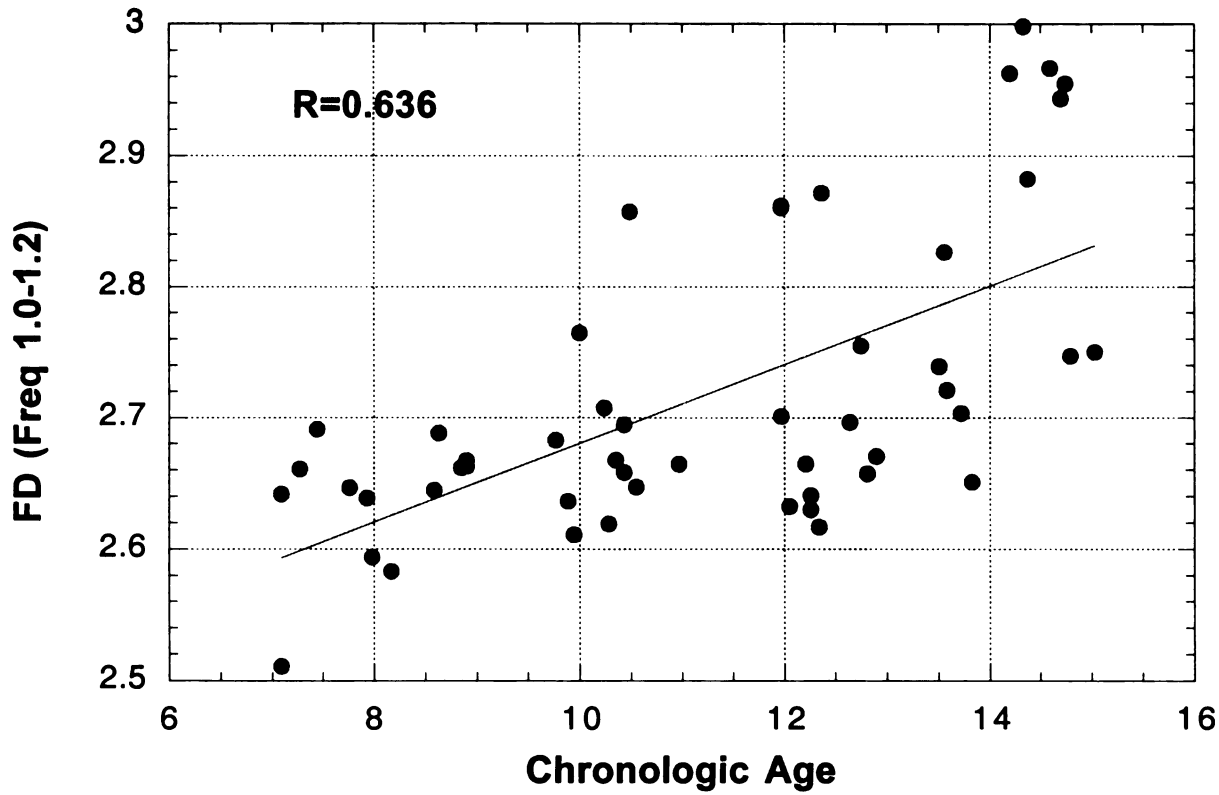

Figure 4: Correlations between chronologic age and the fractal dimension of each of the three frequency ranges for the middle finger.

Figure 4b: Chronologic Age vs FD (Freq 1.2-1.4) - Middle Finger

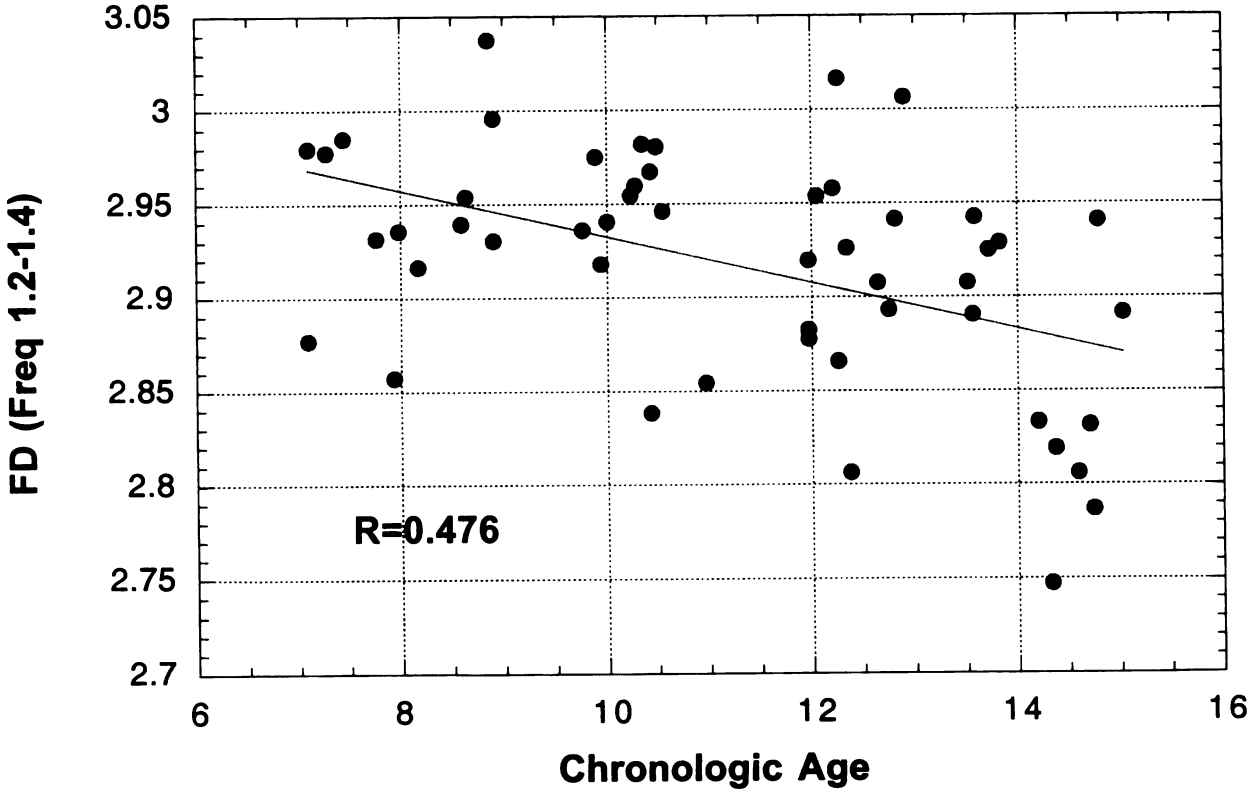

Figure 4c: Chronologic Age vs FD (Freq 1.3-1.4) - Middle Finger

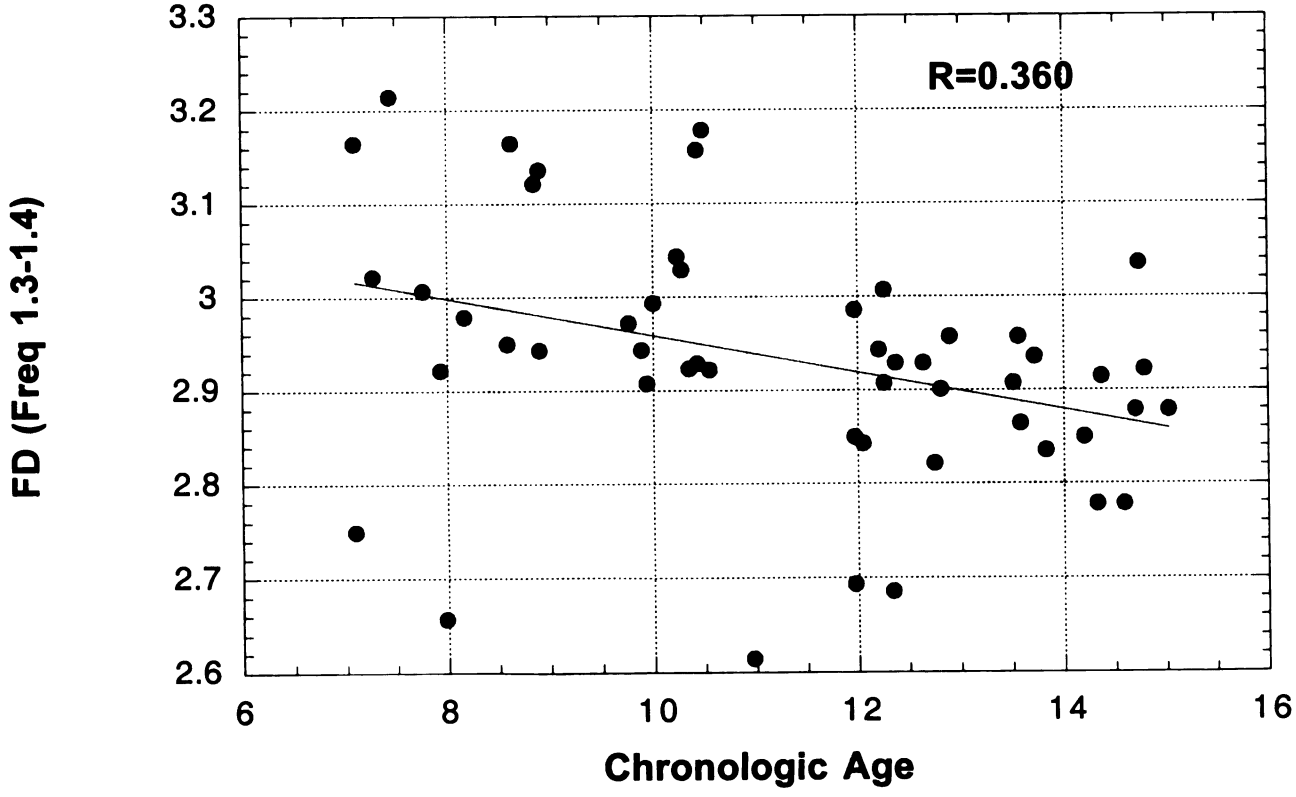

Figure 5a: Tanner Maturation Index vs FD (Freq 1-1.2) - Middle Finger

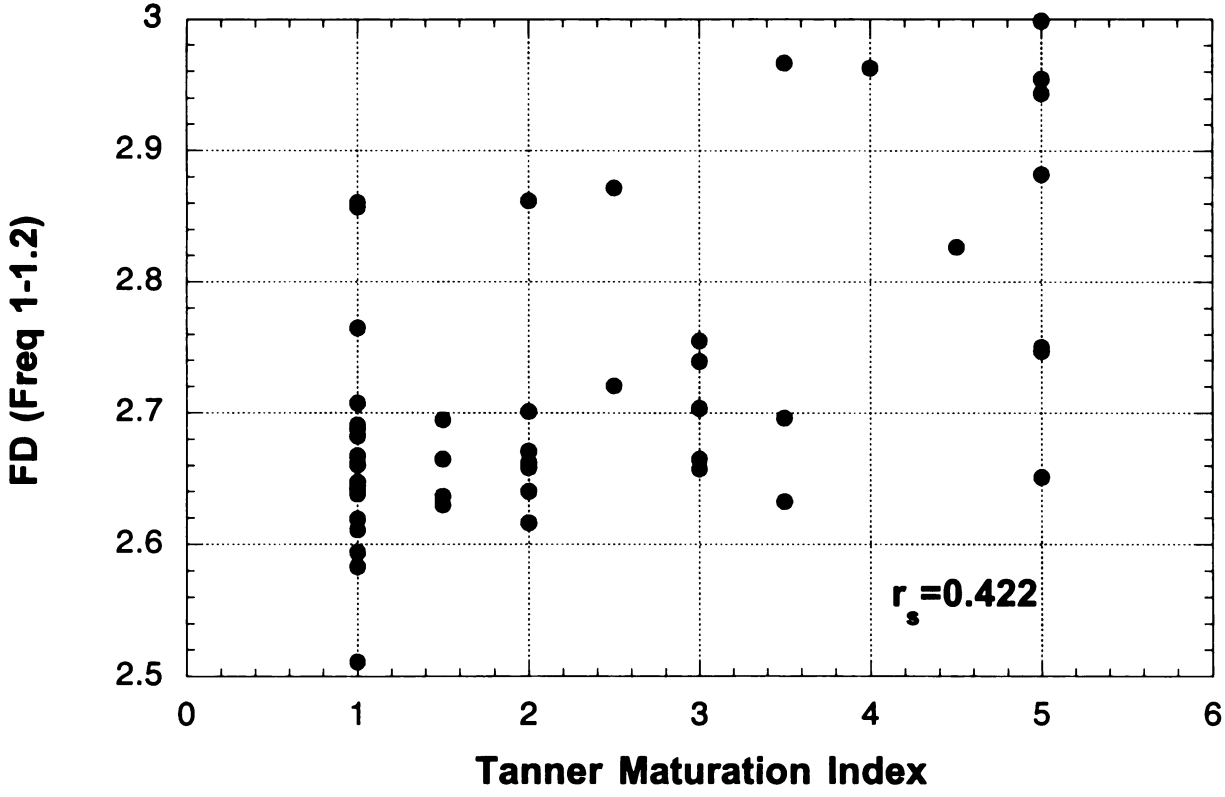

Figure 5: Correlation between Tanner Maturation Index and FD of each of the three frequency ranges for the middle finger

Figure 5b: Tanner Maturation Index vs FD (Freq 1.2-1.4) - Middle Finger

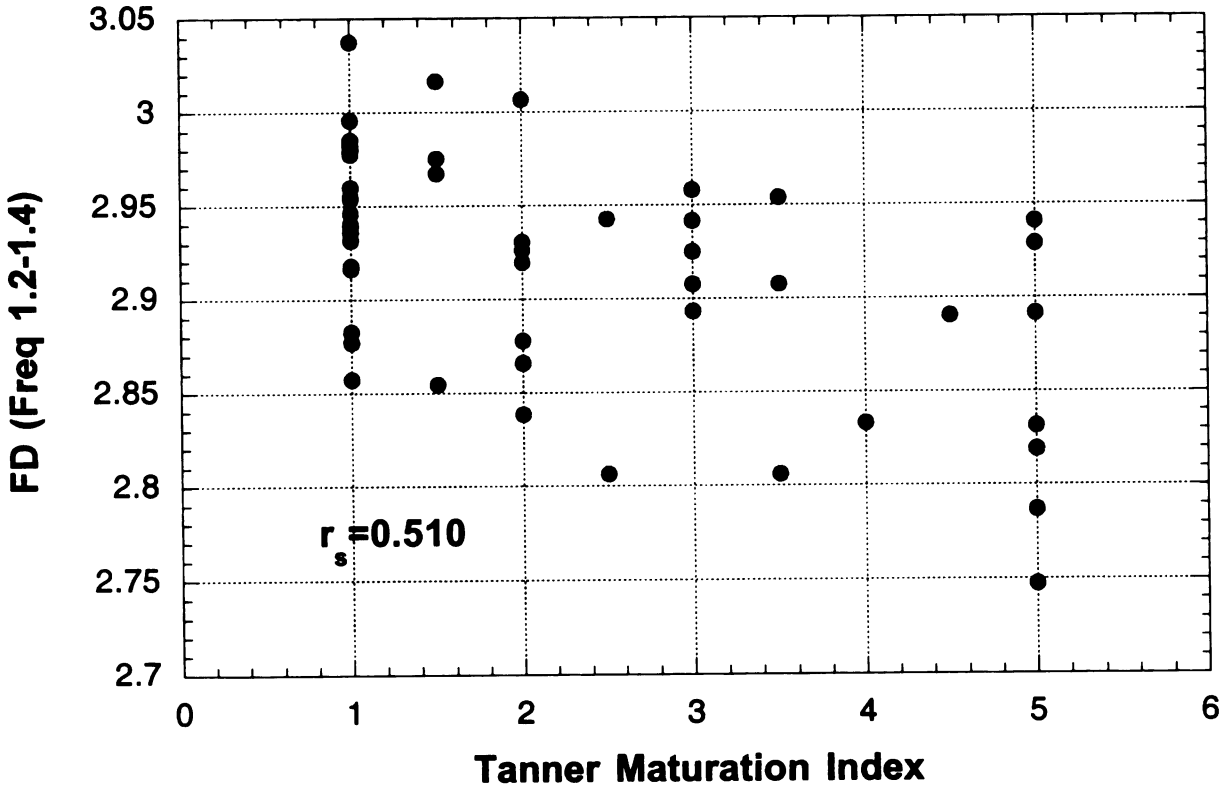

Figure 5c: Tanner Maturation Index vs FD (Freq 1.3-1.4) - Middle Finger

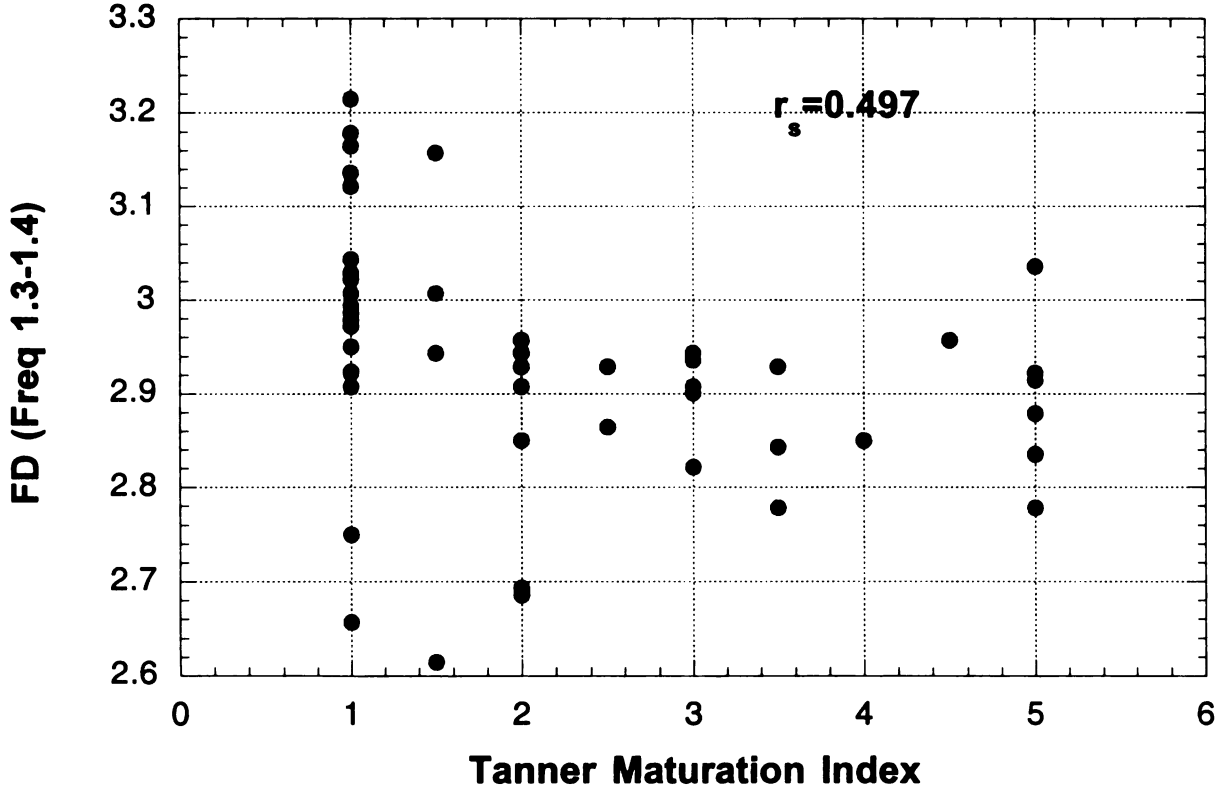

Figure 6a: Skeletal Age (TW2) vs FD (Freq 1-1.2) - Middle Finger

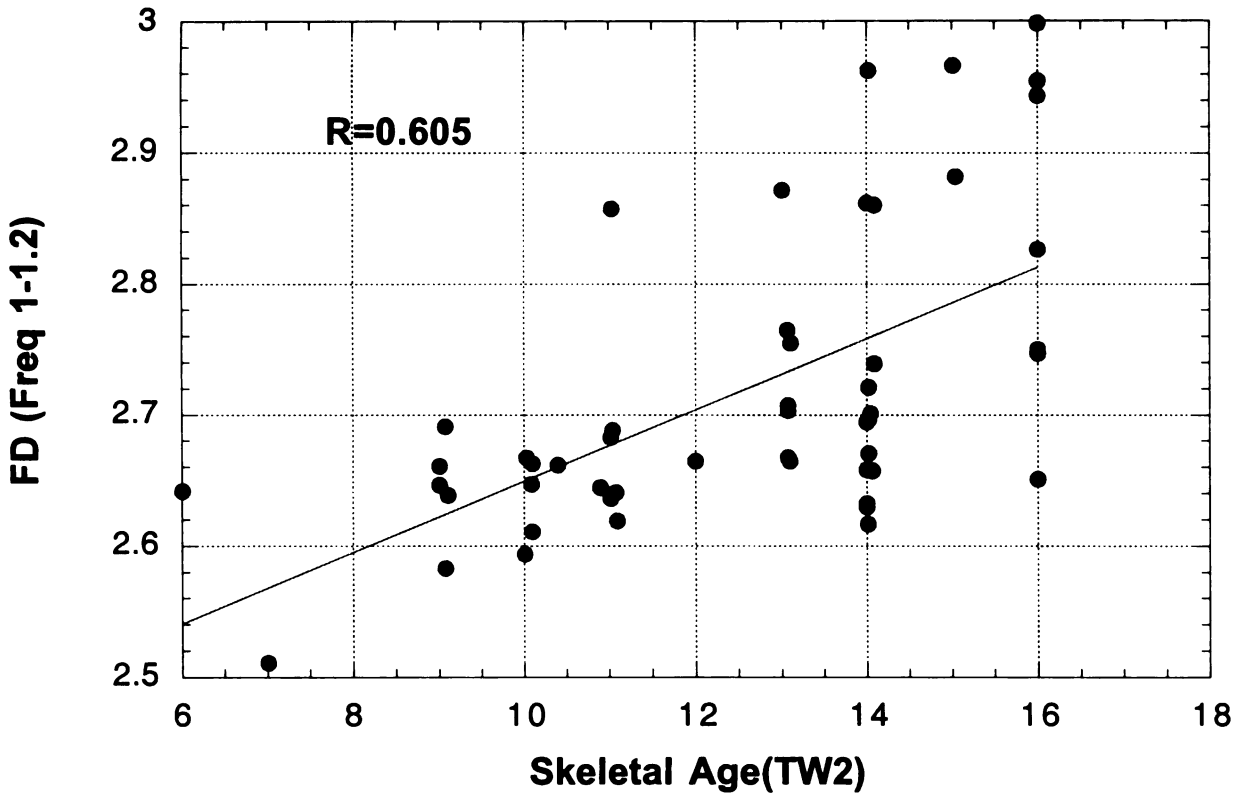

Figure 6: Correlation between skeletal age and FD of each of the three frequency ranges for the middle finger.

Figure 6b: Skeletal Age (TW2) vs FD (Freq 1.2-1.4) - Middle Finger

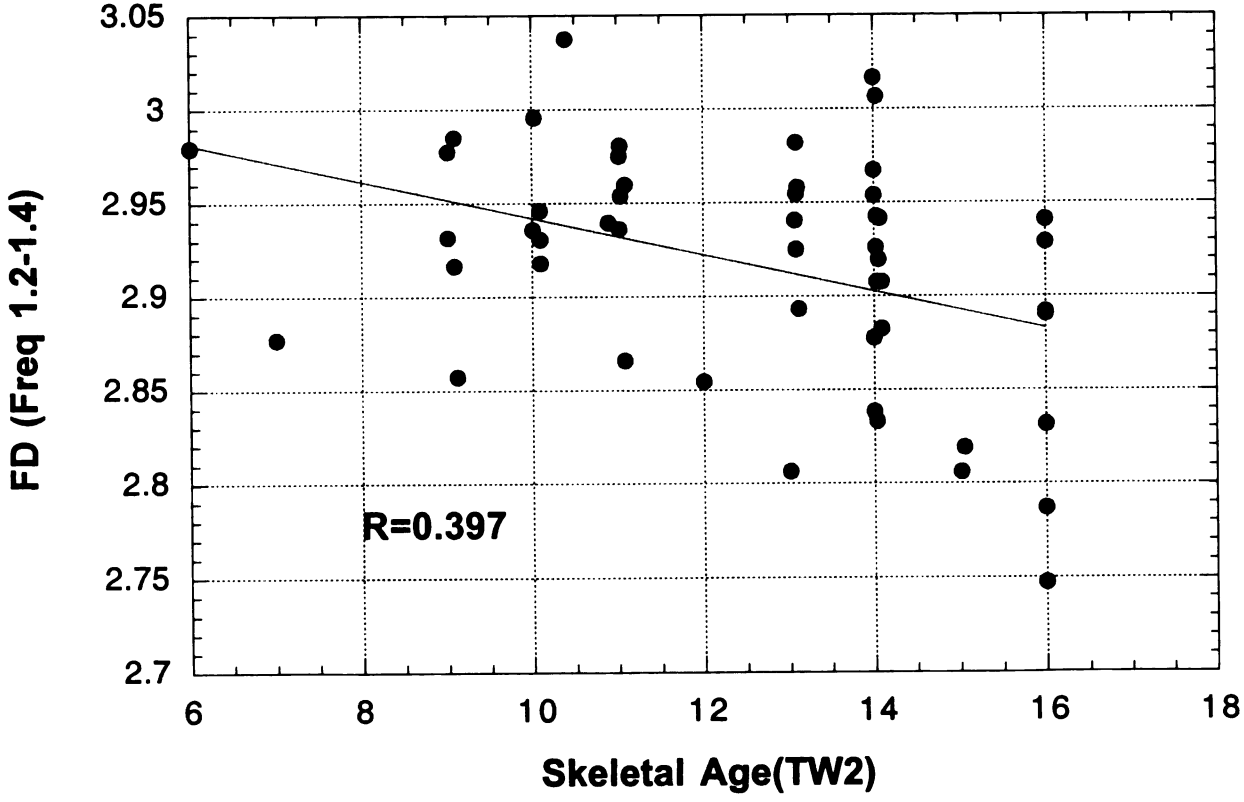

Figure 6c: Skeletal Age (TW2) vs FD (1.3-1.4) - Middle Finger

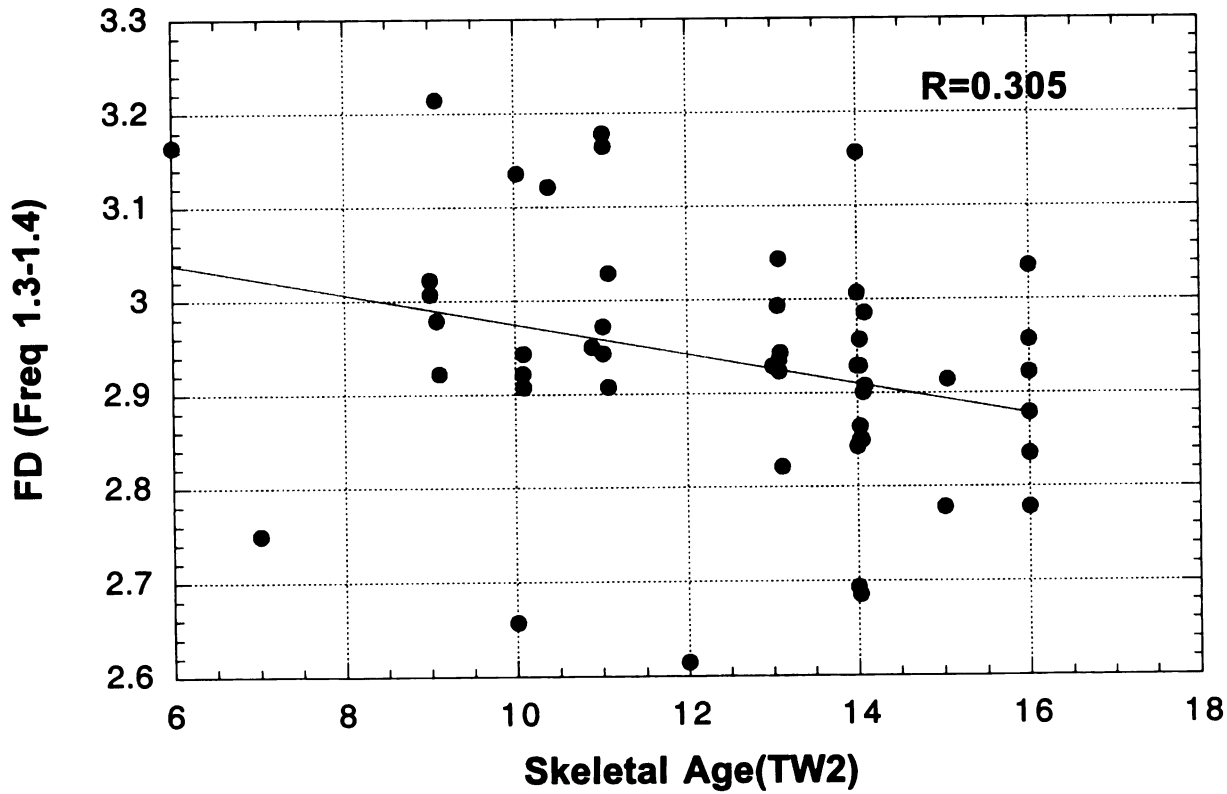

Figure 7a: Chronologic Age vs FD (Freq 0.6-1.0) - Distal of Radius

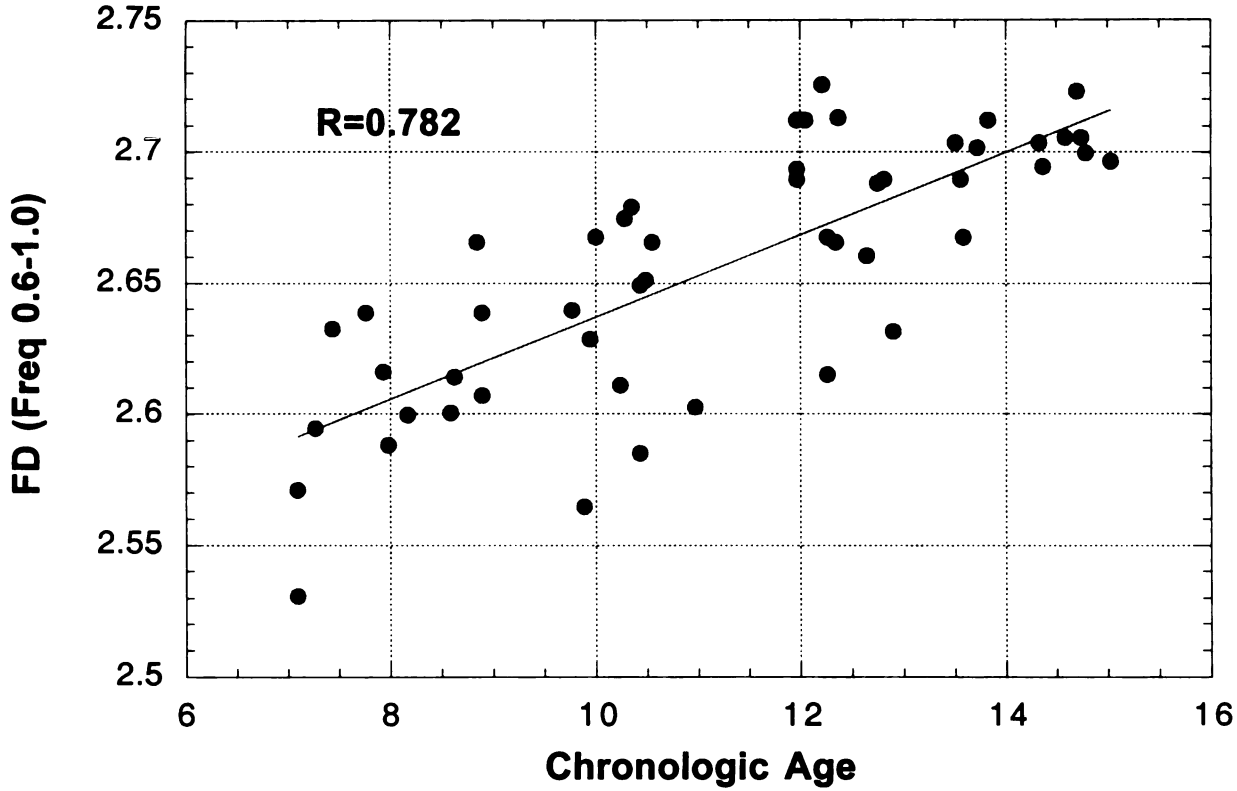

Figure 7: Correlations between chronologic age and FD of each of the four frequency ranges for the distal of radius.

Figure 7b: Chronologic Age vs FD (Freq 1-1.2) - Distal of Radius

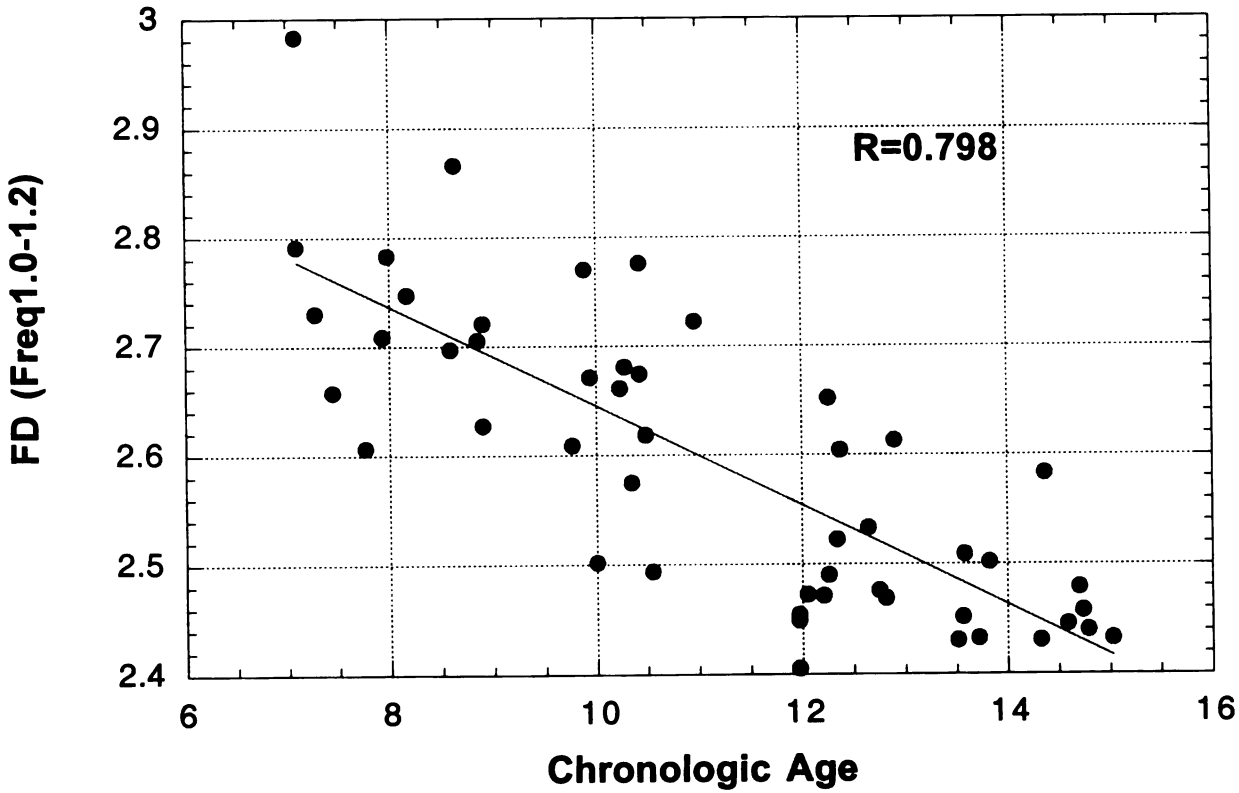

Figure 7c: Chronologic Age vs FD (Freq 1-1.4) - Distal of Radius

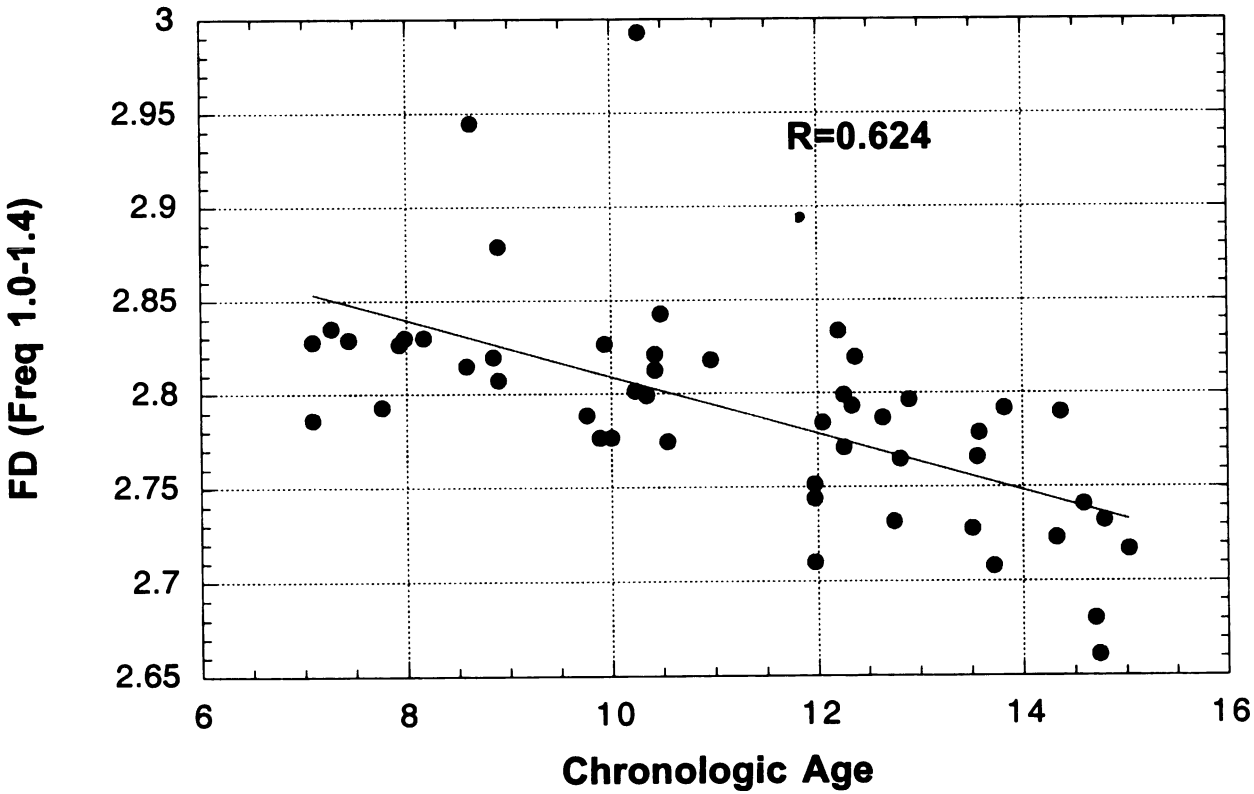

Figure 7d: Chronologic Age vs FD (1.2-1.4) - Distal of Radius

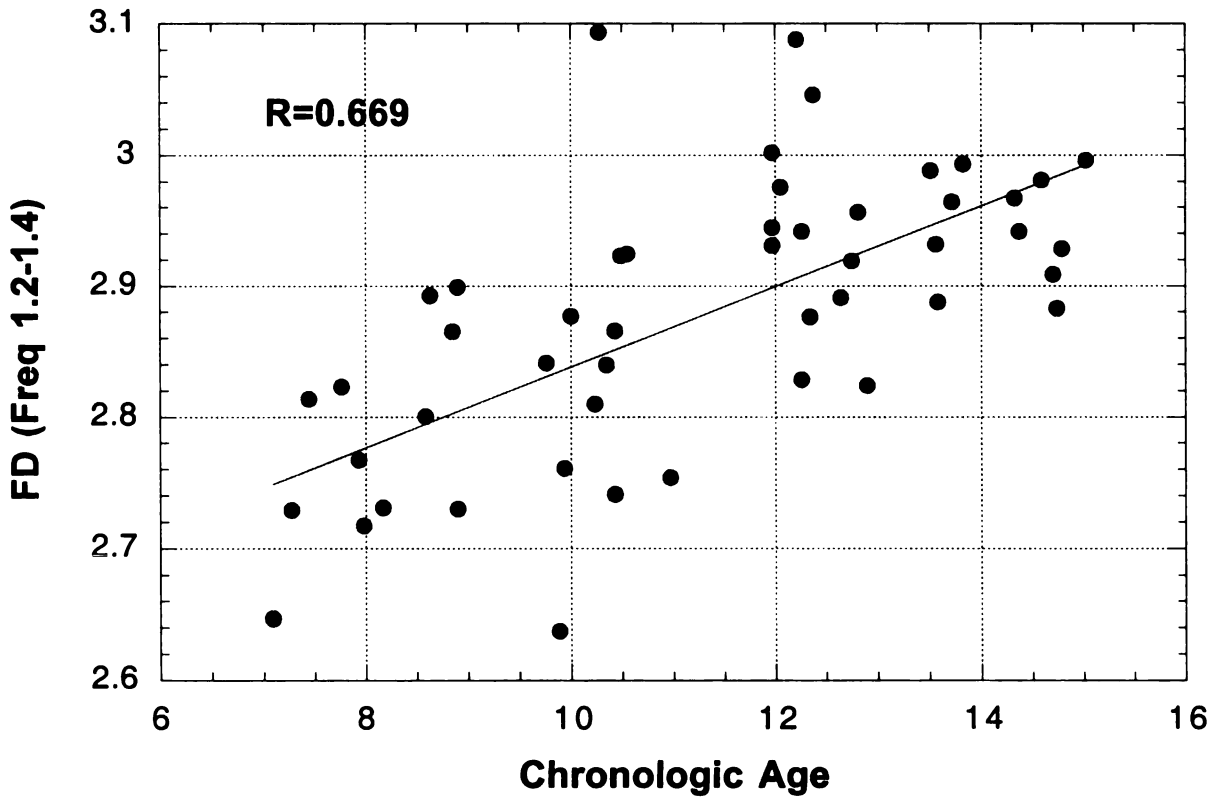

Figure 8a: Tanner Maturation Index vs FD (0.6-1.0) - Distal of Radius

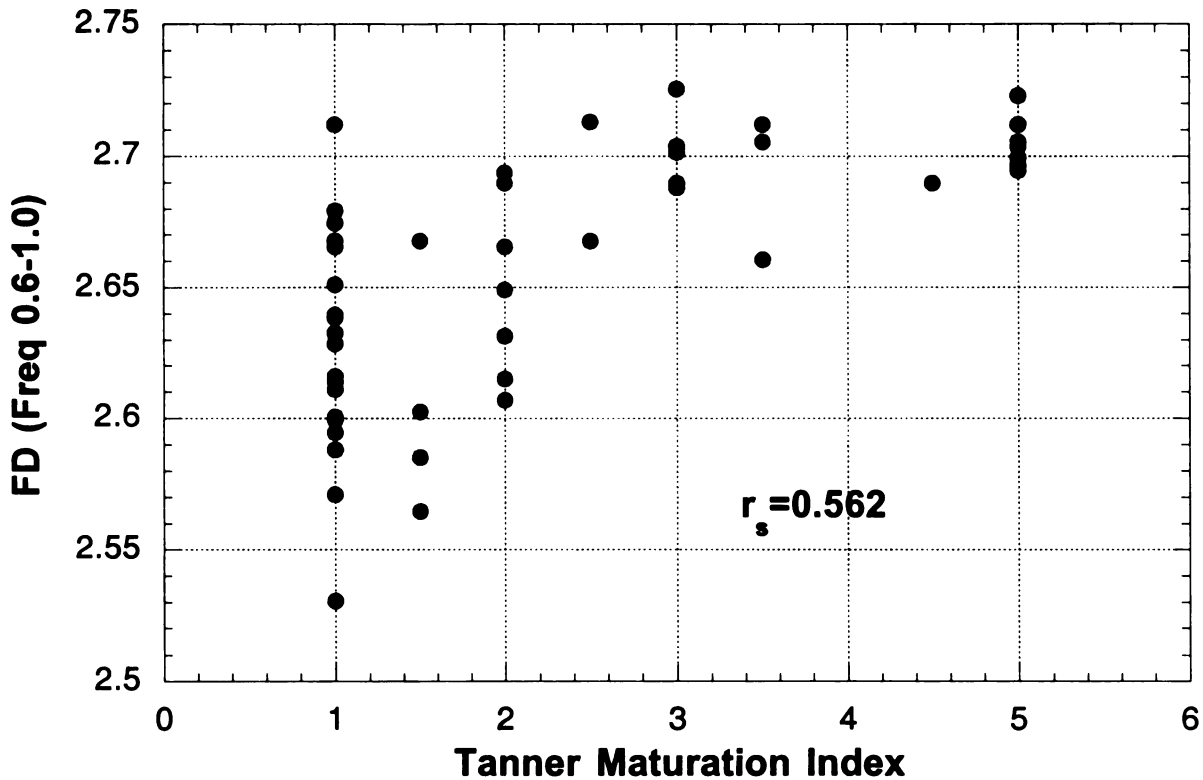

Figure 8: Correlations between Tanner Maturation Index and FD of each of the four frequency ranges for the distal of radius.

Figure 8b: Tanner Maturation Index vs FD (Freq1.0-1.2) - Distal of Radius

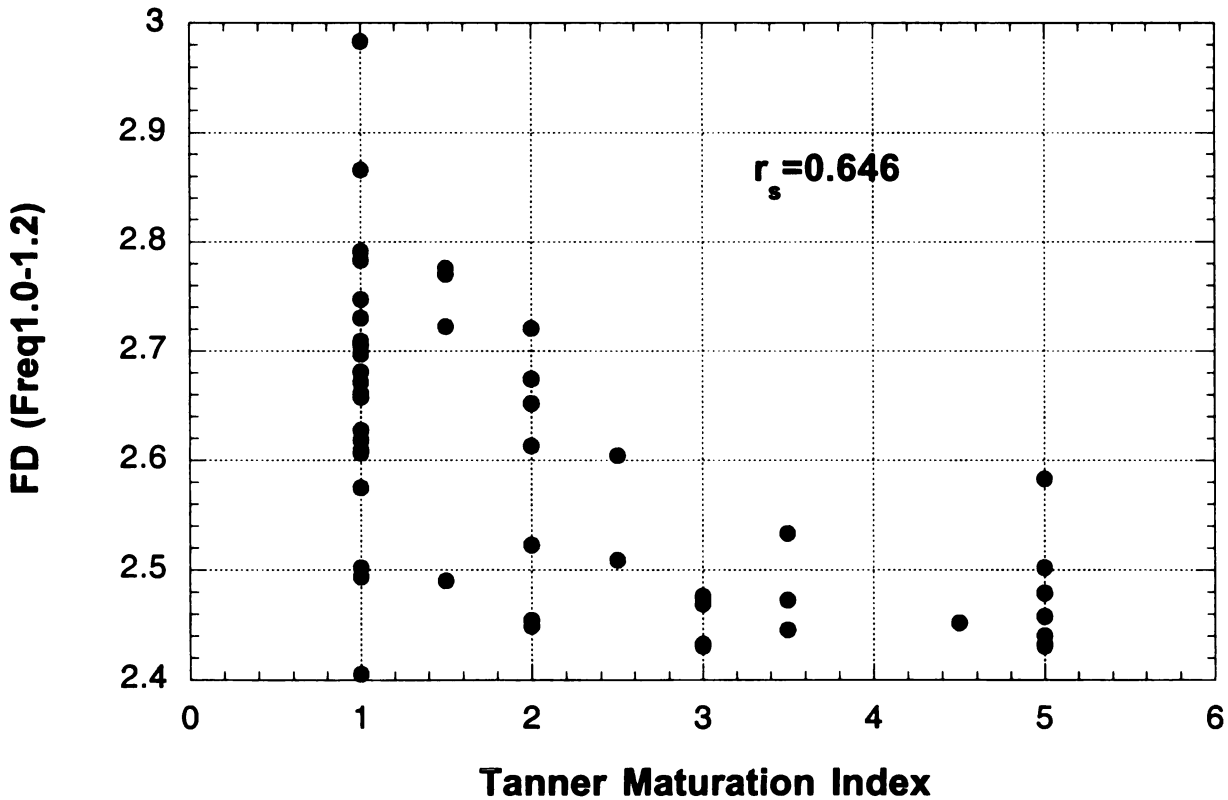

Figure 8c: Tanner Maturation Index vs FD (Freq 1.0-1.4) - Distal of Radius

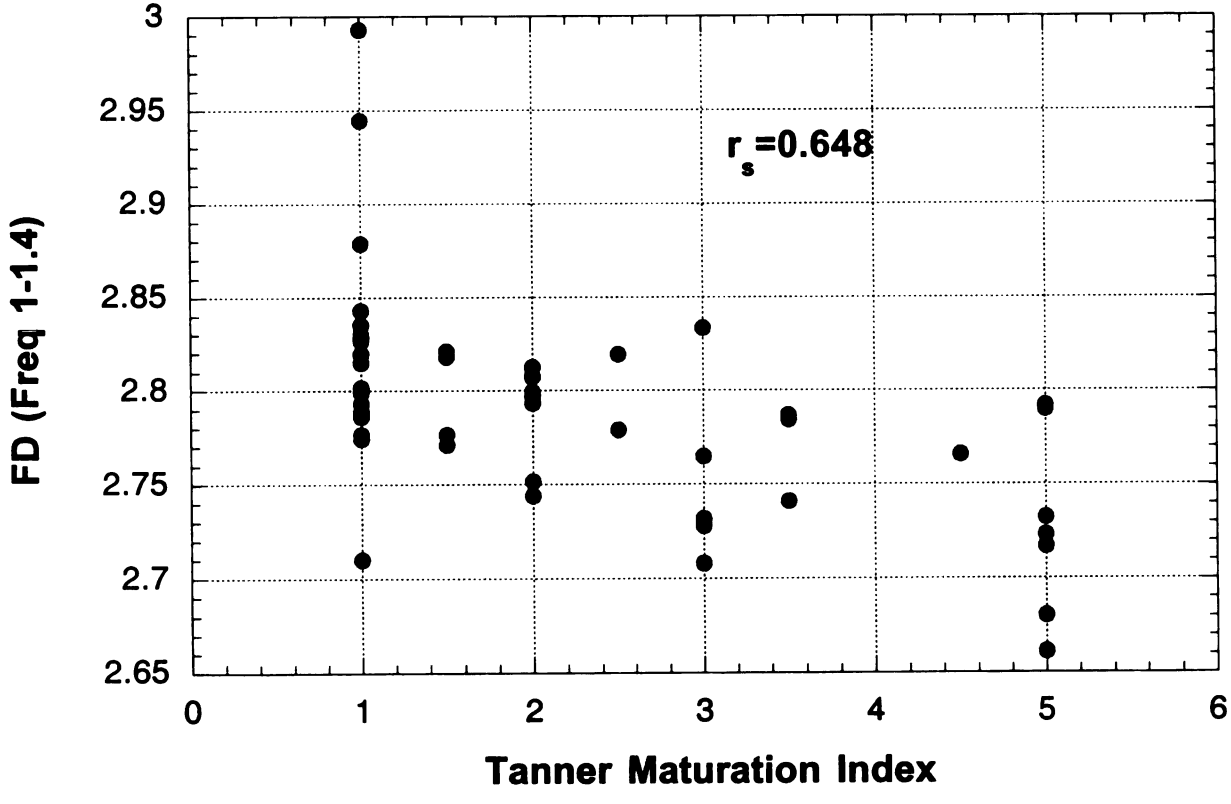

Figure 8d: Tanner Maturation Index vs FD(Freq 1.2-1.4) - Distal of Radius

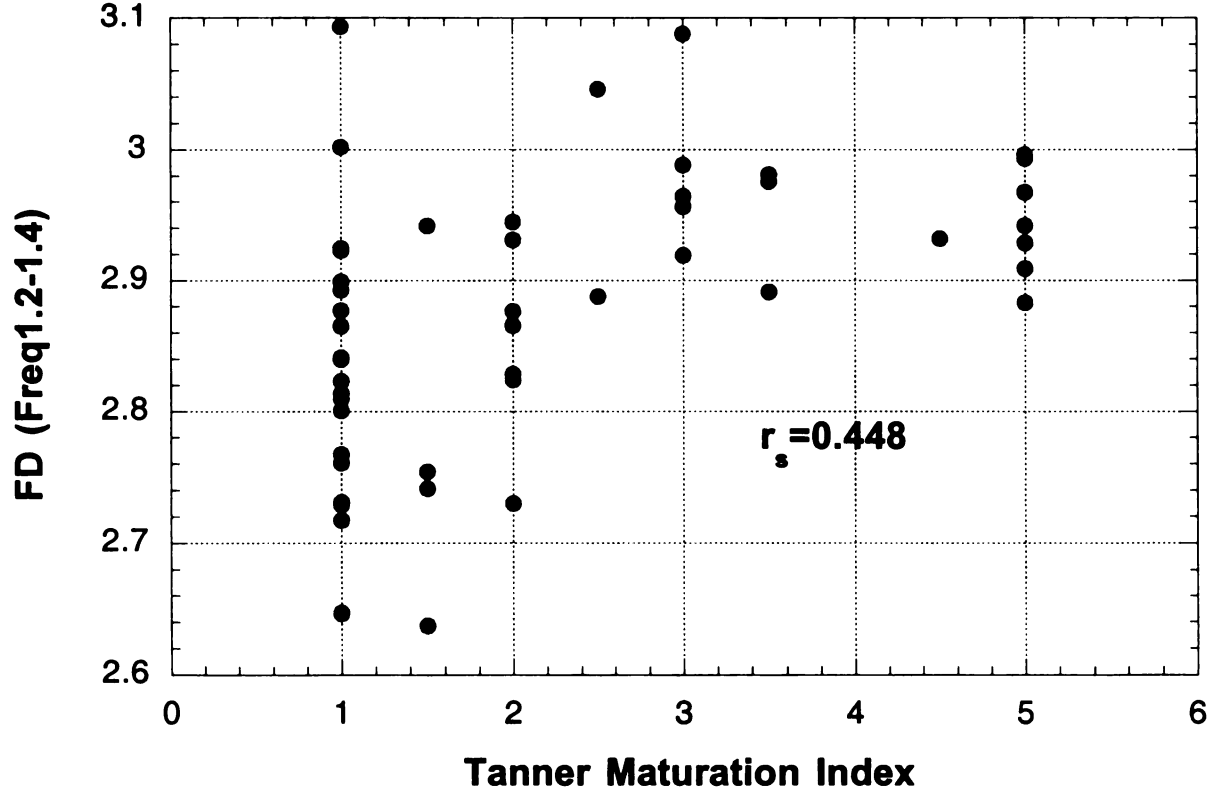

Figure 9a: Skeletal Age vs FD (Freq 0.6-1.0) - Distal of Radius

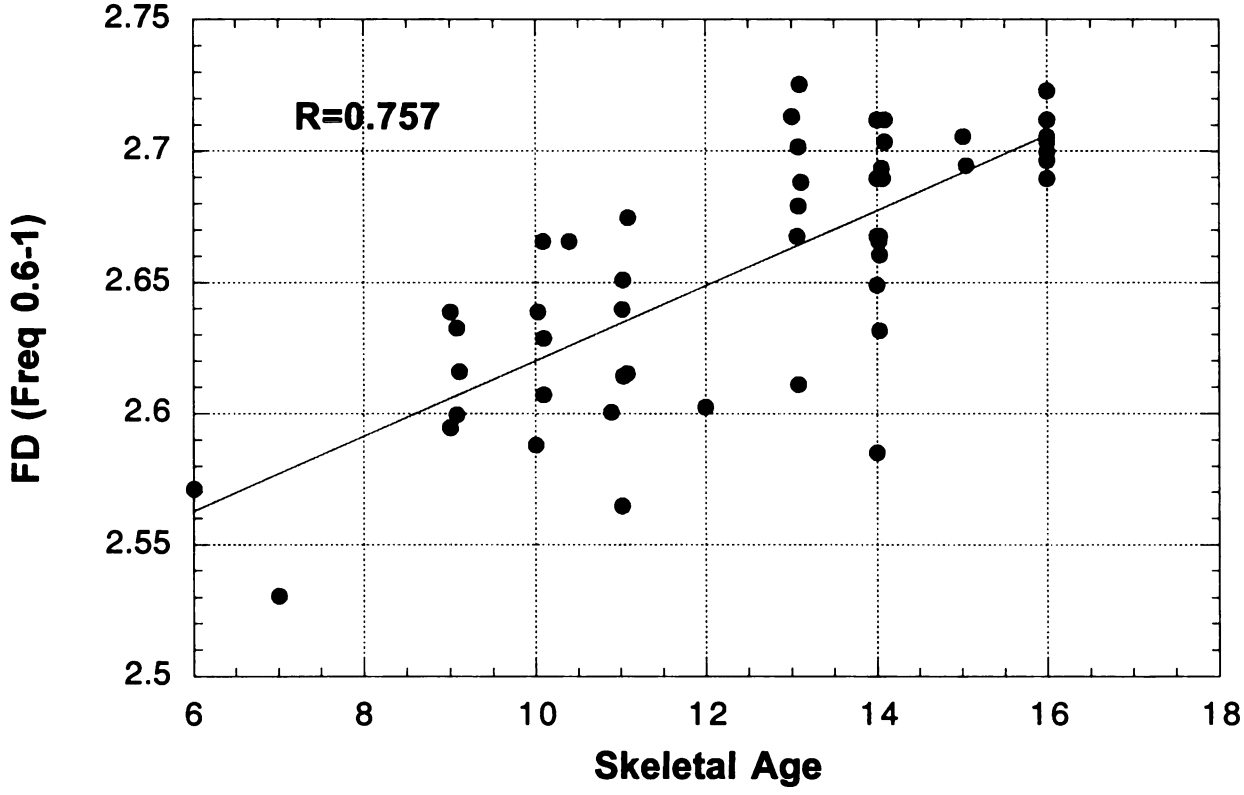

Figure 9: Correlations between Skeletal Age and FD of each of the four frequency ranges for the distal of radius.

Figure 9b: Skeletal Age vs FD (Freq 1.0-1.2) - Distal of Radius

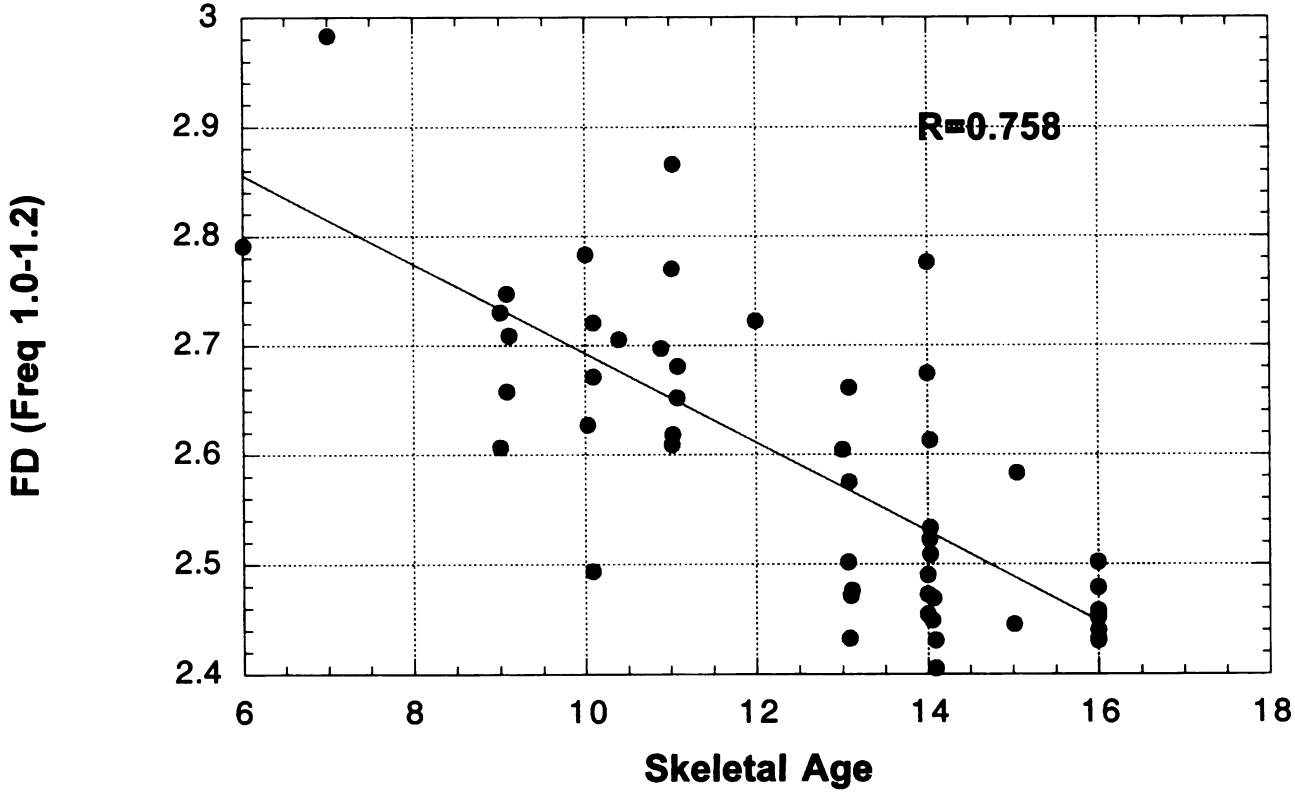

Figure 9c: Skeletal Age vs FD (Freq 1.0-1.4) - Distal of Radius

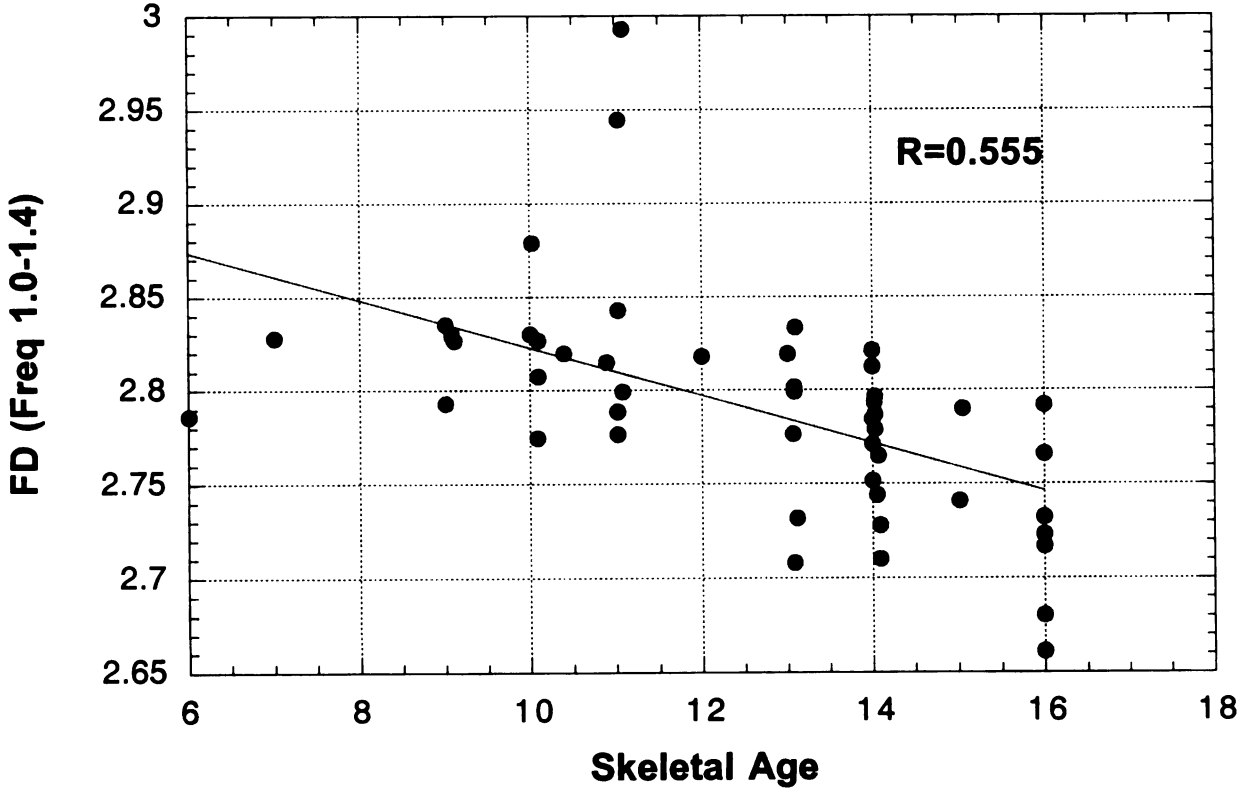

Figure 9d: Skeletal Age vs FD (Freq 1.2-1.4) - Distal of Radius

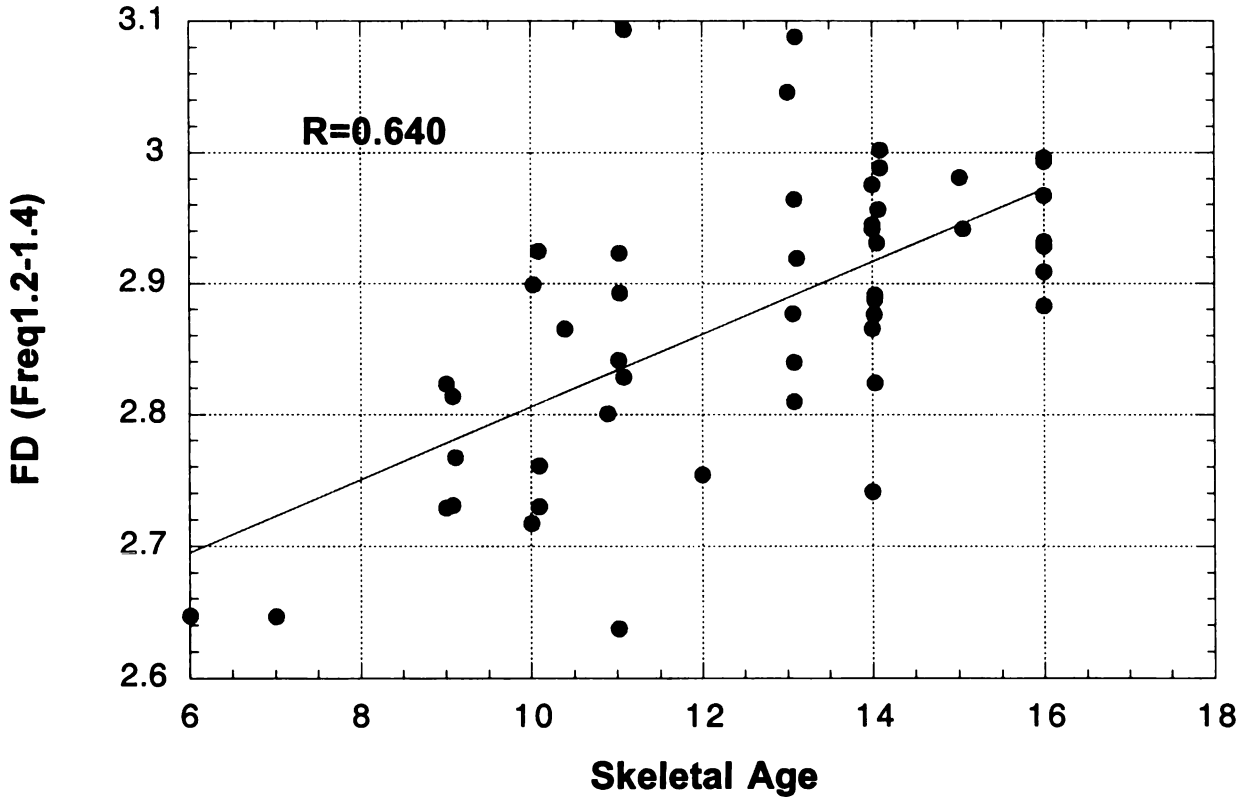

Figure 10a: Interoperator Location Difference vs the Average ROI Size The Middle Finger

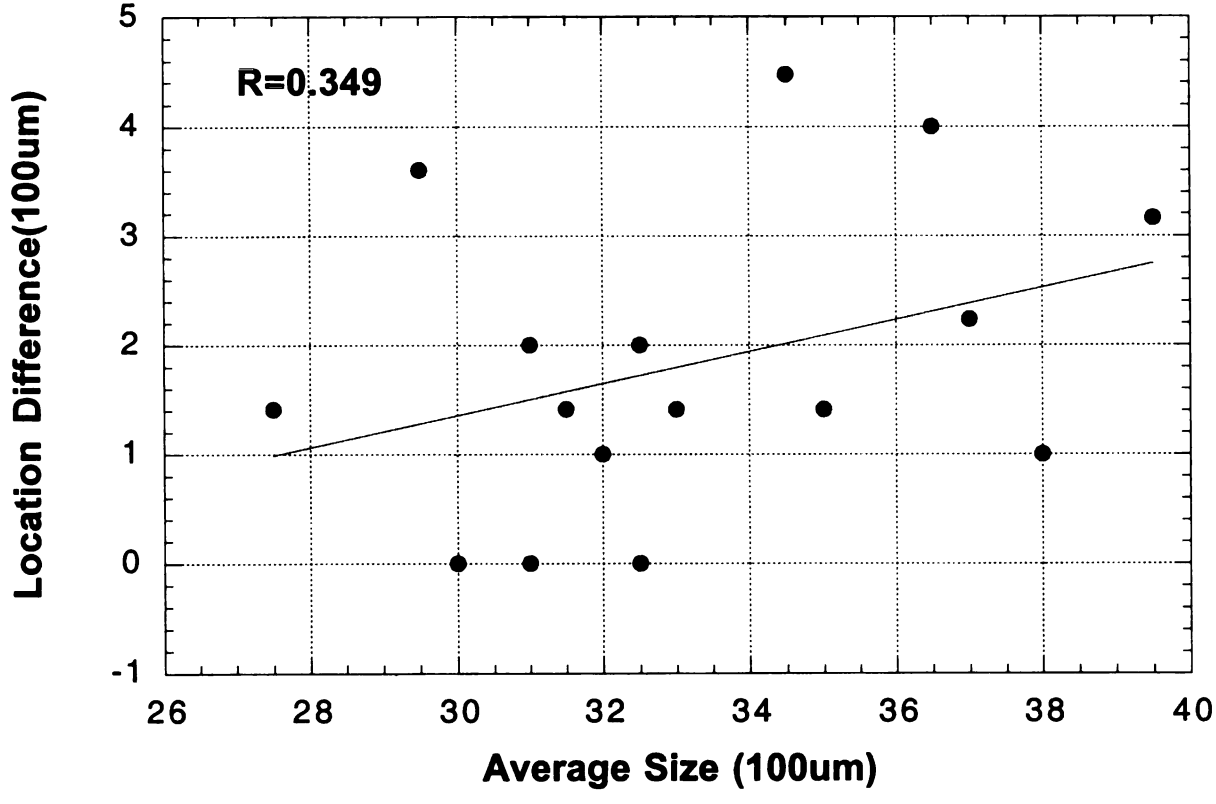

Figure 10: Interoperator reliability study for the middle finger.

Figure 10b: Interoperator Percent Location Difference vs the Average ROI Size The Middle Finger

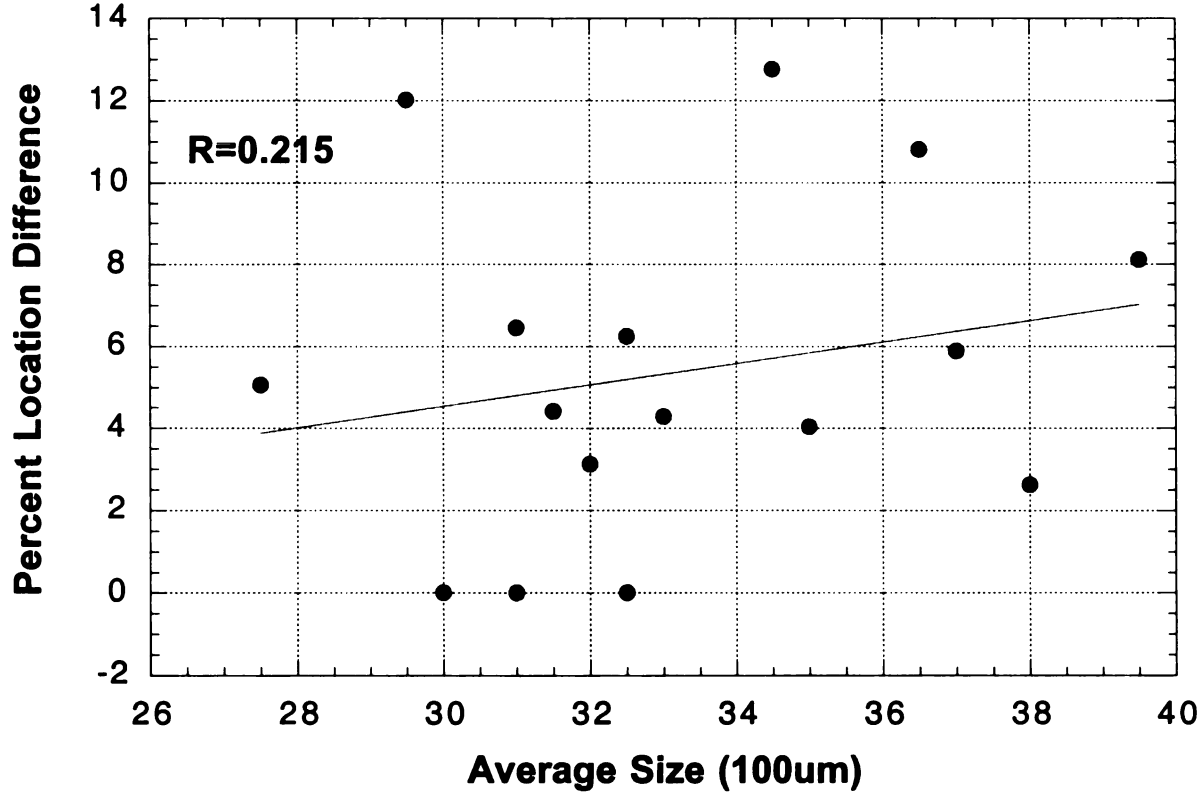

Figure 10c: Interoperator Size Difference vs the Average ROI Size
The Middle Finger

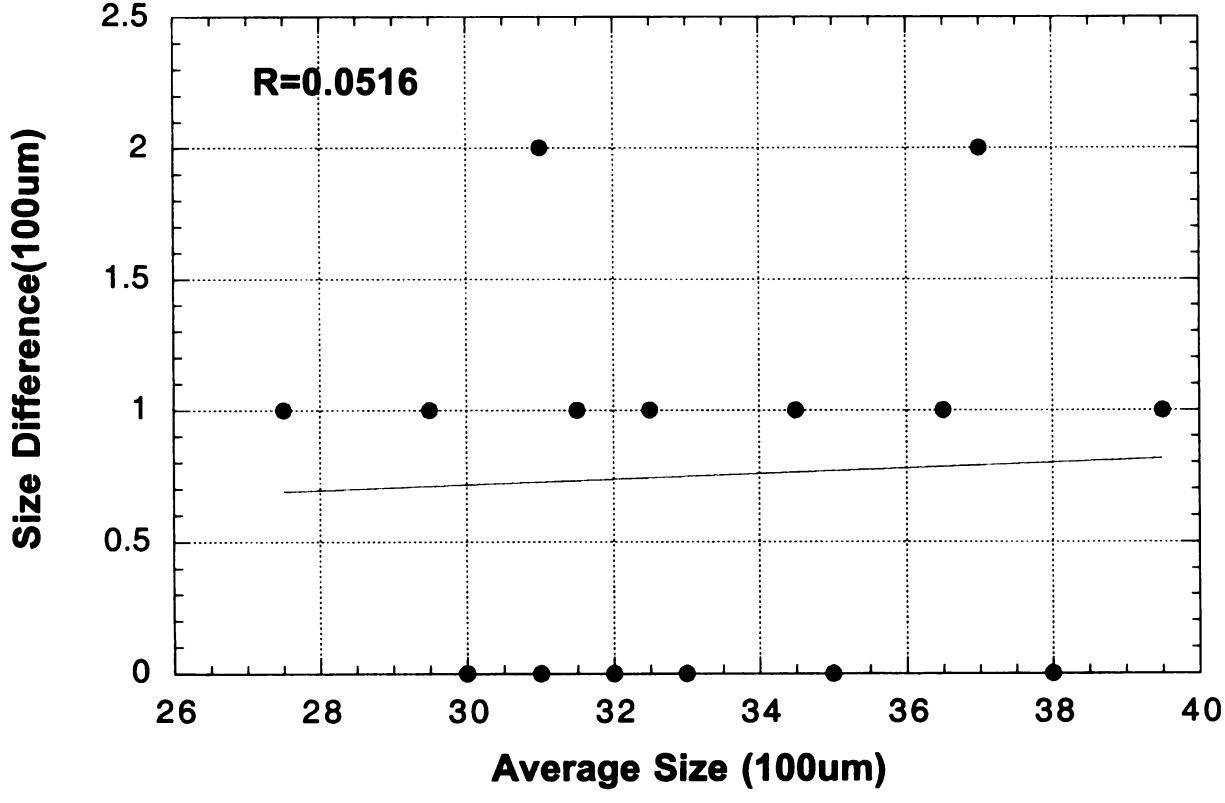

Figure 10d: Interoperator Percent Size Difference vs the Average ROI Size The Middle Finger

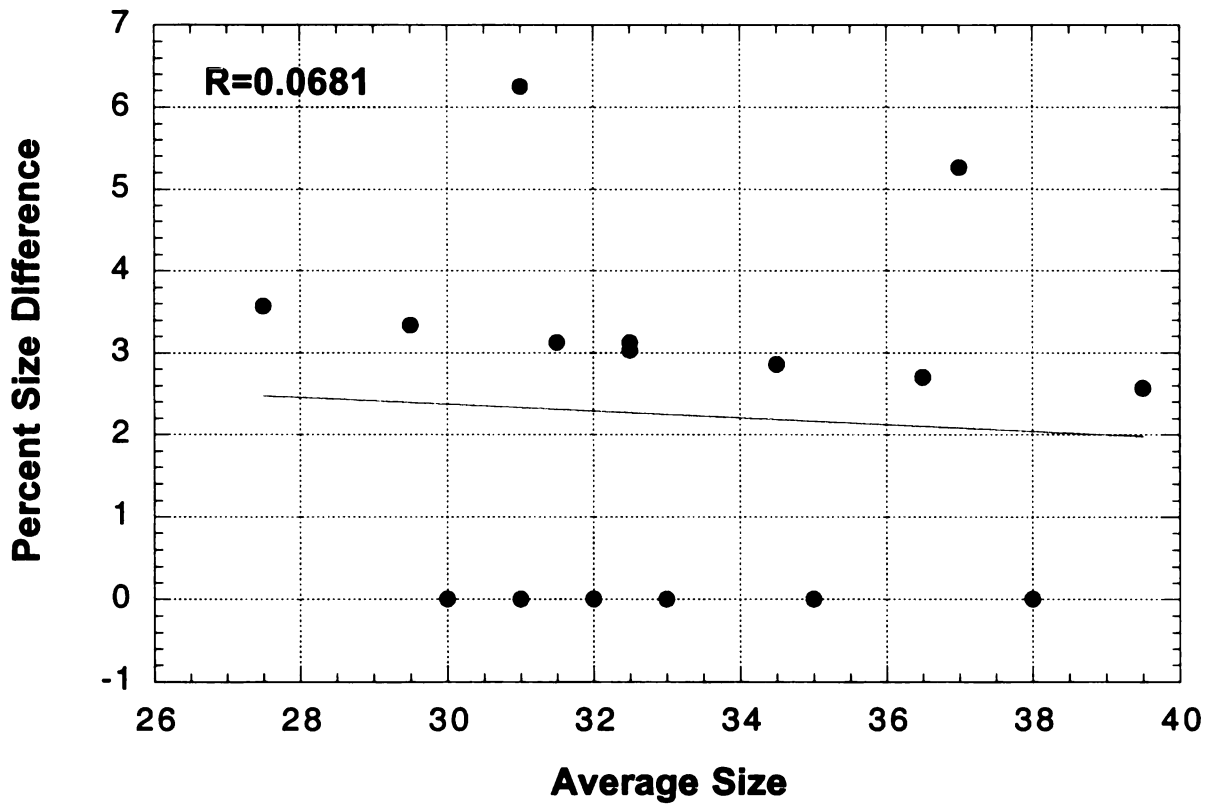

Figure 10e: Interoperator FD Difference (Freq 1.0-1.2)
vs
the Average Size of the ROI Circle
The Middle Finger

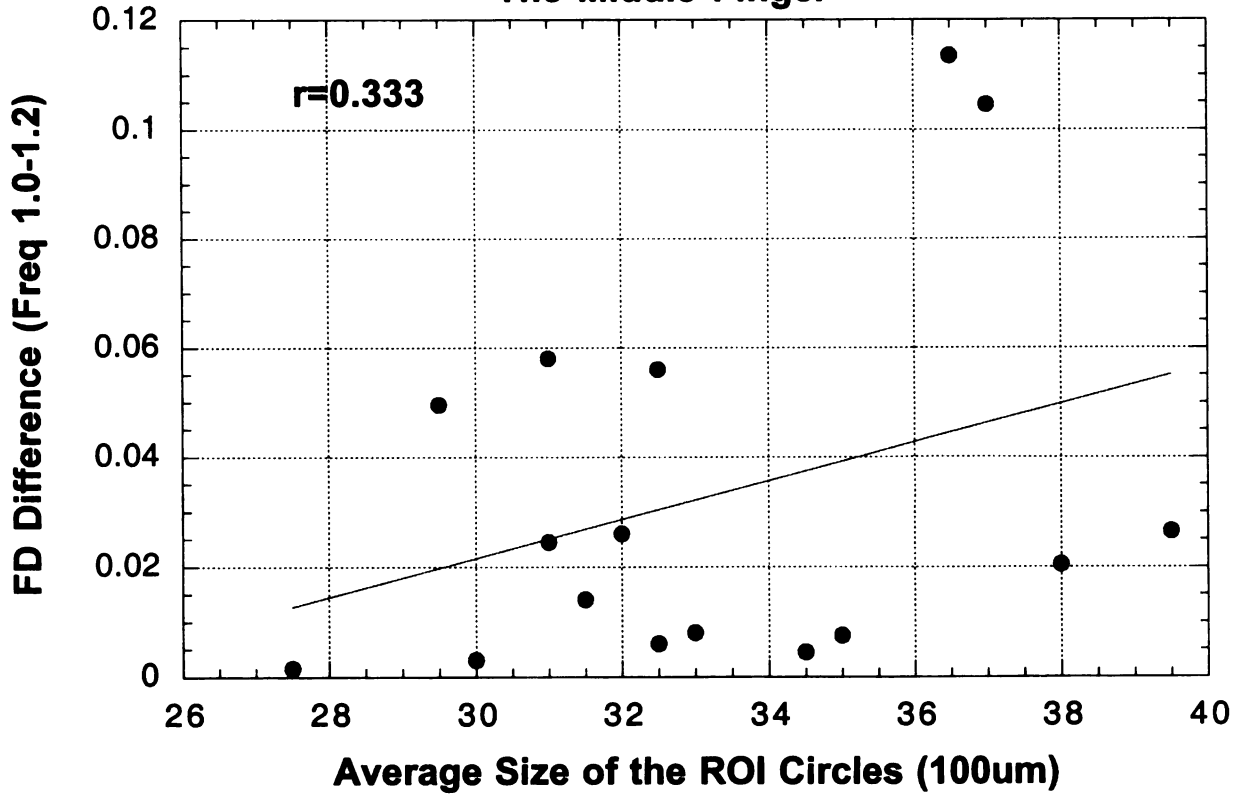

Figure 10f: Interoperator Percent FD Difference (Freq 1.0-1.2)
vs
the Average Size of the ROI Circle
The Middle Finger

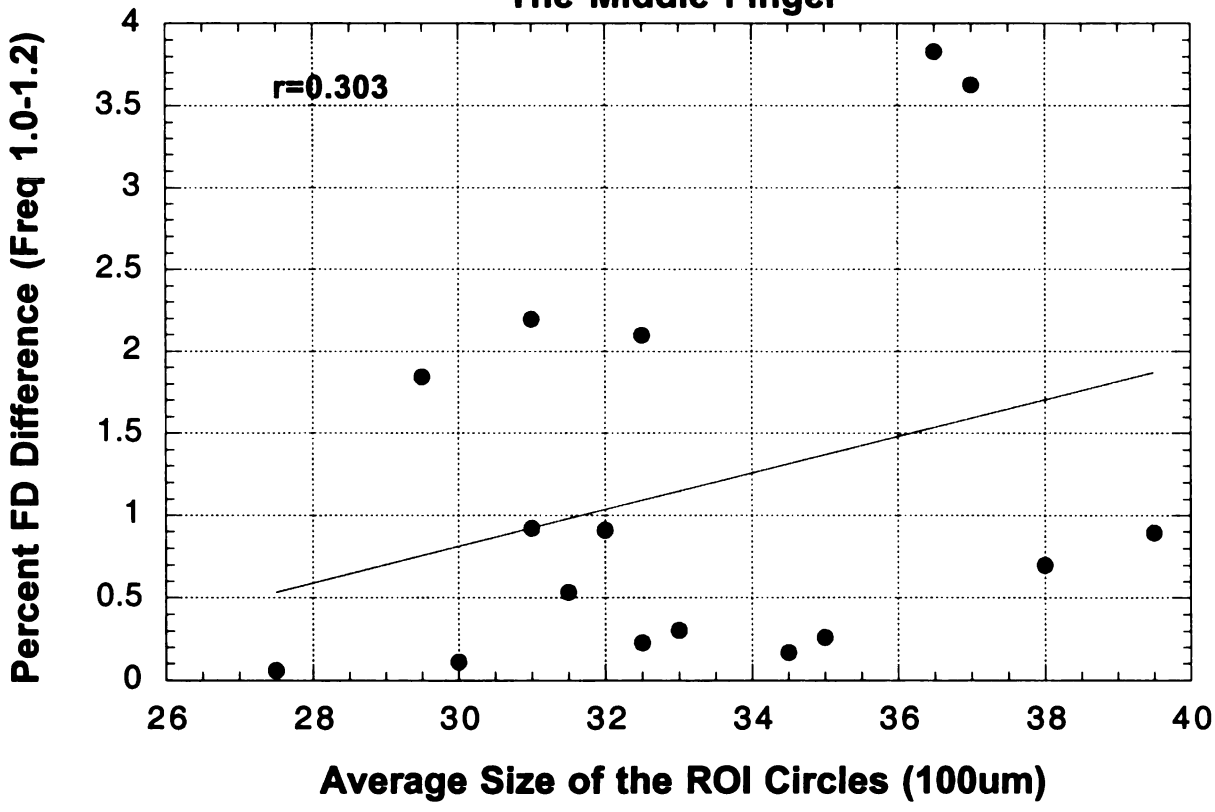

Figure 10g: Interoperator FD Difference (Freq 1.2-1.4)
vs
the Average Size of the ROI Circle
The Middle Finger

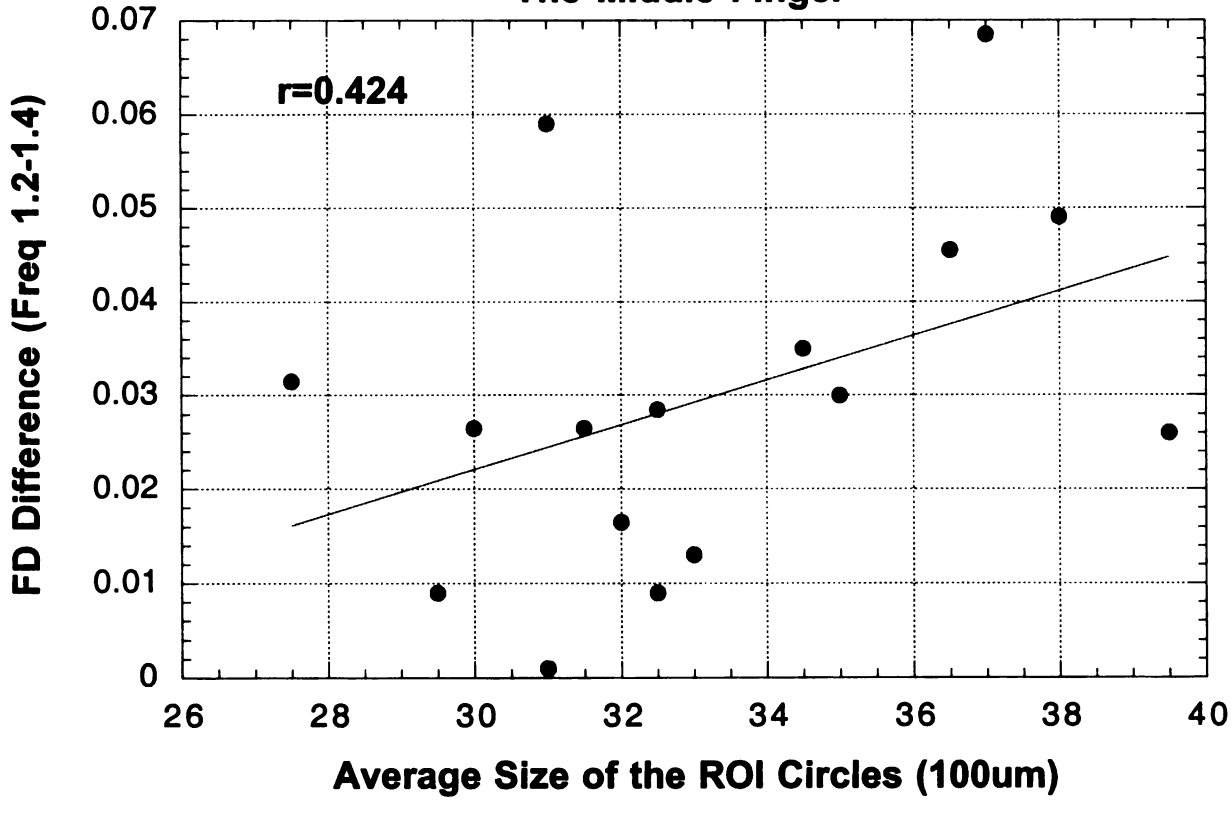

Figure 10h: Interoperator Percent FD Difference (Freq 1.2-1.4)
vs
the Average Size of the ROI Circle
The Middle Finger

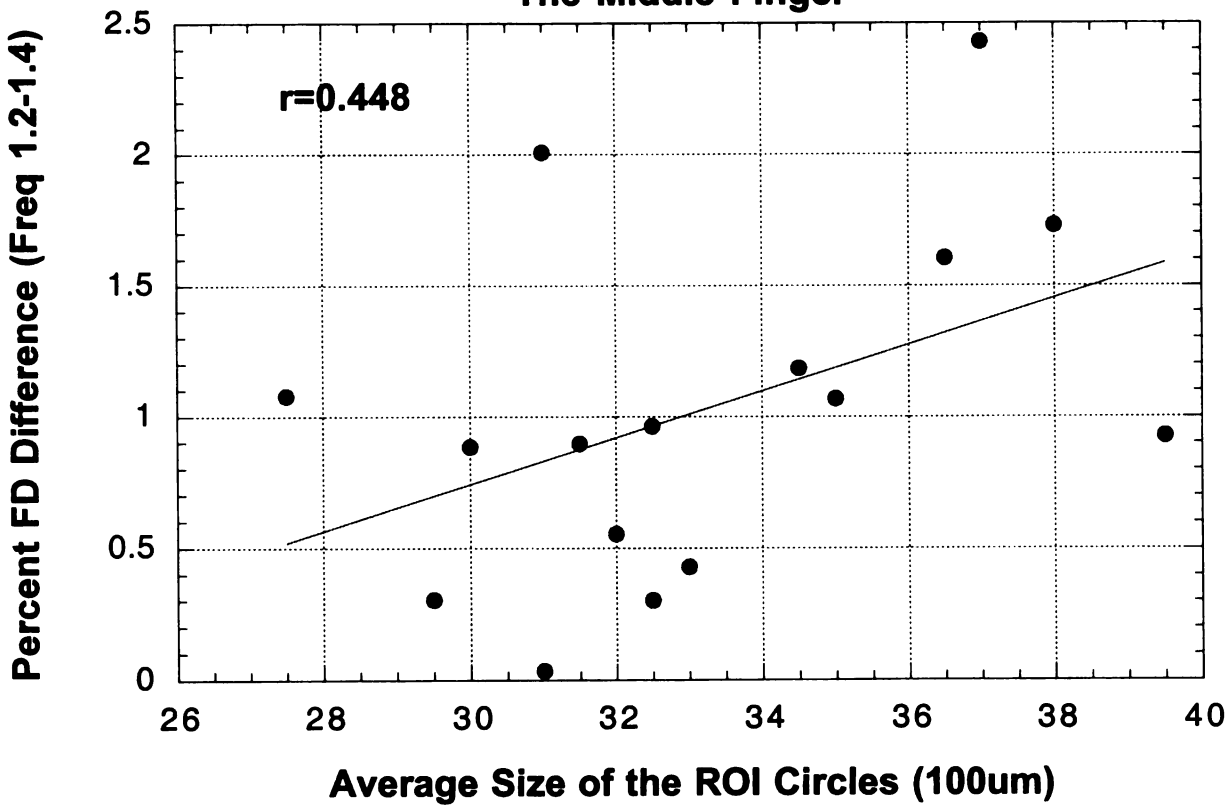

Figure 10i: Interoperator FD Difference (Freq 1.3-1.4)
vs
the Average Size of the ROI Circle
The Middle Finger

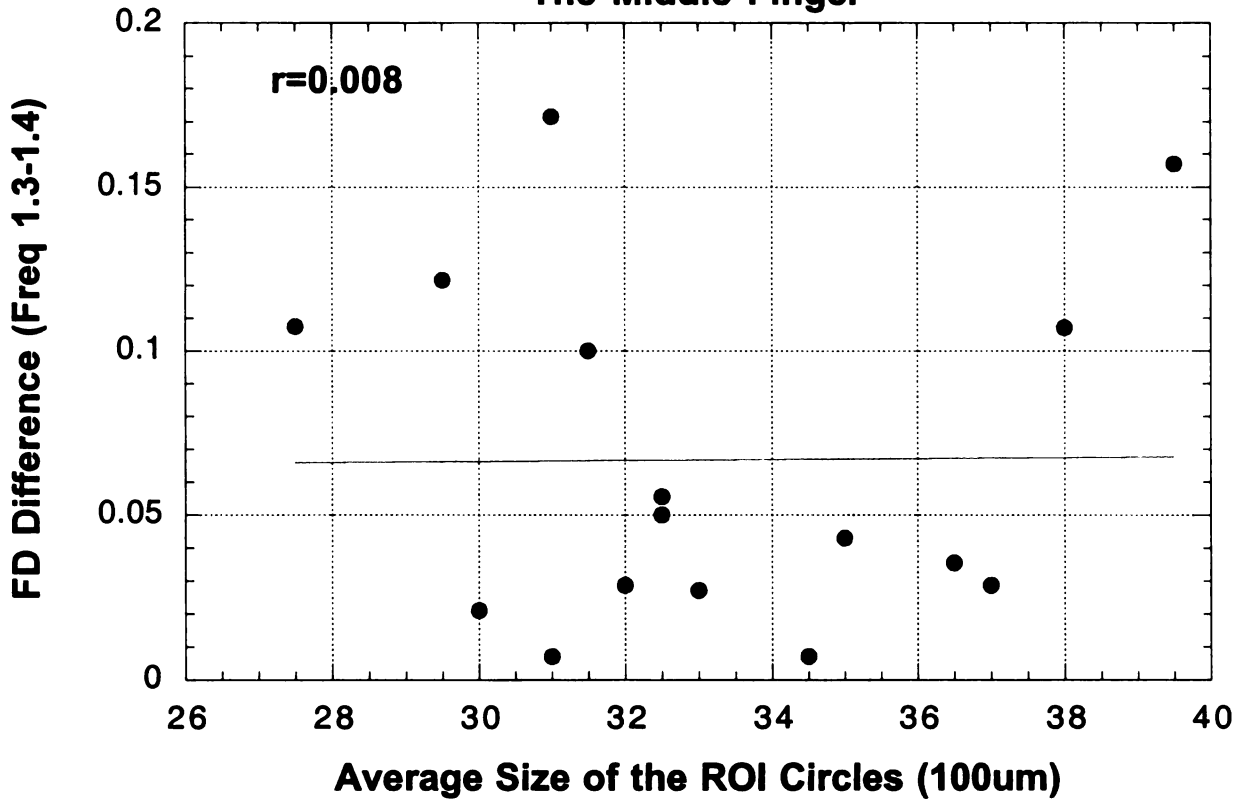

Figure 10j: Interoperator Percent FD Difference (Freq 1.3-1.4)
vs
the Average Size of the ROI Circle
The Middle Finger

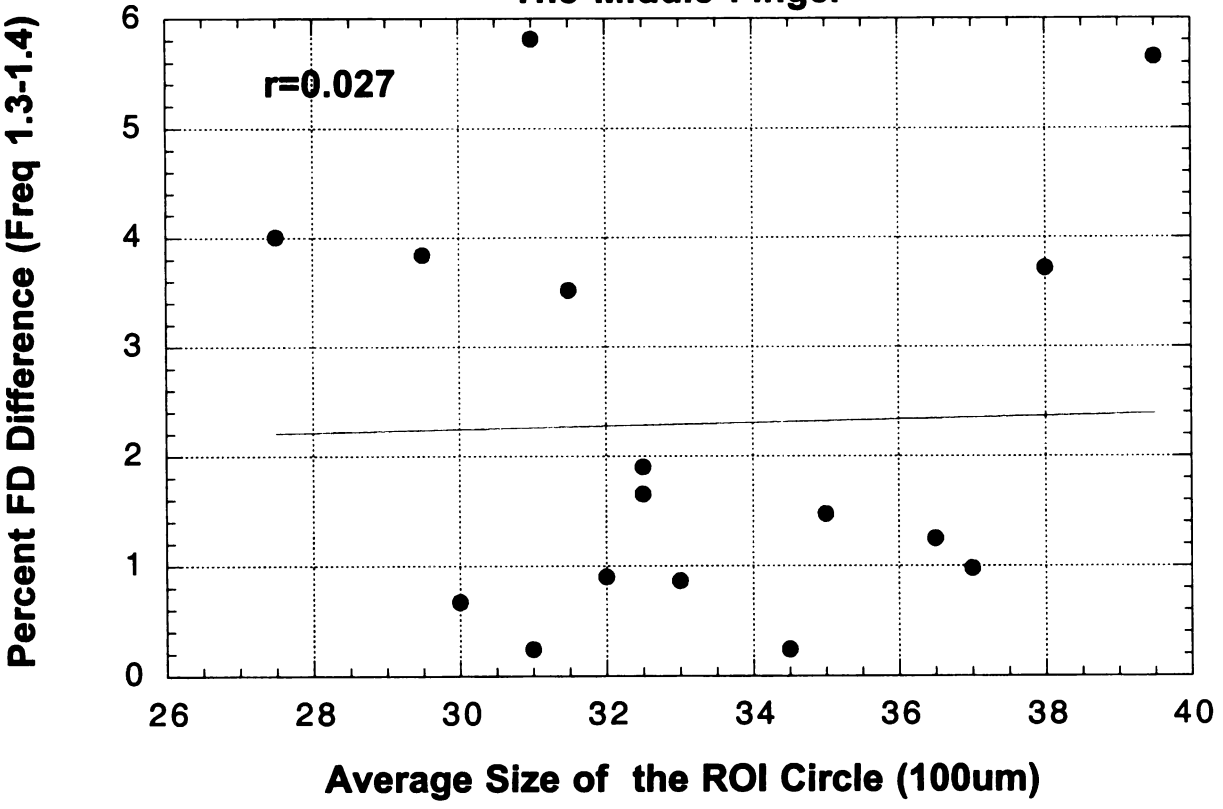

Figure 11a: Interoperator Location Difference vs the Average ROI Size The Distal of Radius

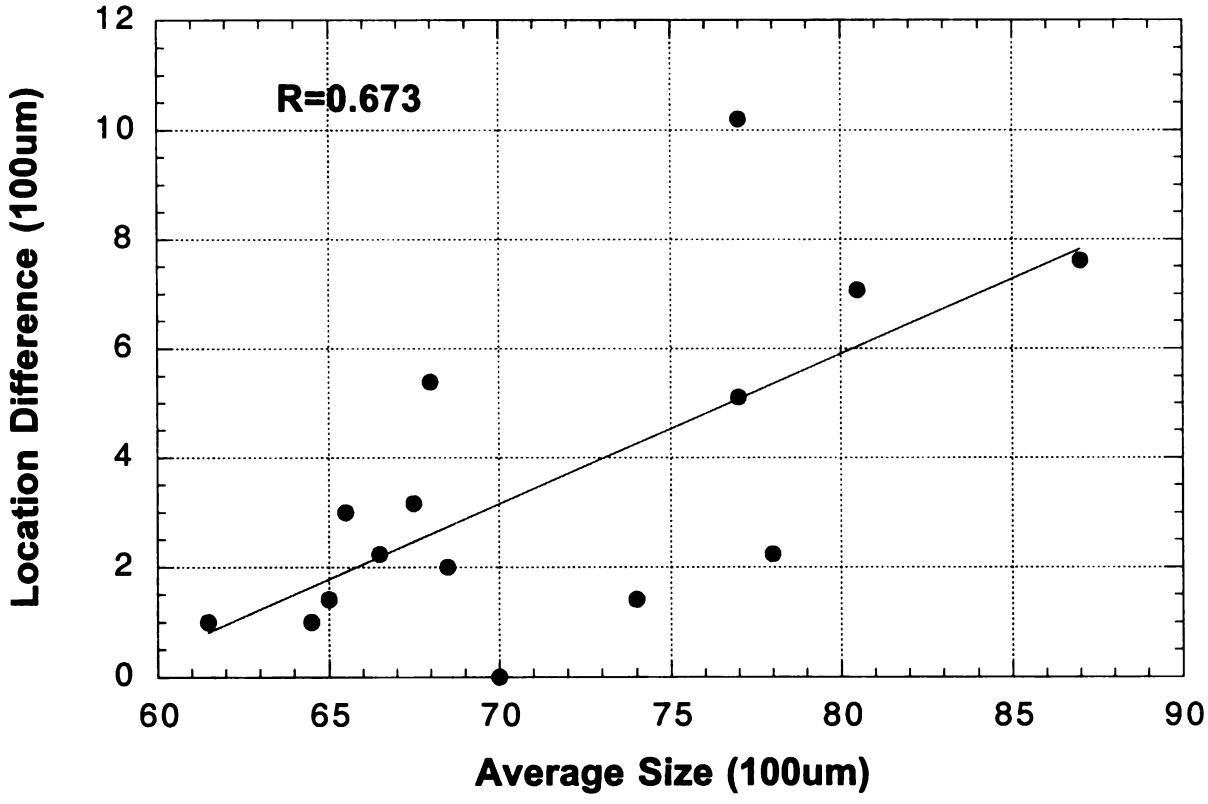

Figure 11: Interoperator reliability study for the distal of radius

Figure 11b: Interoperator Percent Location Difference vs the Average ROI Size The Distal of Radius

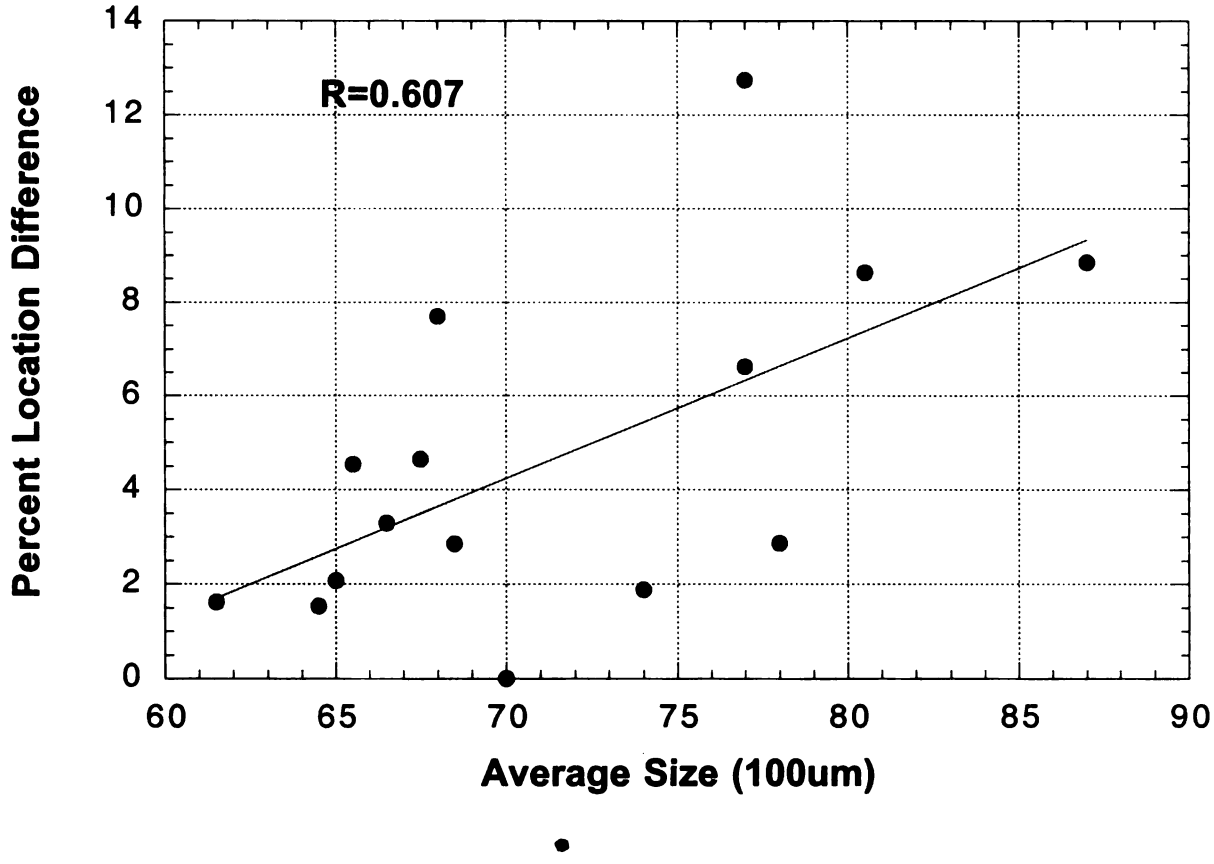

Figure 11c: Interoperator Size Difference vs the Average ROI Size The Distal of Radius

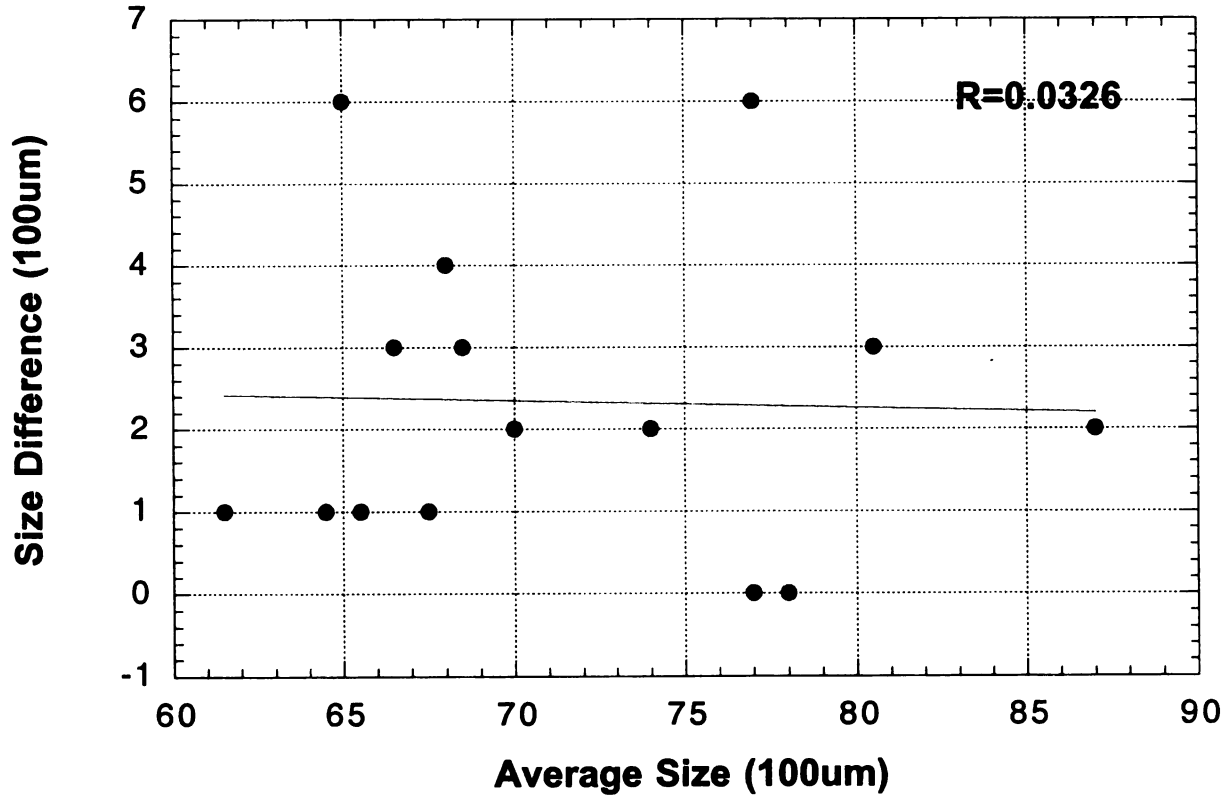

Figure 11d: Interoperator Percent Size Difference vs the Average ROI Size The Distal of Radius

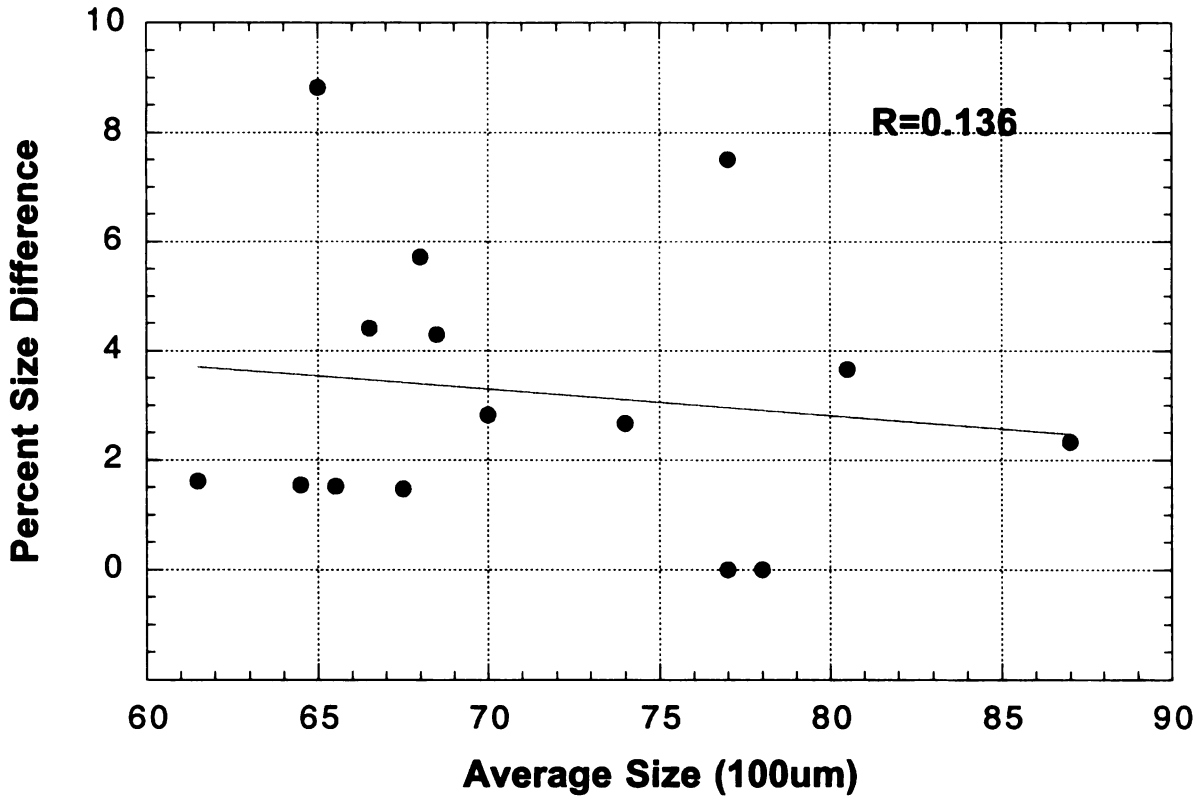

Figure 11e: Interoperator FD Difference (Freq 0.6-1.0)
vs
the Average Size of the ROI Circle
The Distal of Radius

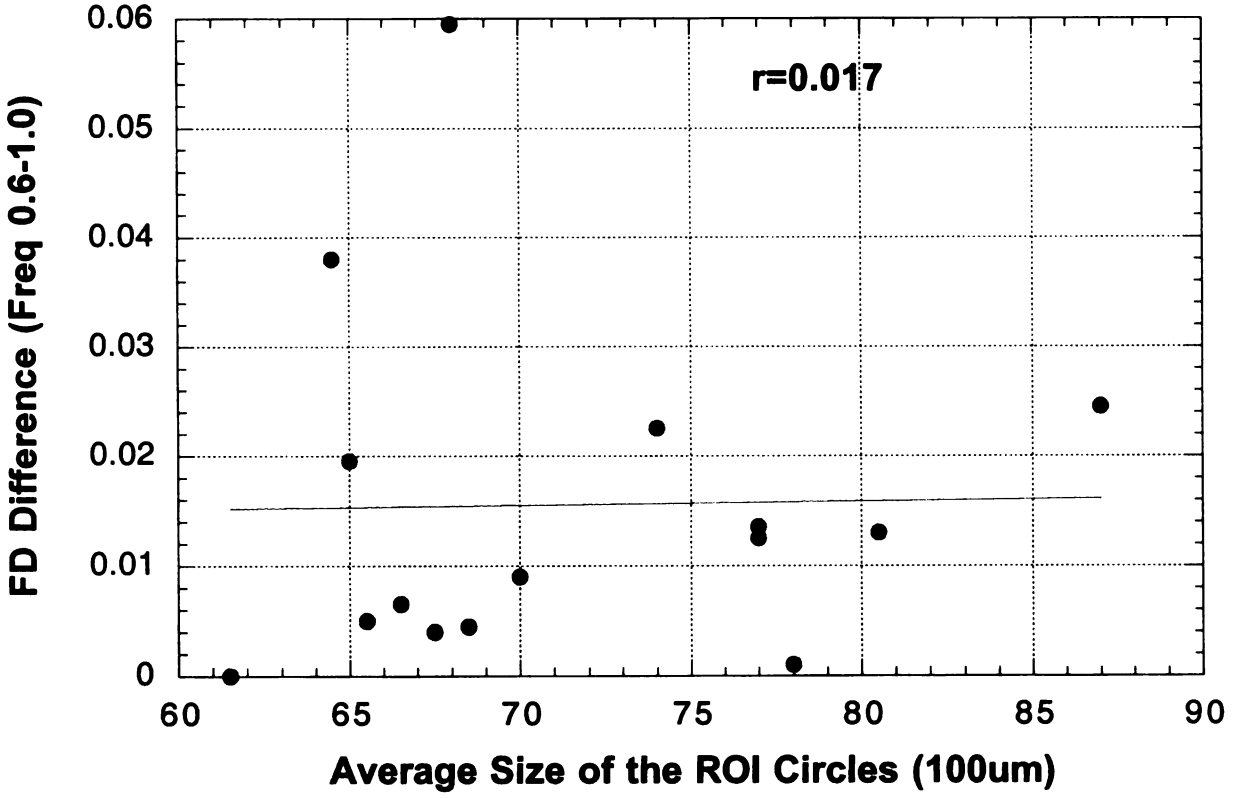

Figure 11f: Interoperator Percent FD Difference (Freq 0.6-1.0)
vs
the Average Size of the ROI Circle
The Distal of Radius

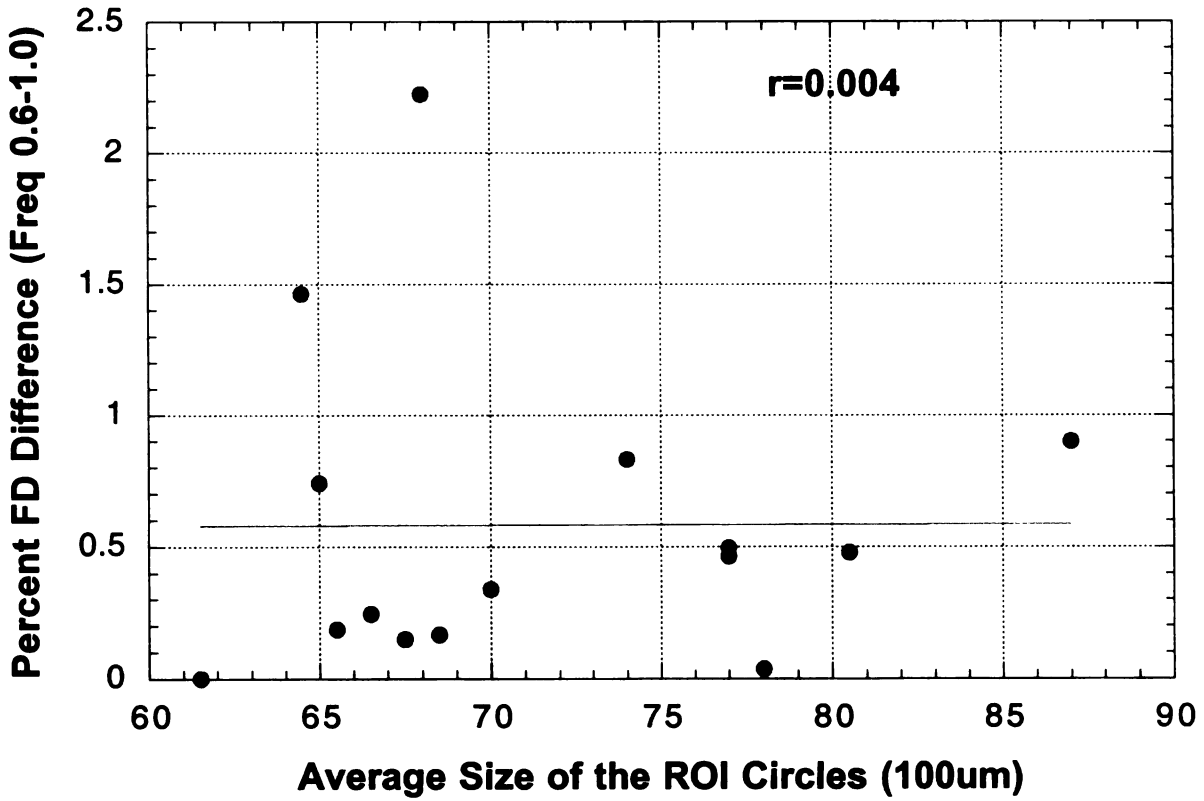

Figure 11g: Interoperator FD Difference (Freq 1.0-1.2)
vs
the Average Size of the ROI Circle
The Distal of Radius

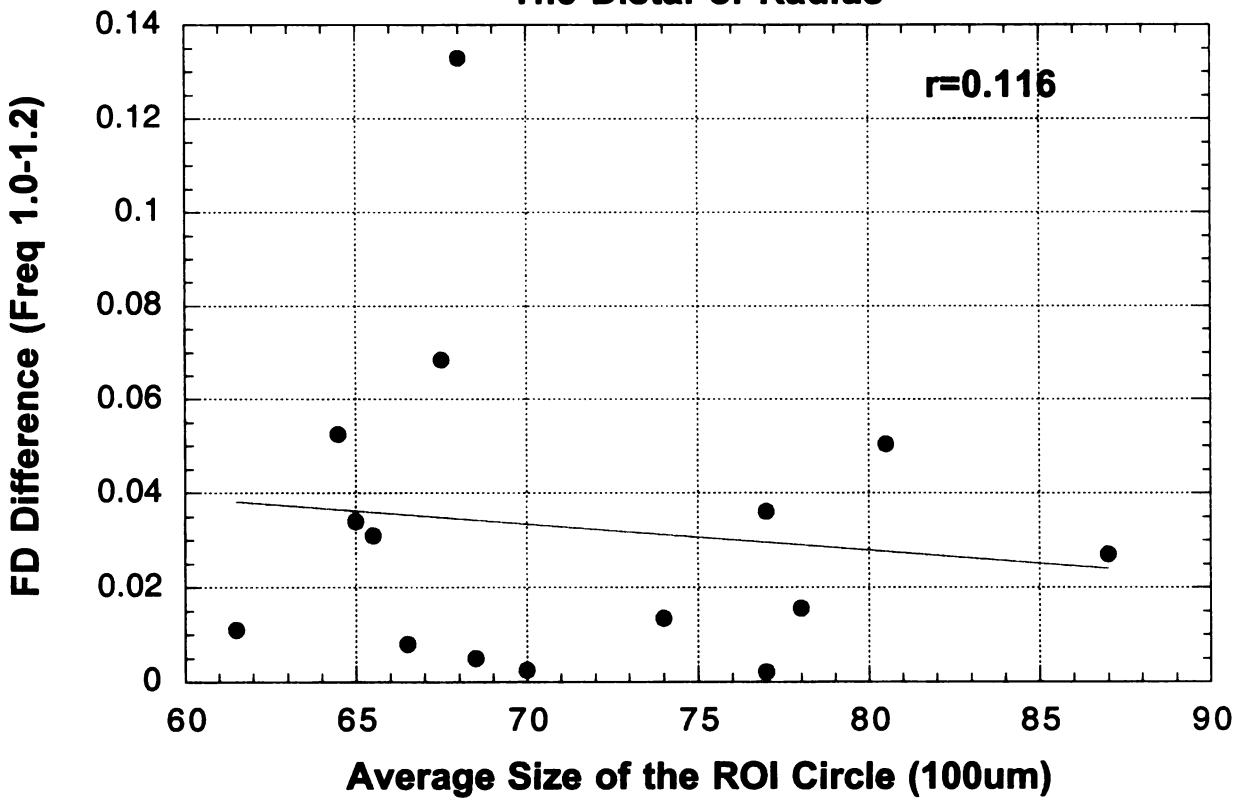

Figure 11h: Interoperator Percent FD Difference (Freq 1.0-1.2)
vs
the Average Size of the ROI Circle
The Distal of Radius

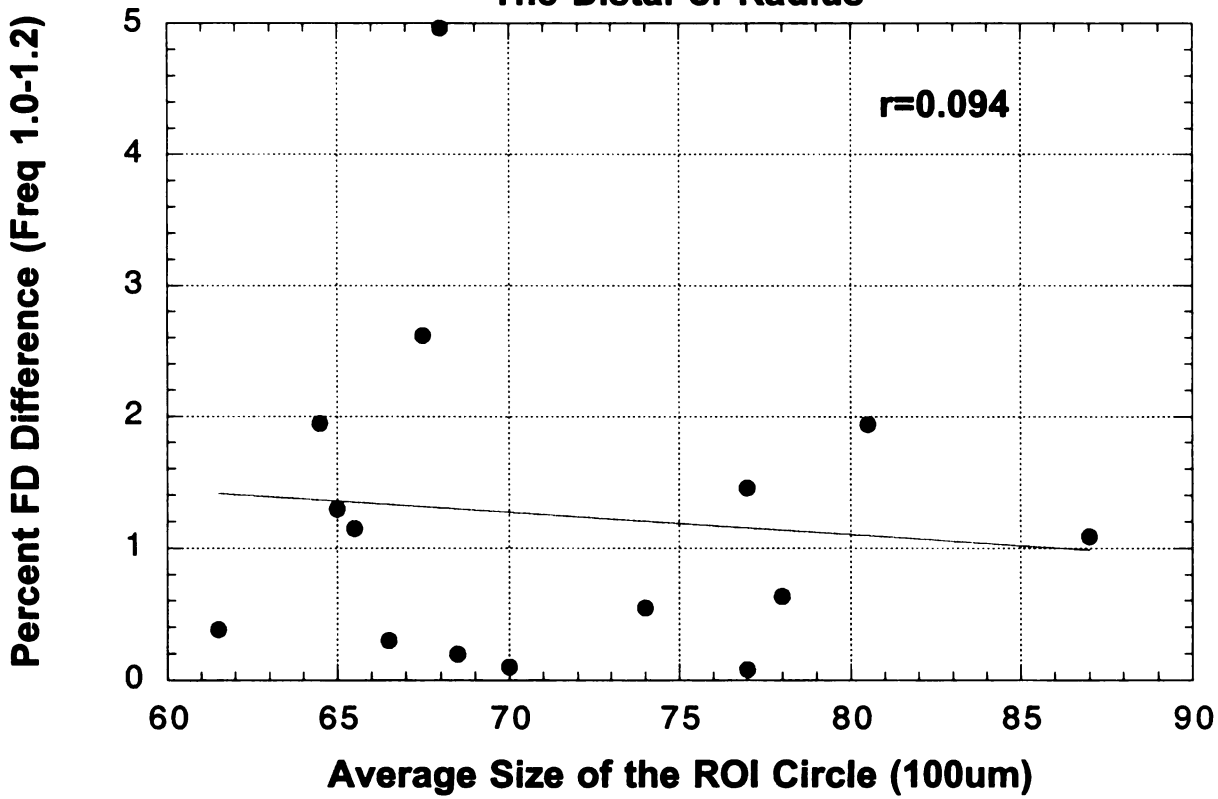

Figure 11i: Interoperator FD Difference (Freq 1.0-1.4)
vs
the Average Size of the ROI Circle
The Distal of Radius

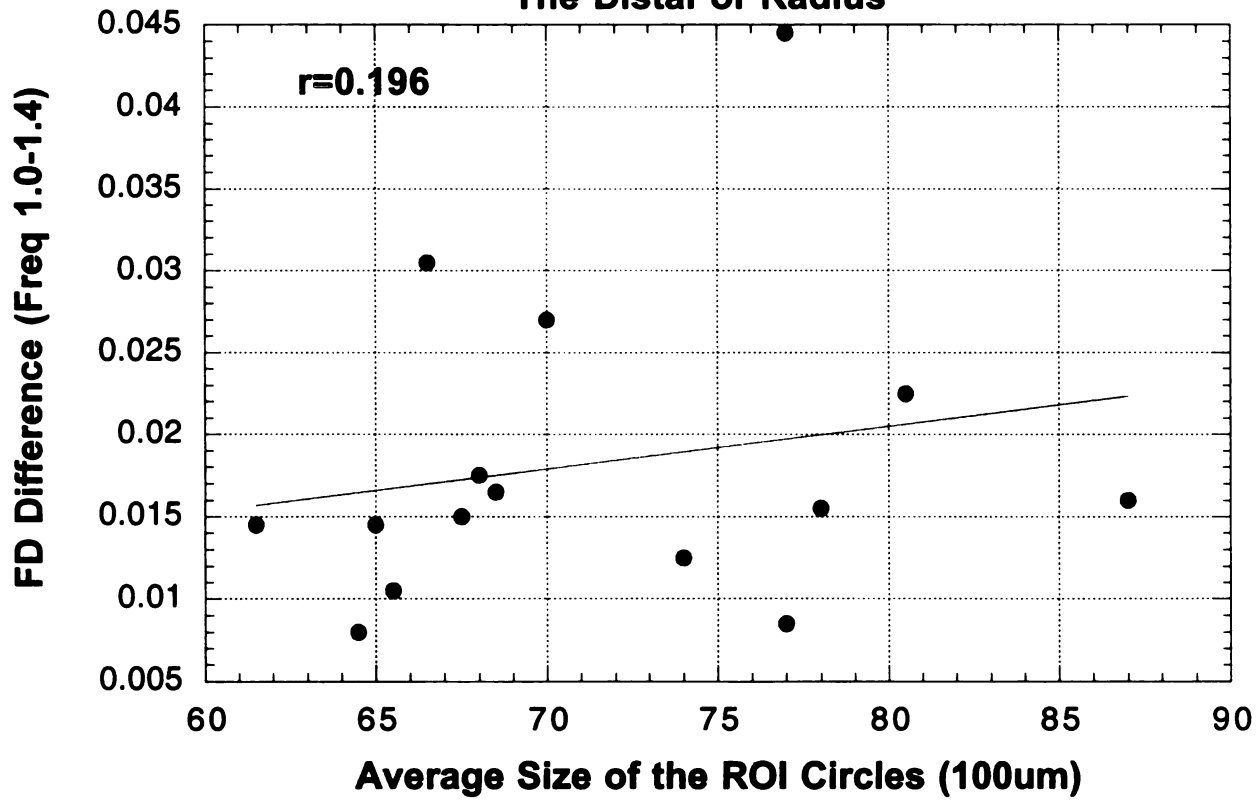

Figure 11j: Interoperator Percent FD Difference (Freq 1.0-1.4)
vs
the Average Size of the ROI Circle
The Distal of Radius

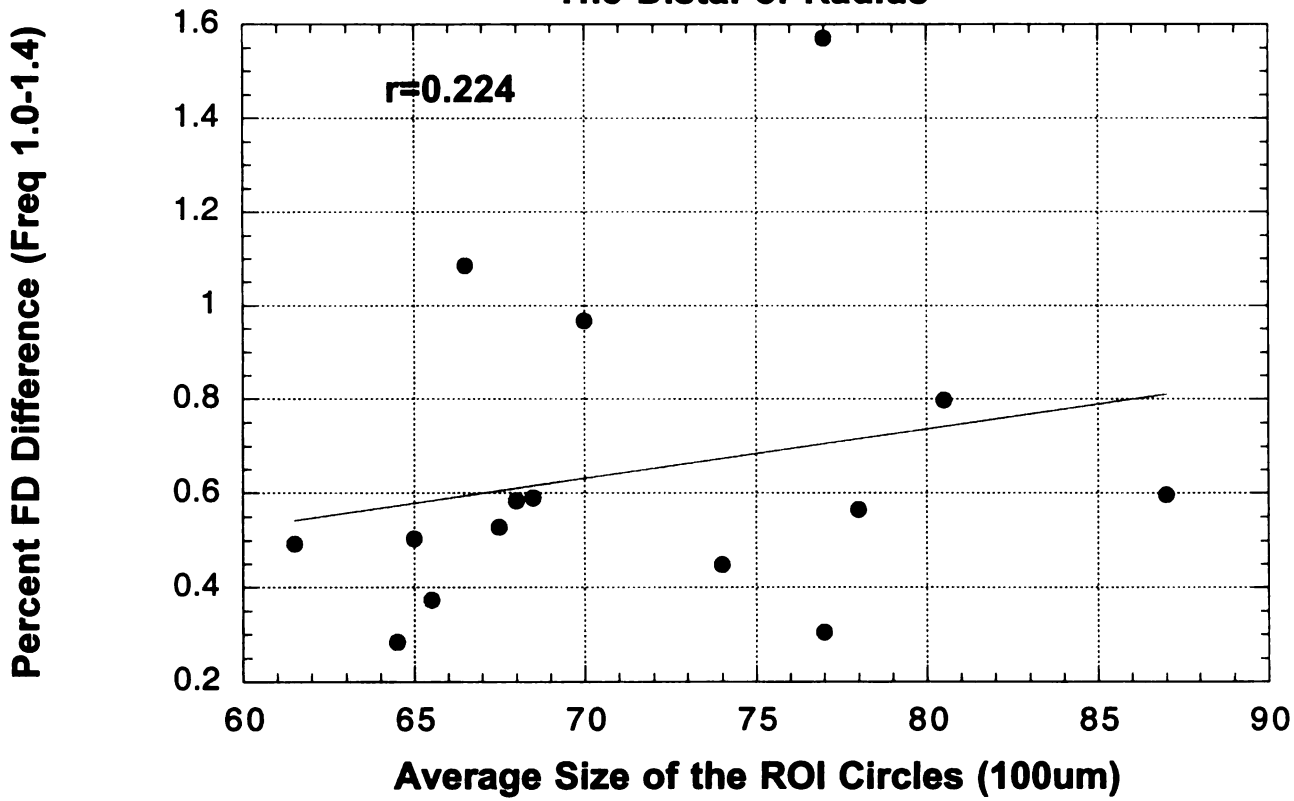

Figure 11k: Interoperator FD Difference (Freq 1.2-1.4)
vs
the Average Size of the ROI Circle
The Distal of Radius

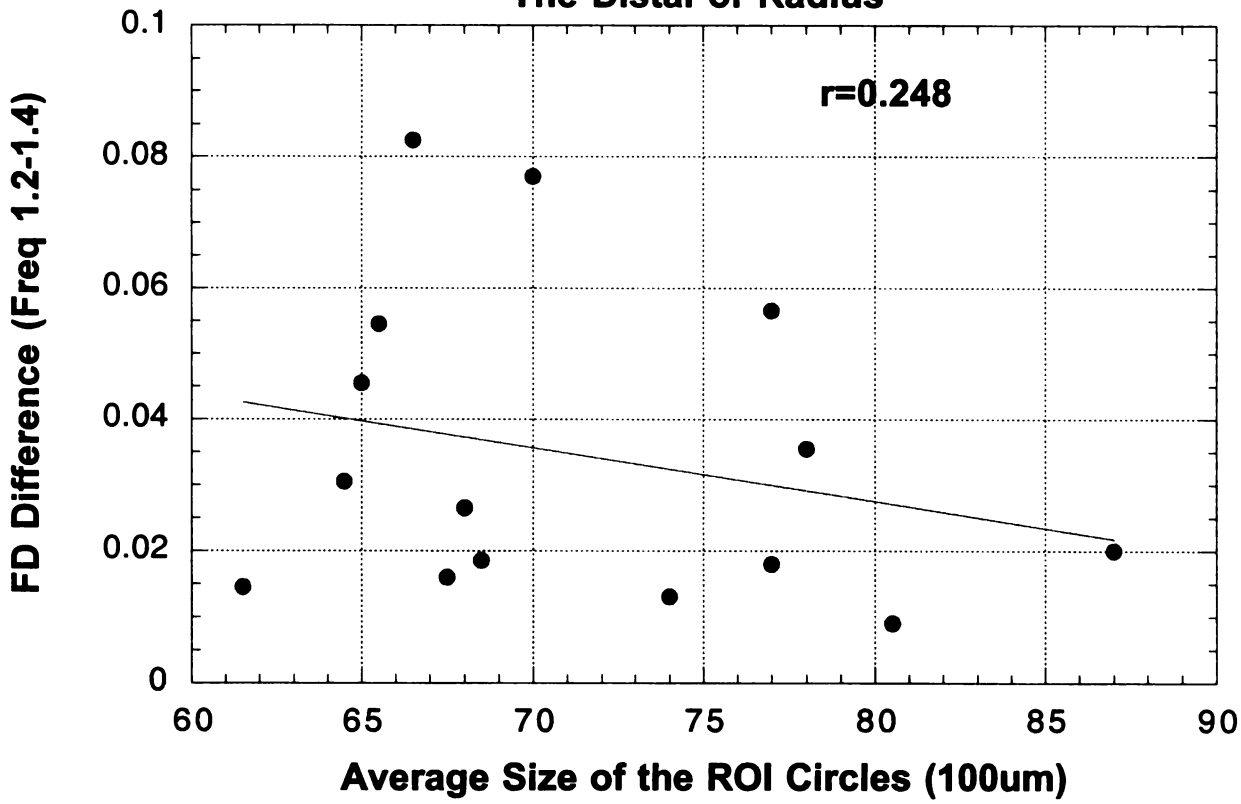

Figure 11l: Interoperator Percent FD Difference (Freq 1.2-1.4)
vs
the Average Size of the ROI Circle
The Distal of Radius

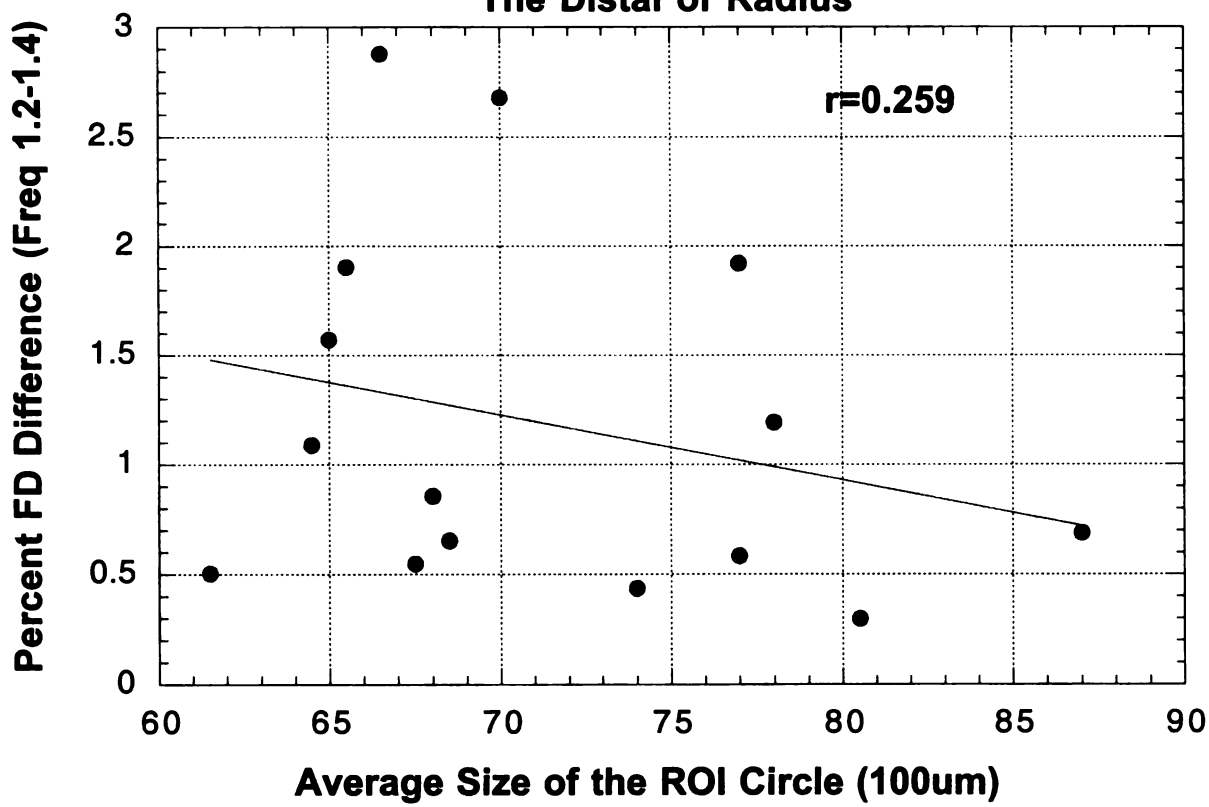

Figure 11m: Interoperator FD Correlation
Freq 0.6-1.0
Distal of Raduis

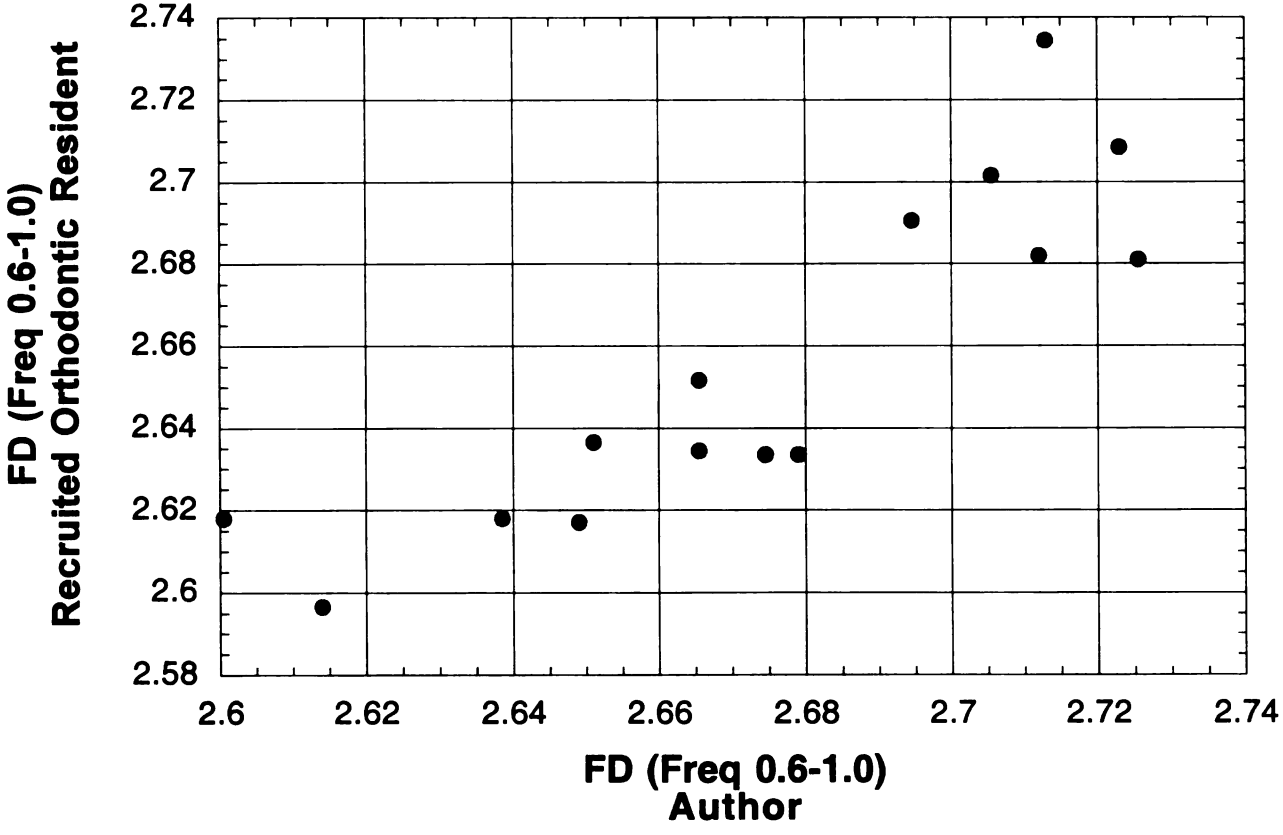

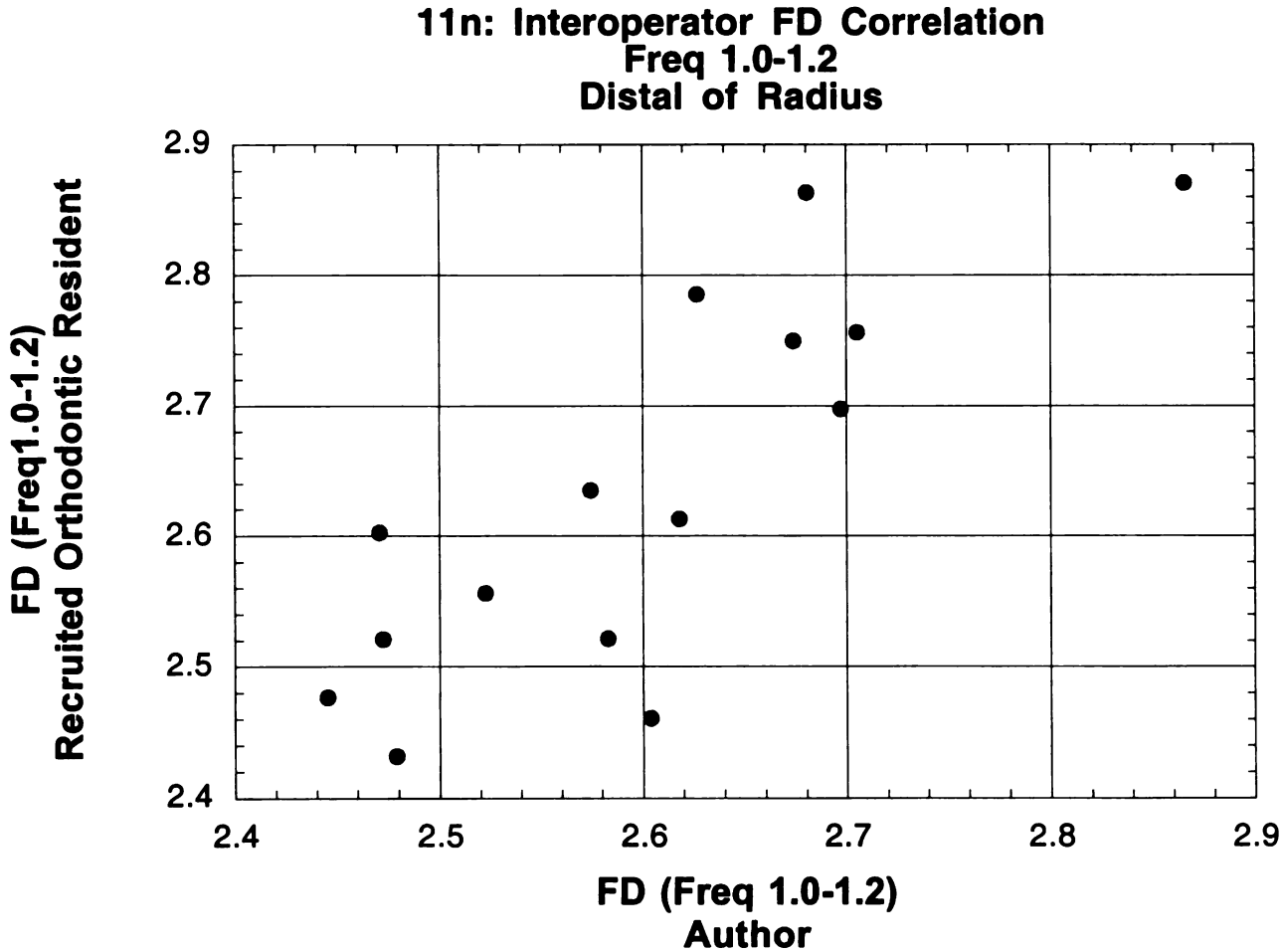
11n: Interoperator FD Correlation
Freq 1.0-1.2
Distal of Radius
FD (Freq1.0-1.2)
Recruited Orthodontic Resident
2.9
2.8
2.7
2.6
2.5
2.4
2.4
2.5
2.6
2.7
2.8
2.9
FD (Freq 1.0-1.2)
Author

Figure 12a: Intraoperator Location Difference vs the Average ROI Size The Middle Finger

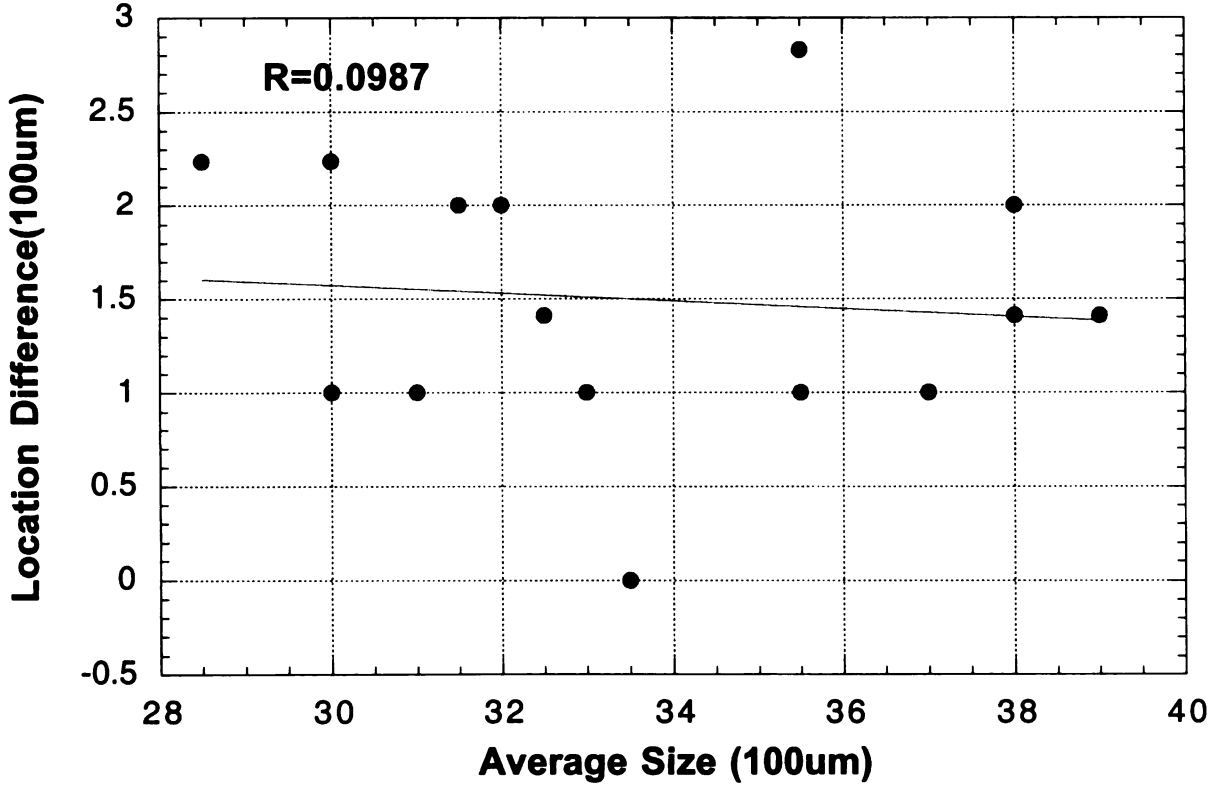

Figure 12: Intraoperator reliability study for the middle finger.

Figure 12b: Intraoperator Percent Location Difference vs the Average ROI Size The Middle Finger

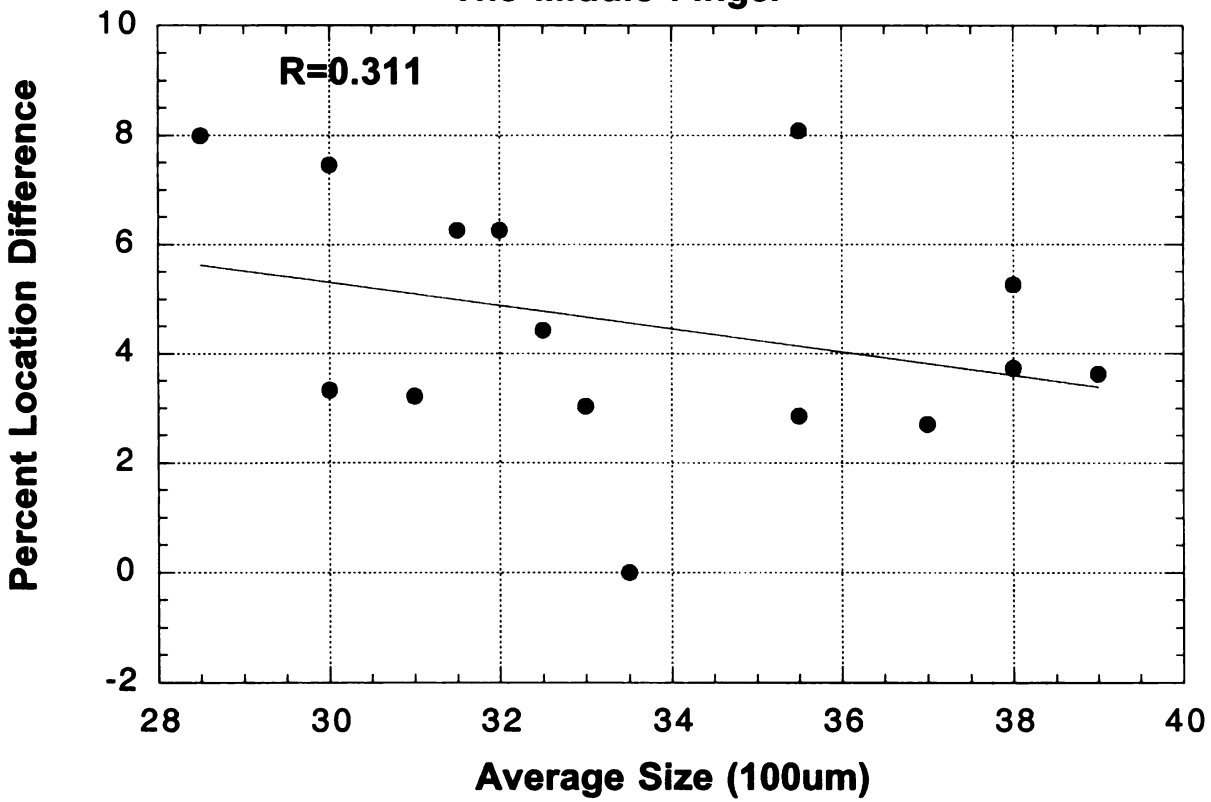

Figure 12c: Intraoperator Size Difference vs the Average ROI Size The Middle Finger

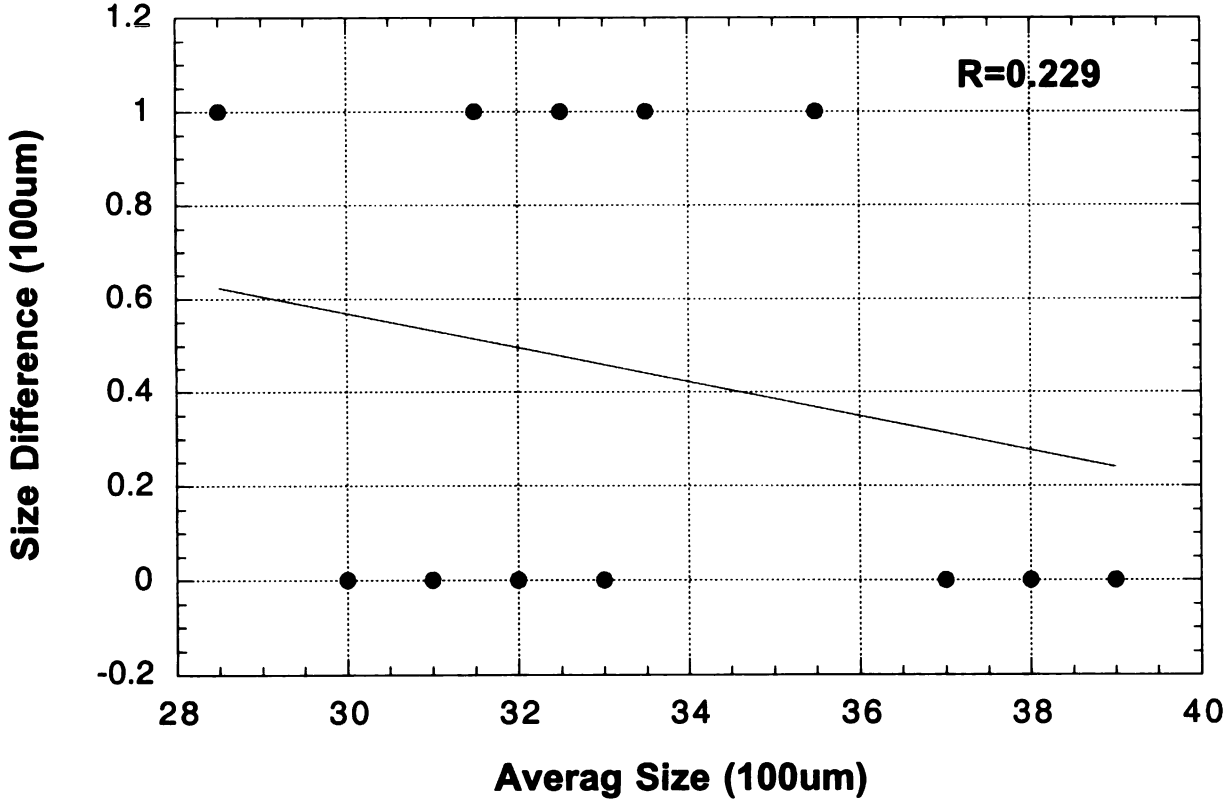

Figure 12d: Intraoperator Percent Size Difference vs the Average ROI Size The Middle Finger

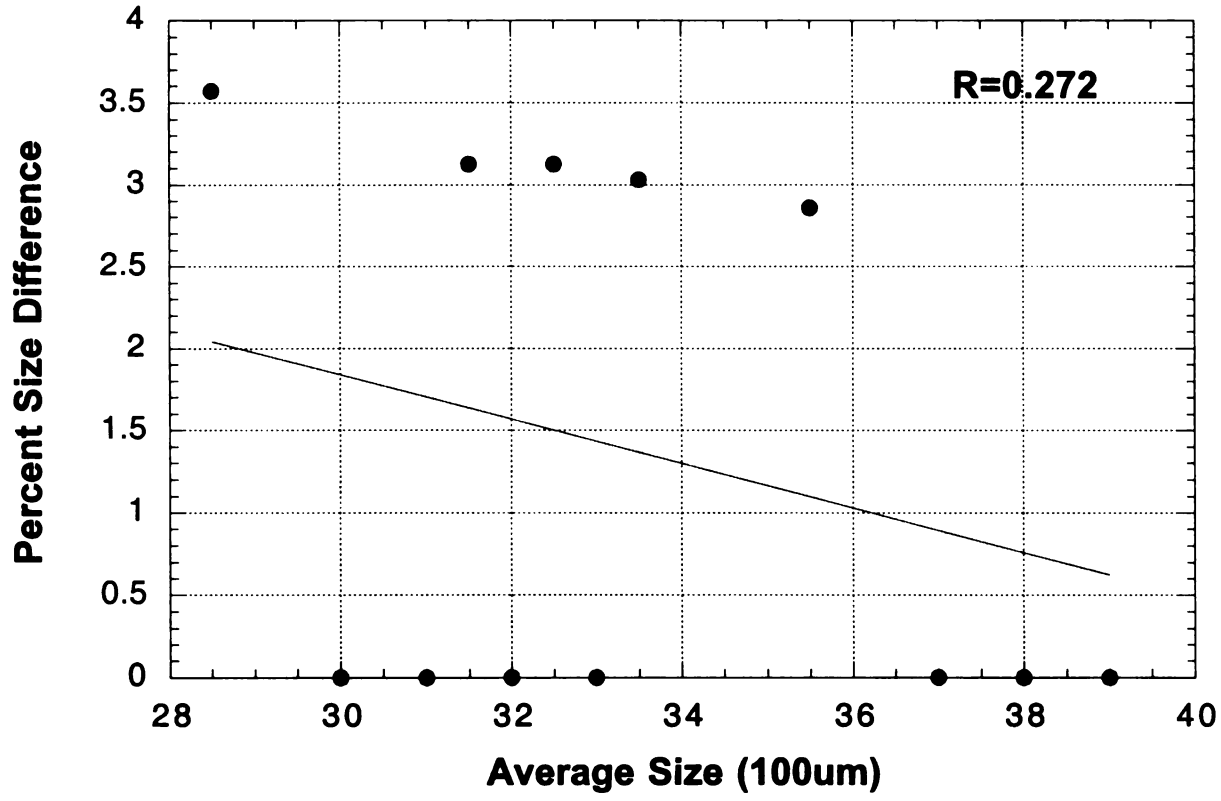

Figure 12e: Intraoperator FD Difference (Freq 1.0-1.2)
vs
the Average Size of the ROI Circle
The Middle Finger

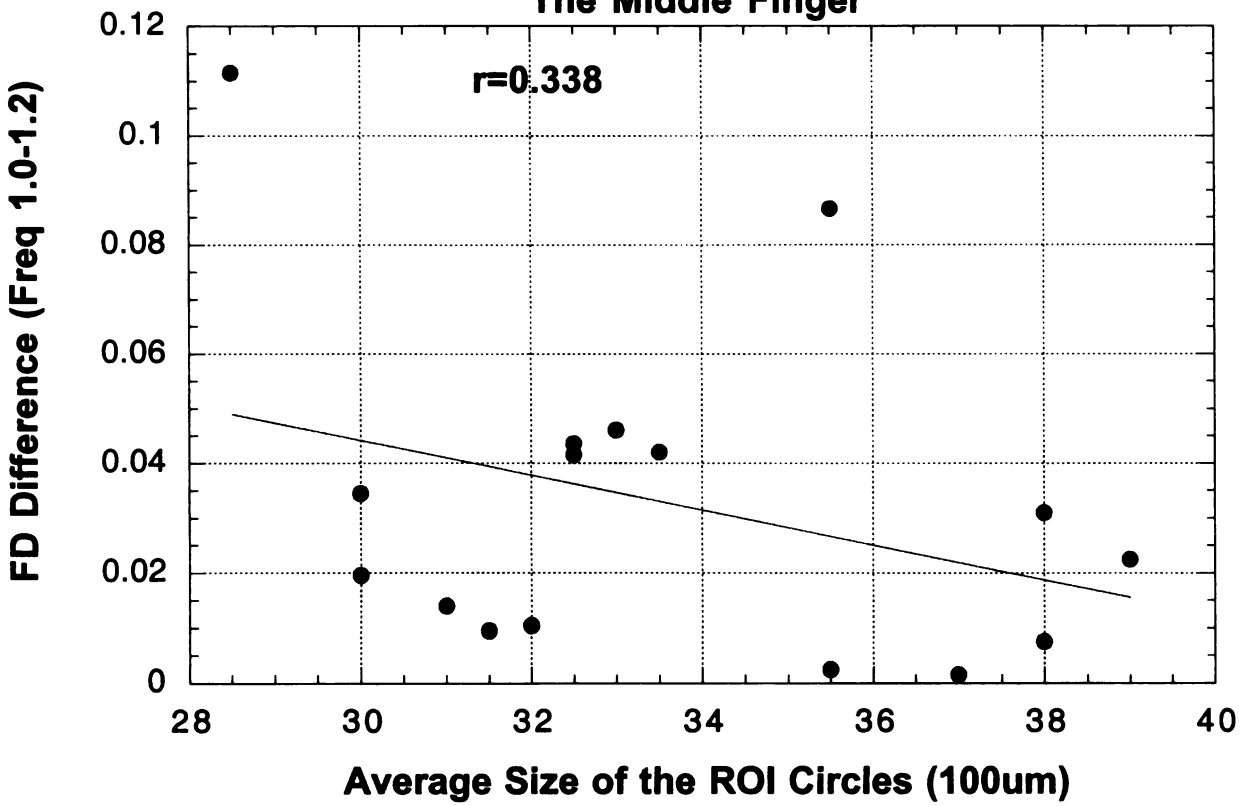

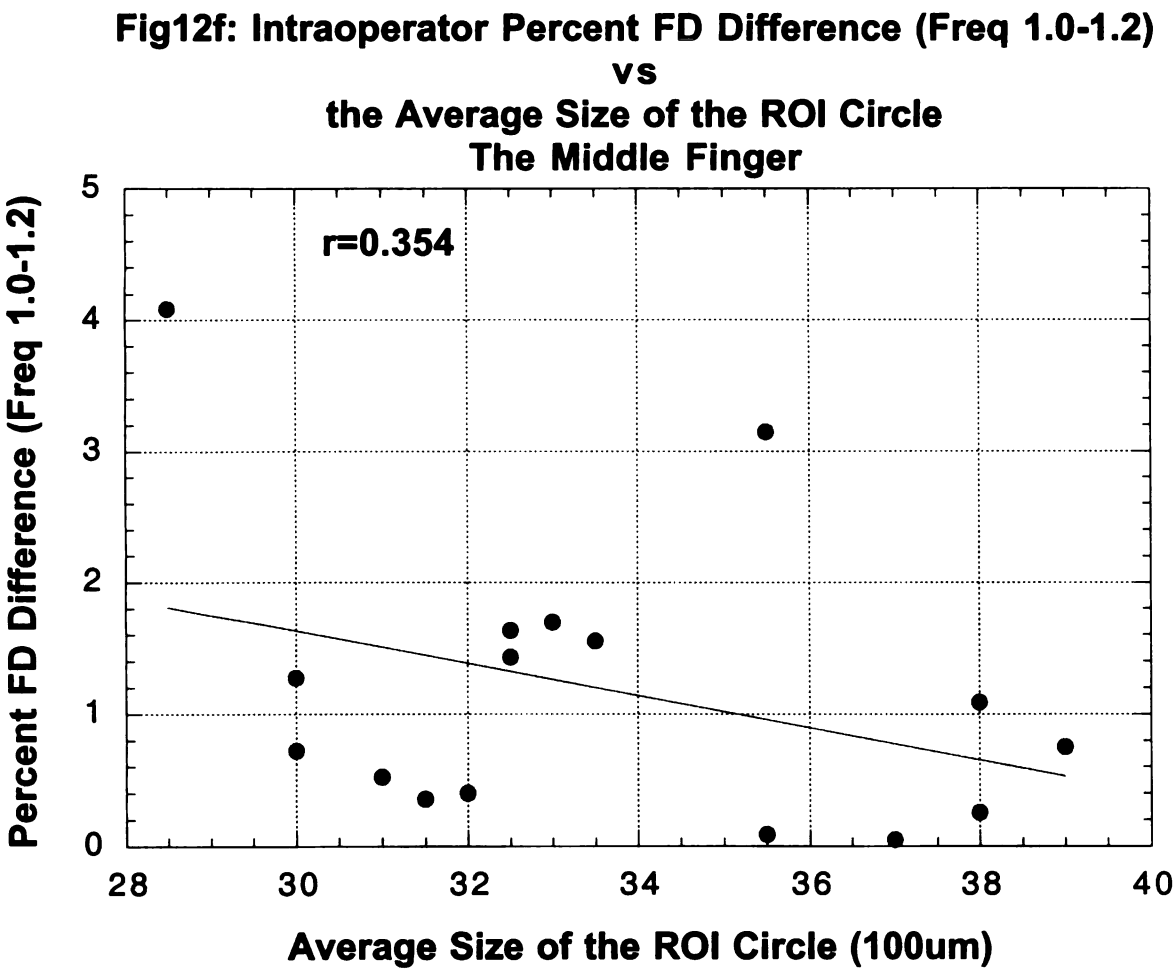
Fig12f: Intraoperator Percent FD Difference (Freq 1.0-1.2)
vs
the Average Size of the ROI Circle
The Middle Finger
r=0.354
Percent FD Difference (Freq 1.0-1.2)
Average Size of the ROI Circle (100um)
0
1
2
3
4
5
28
30
32
34
36
38
40

Figure 12g: Intraoperator FD Difference (Freq 1.2-1.4)
vs
the Average Size of the ROI Circle
The Middle Finger

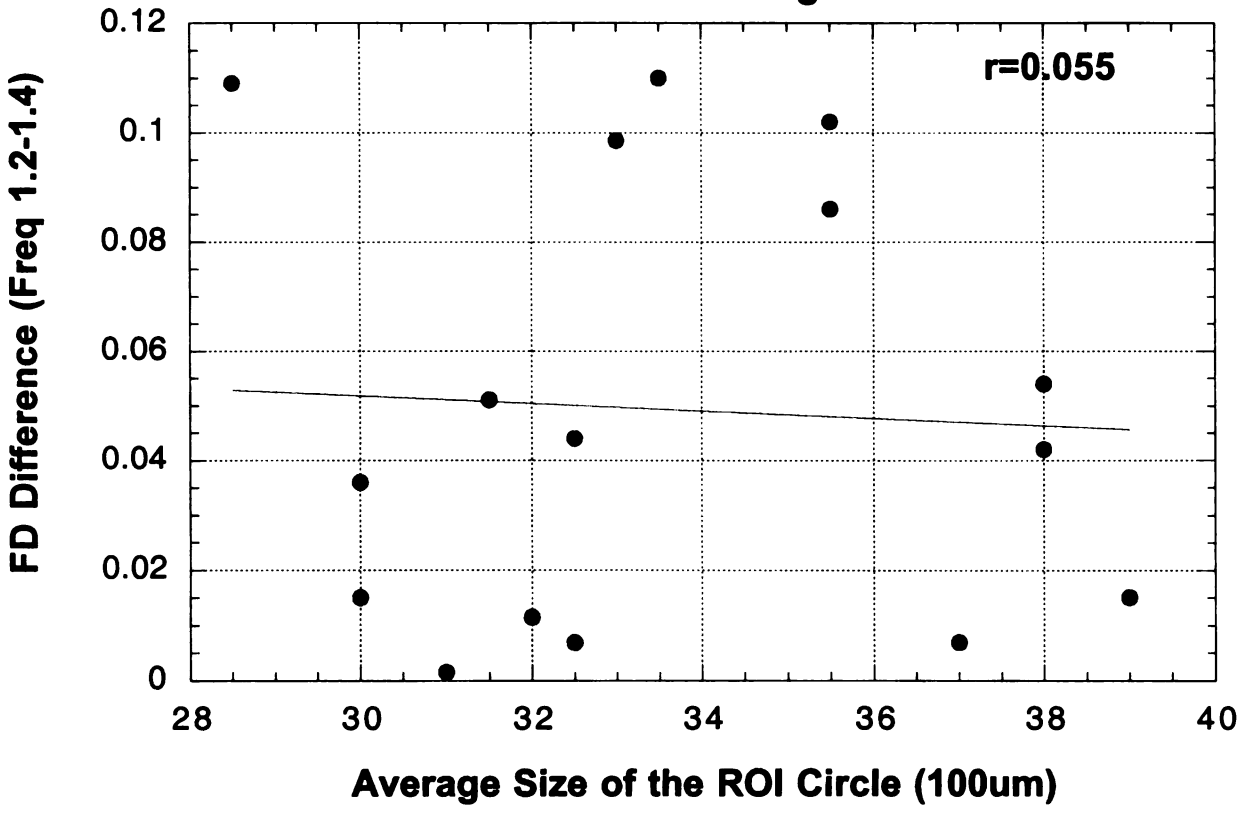

Figure 12h: Intraoperator Percent FD Difference (Freq 1.2-1.4)
vs
the Average Size of the ROI Circles
The Middle Finger

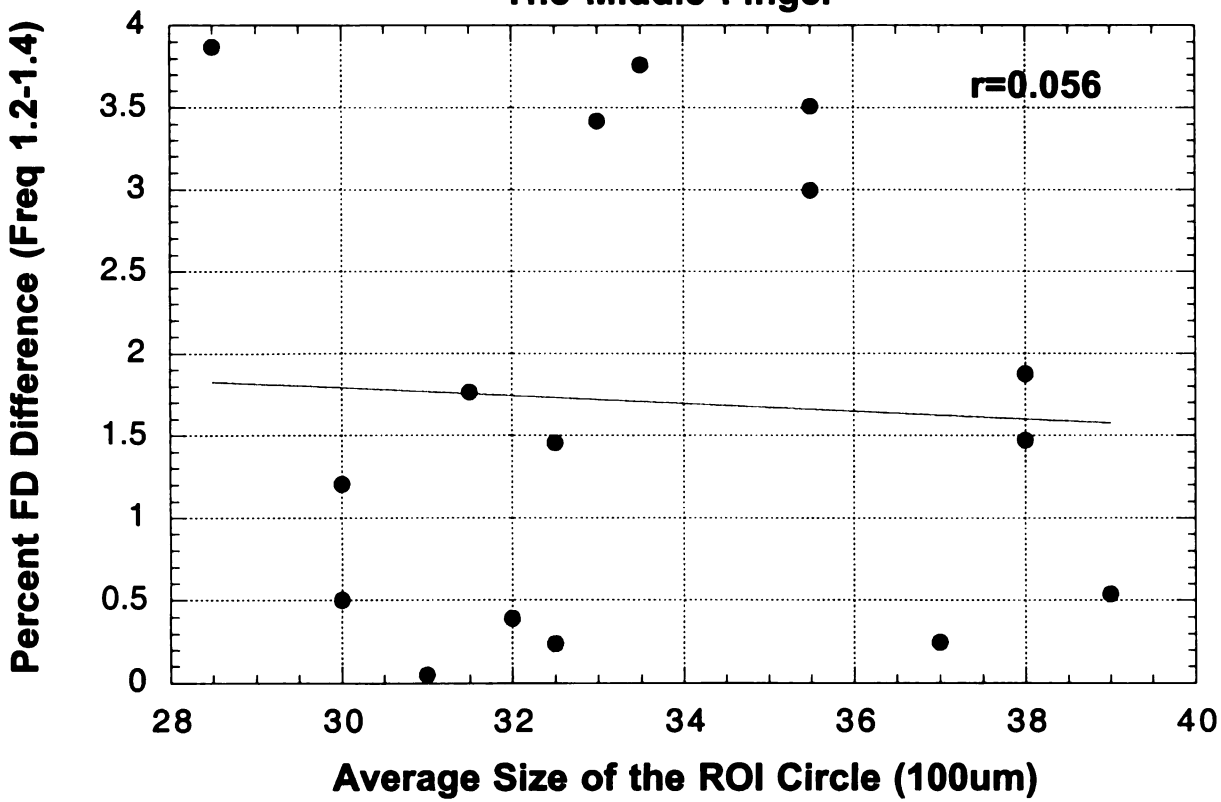

Figure 12i: Intraoperator FD Difference (Freq 1.3-1.4)
vs
the Average Size of the ROI Circles
The Middle Finger

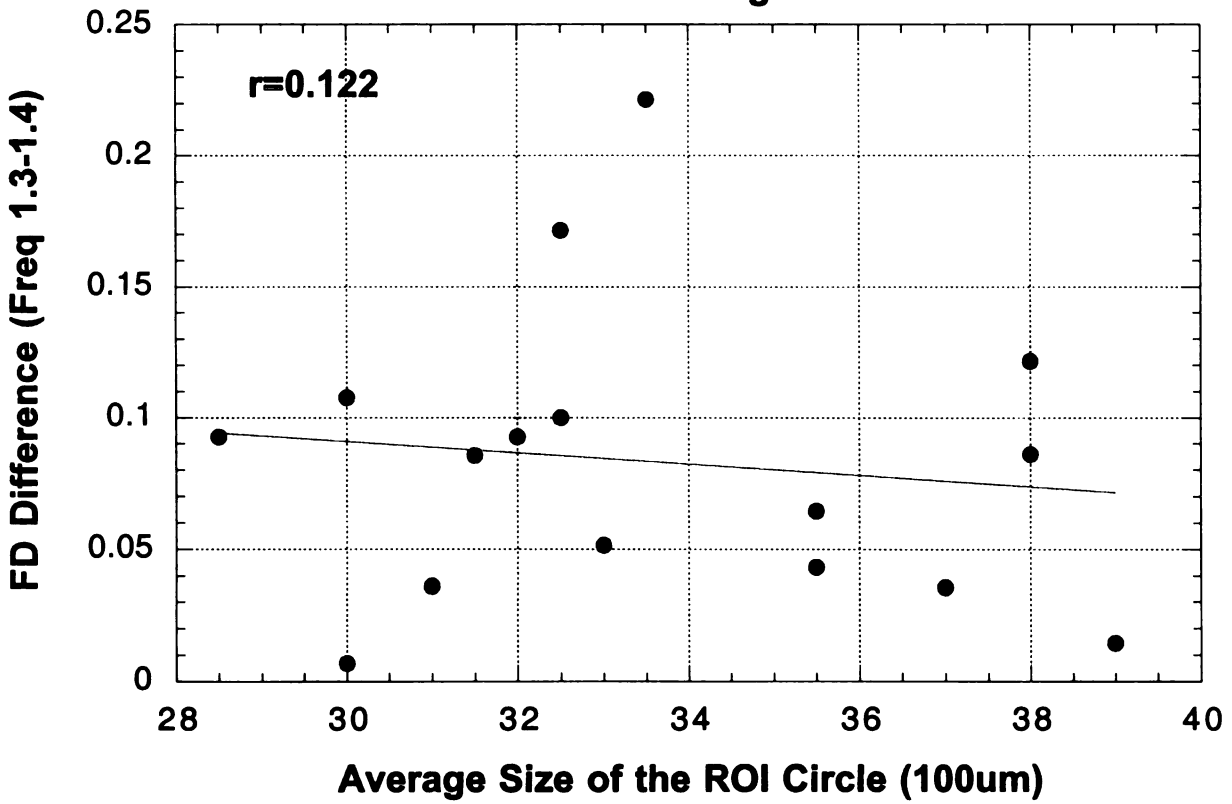

Figure 12j: Intraoperator Percent FD Difference (Freq 1.3-1.4) vs the Average Size of the ROI Circle The Middle Finger

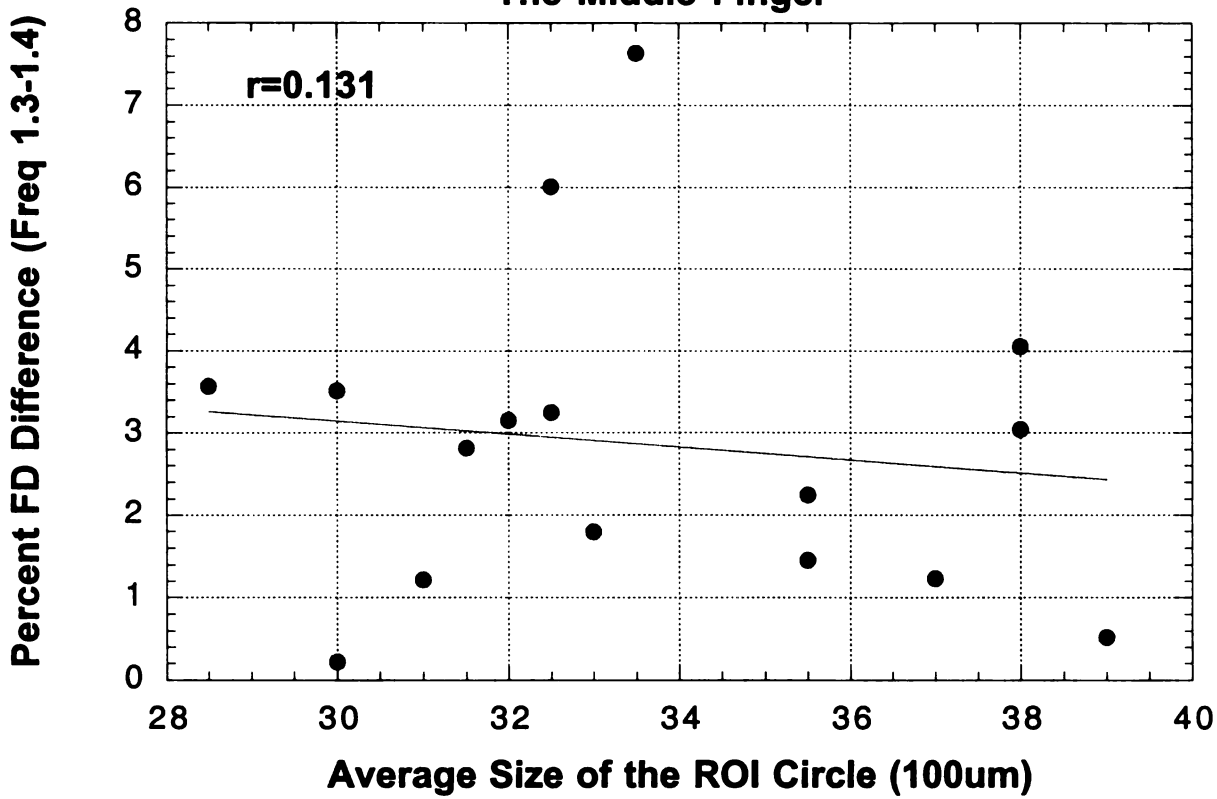

Figure 13a: Intraoperator Location Difference vs the Average ROI Size The Distal of Radius

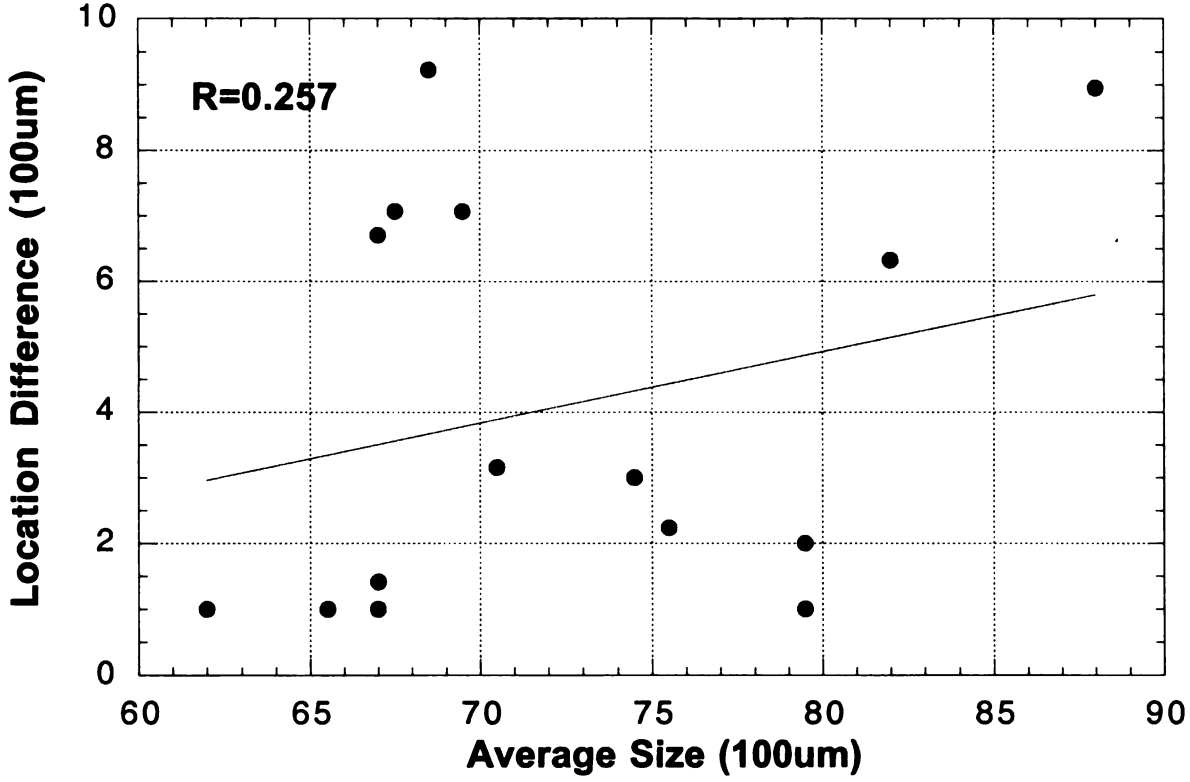

Figure 13: Intraoperator reliability study for the distal of radius

Figure 13b: Intraoperator Percent Location Difference vs the Average ROI Size The Distal of Radius

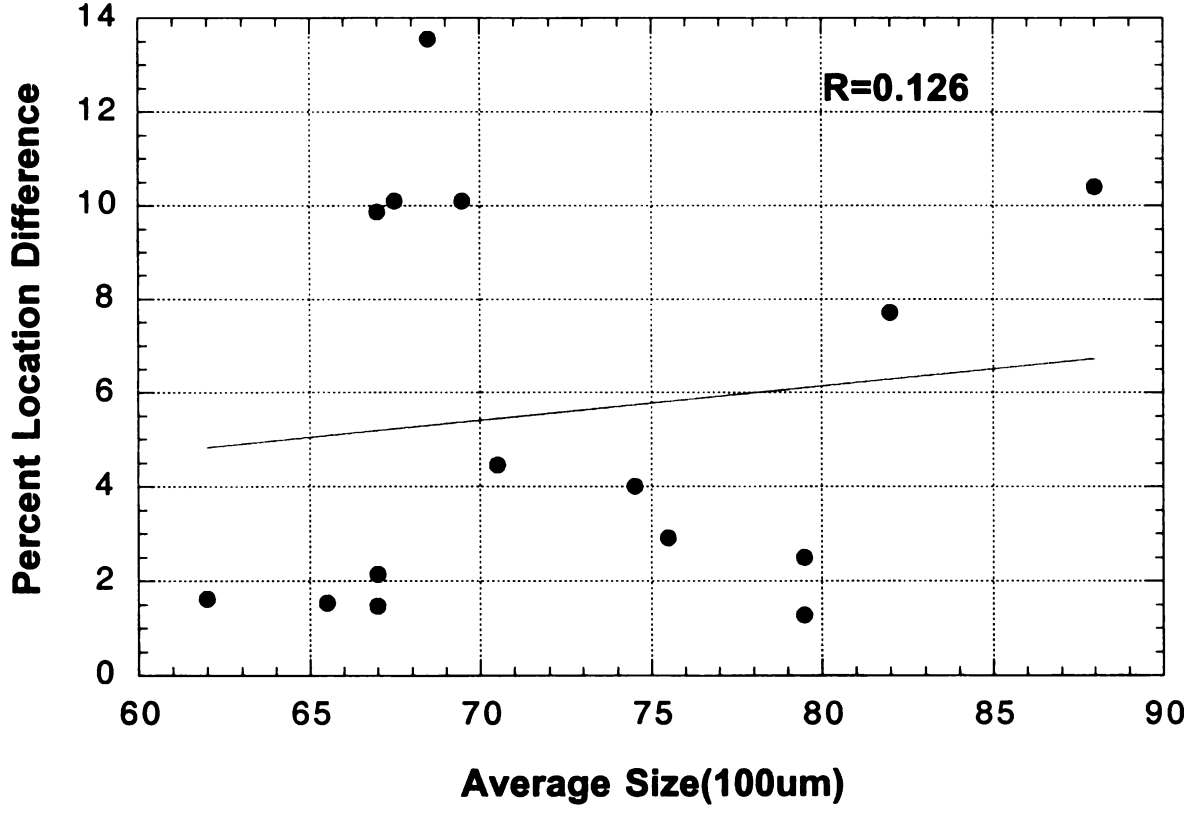

Figure 13c: Intraoperator Size Difference vs the Average ROI Size
The Distal of Radius

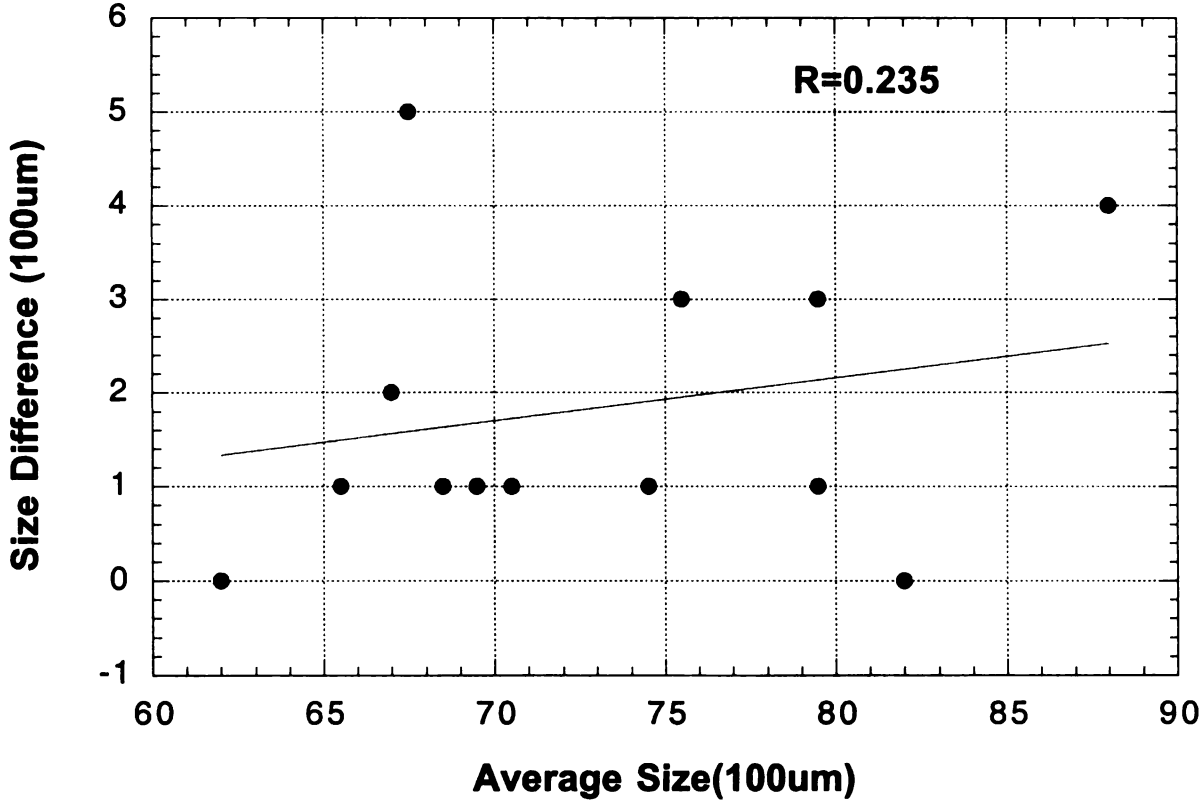

Figure 13d: Intraoperator Percent Size Difference vs the Average ROI Size The Distal of Radius

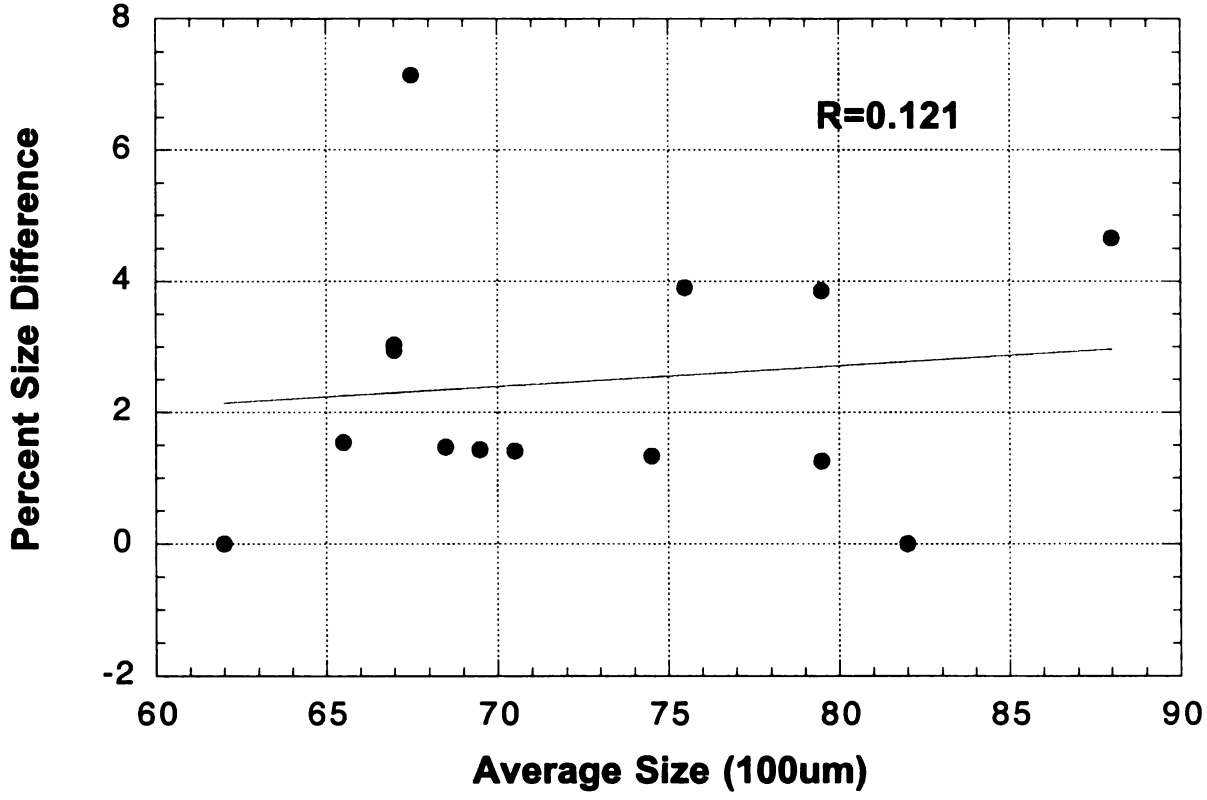

Figure 13e: Intraoperator FD Difference (Freq 0.6-1.0)
vs
the Average ROI Size
The Distal of Radius

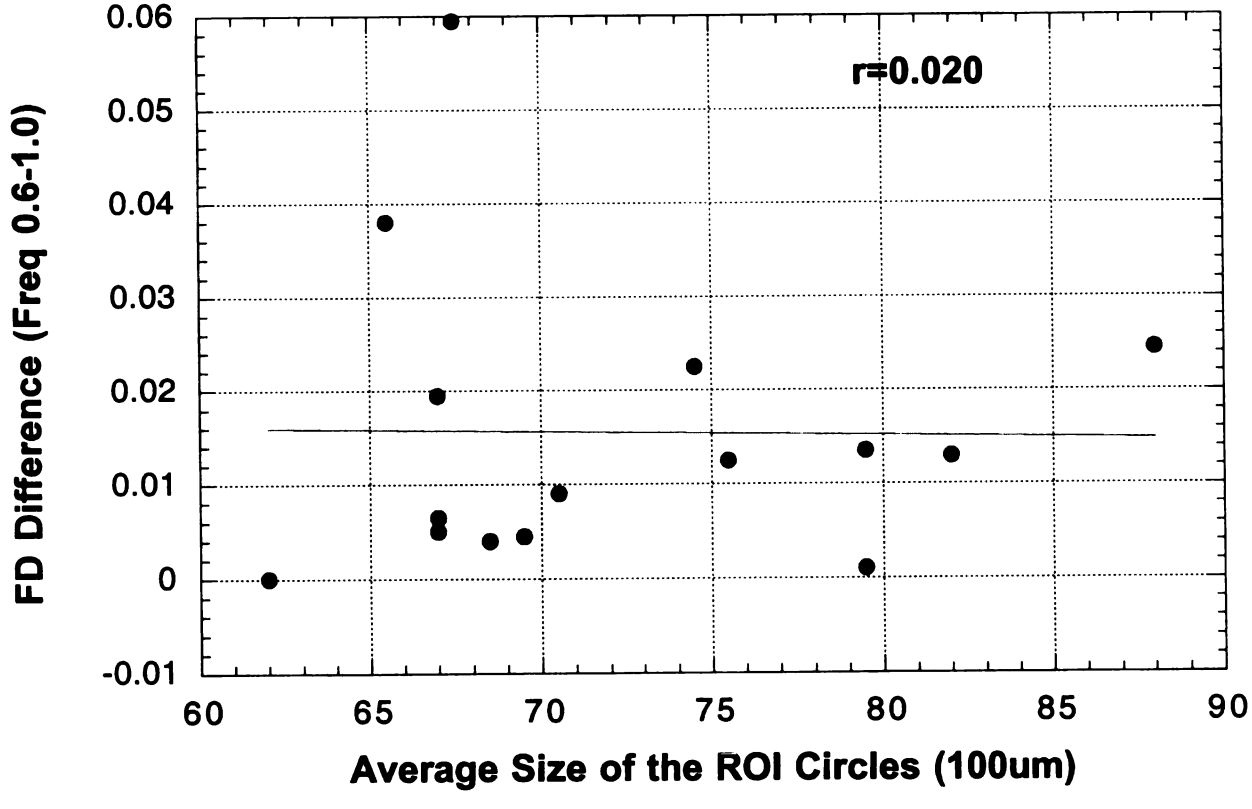

Figure 13f: Intraoperator Percent FD Difference (Freq 0.6-1.0)
vs
the Average ROI Size
The Distal of Radius

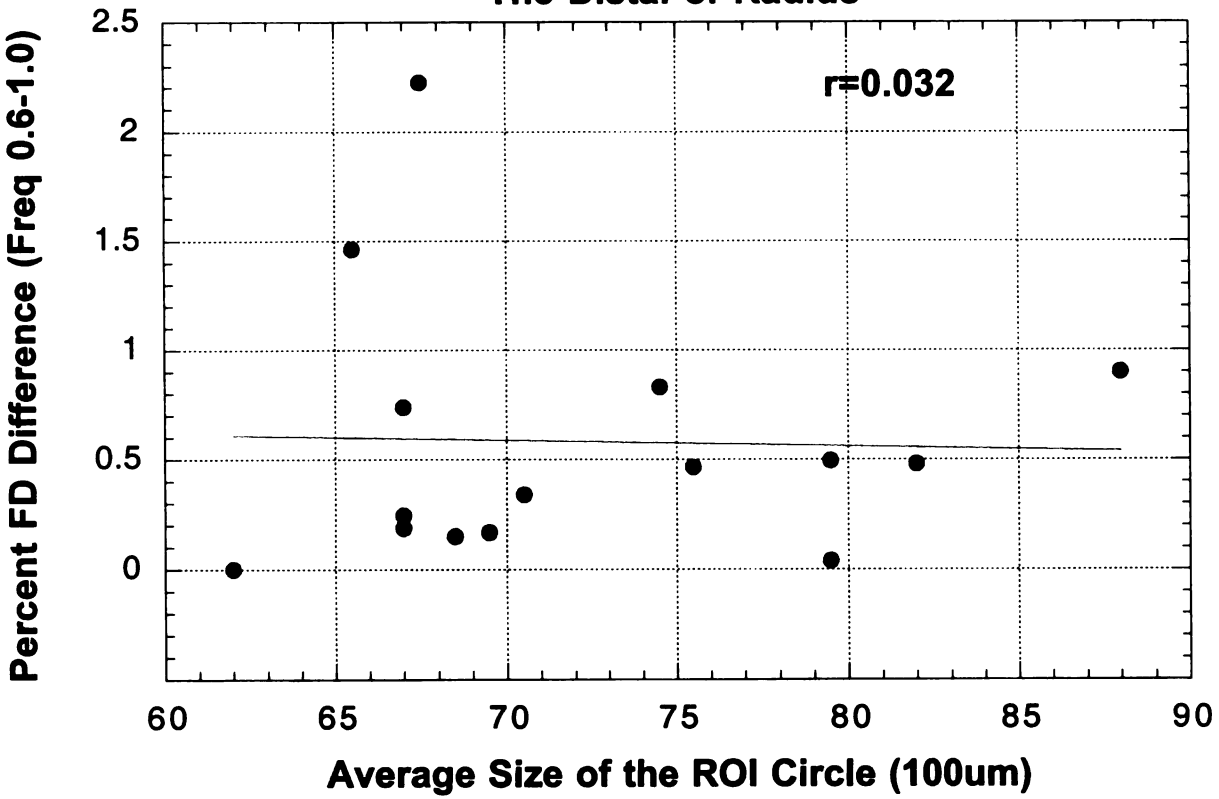

Figure 13g: Intraoperator FD Difference (Freq 1.0-1.2)
vs
the Average ROI Size
The Distal of Radius

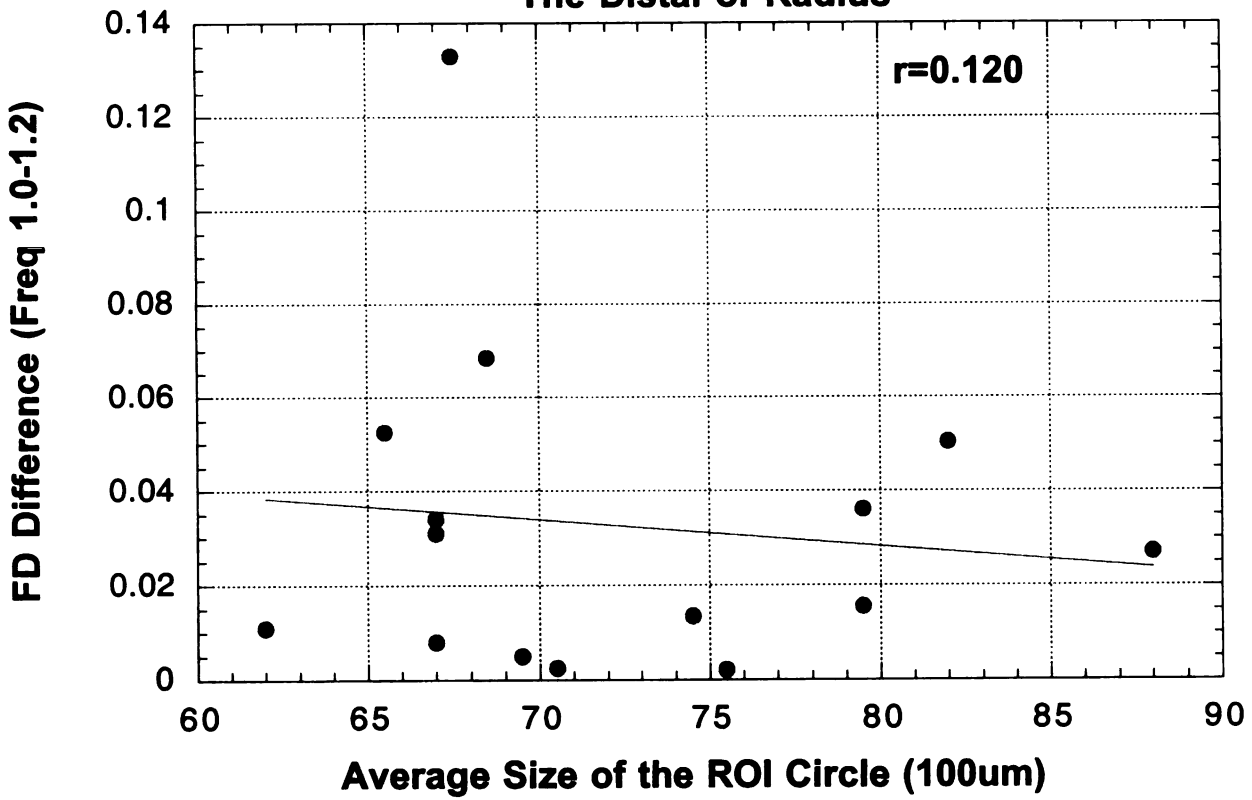

Figure 13h: Intraoperator Percent FD Difference (Freq 1.0-1.2) vs the Average ROI Size The Distal of Radius

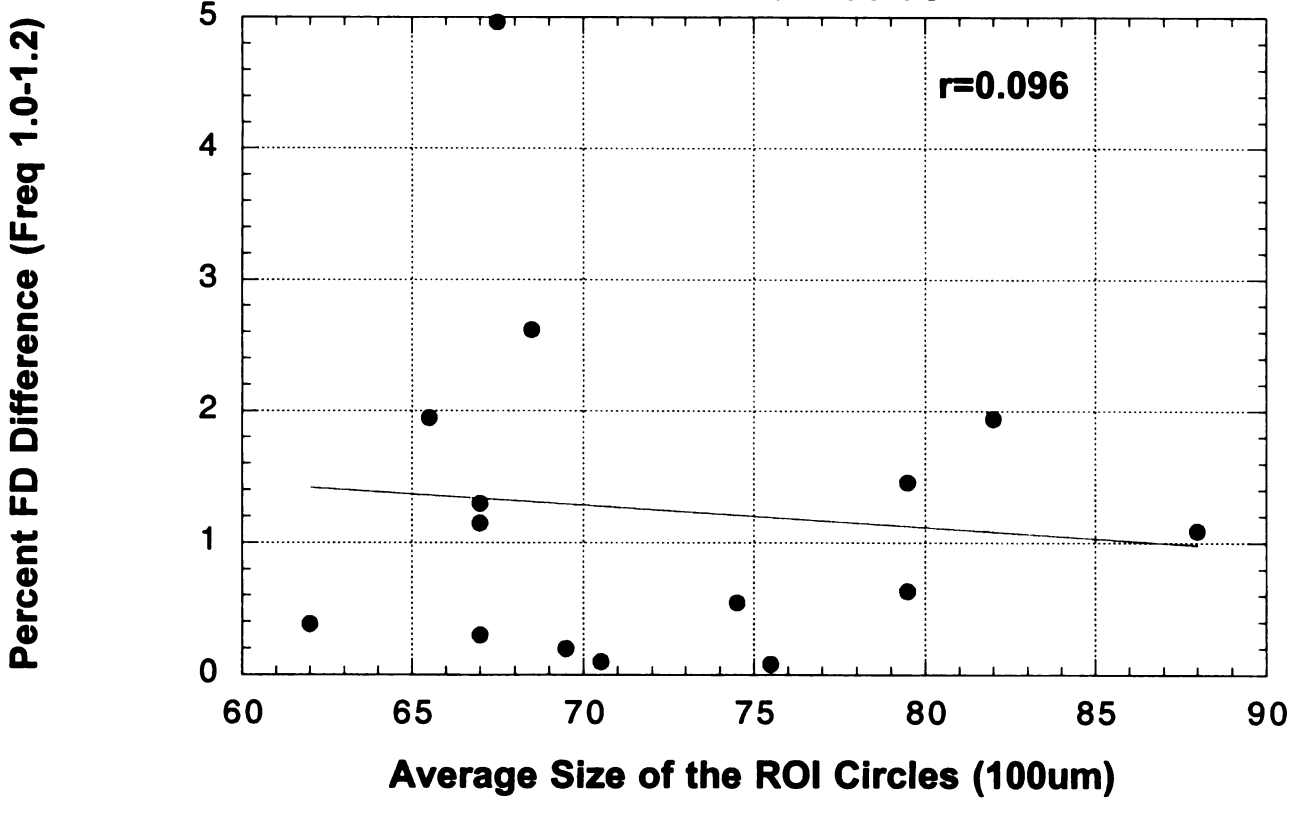

Figure 13i: Intraoperator FD Difference (Freq 1.0-1.4)
vs
the Average ROI Size
The Distal of Radius

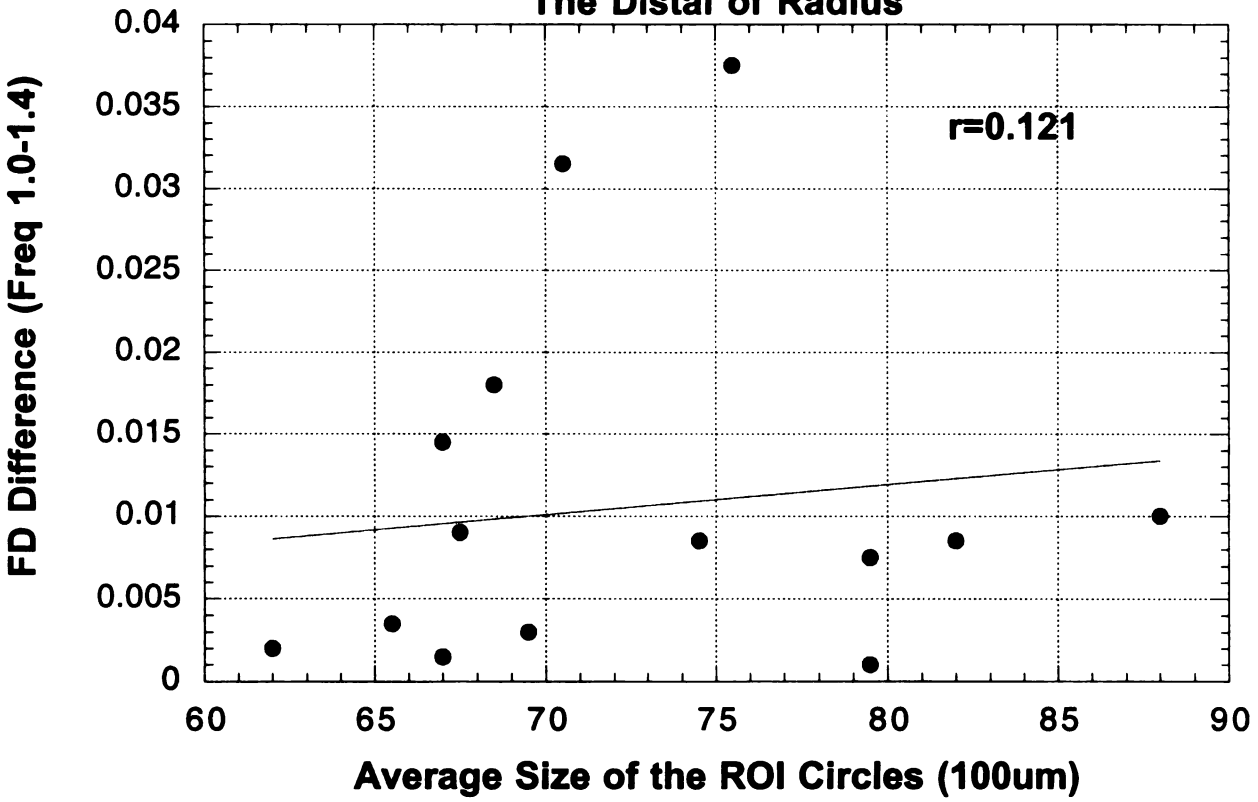

Figure 13j: Intraoperator Percent FD Difference (Freq 1.0-1.4) vs the Average ROI Size The Distal of Radius

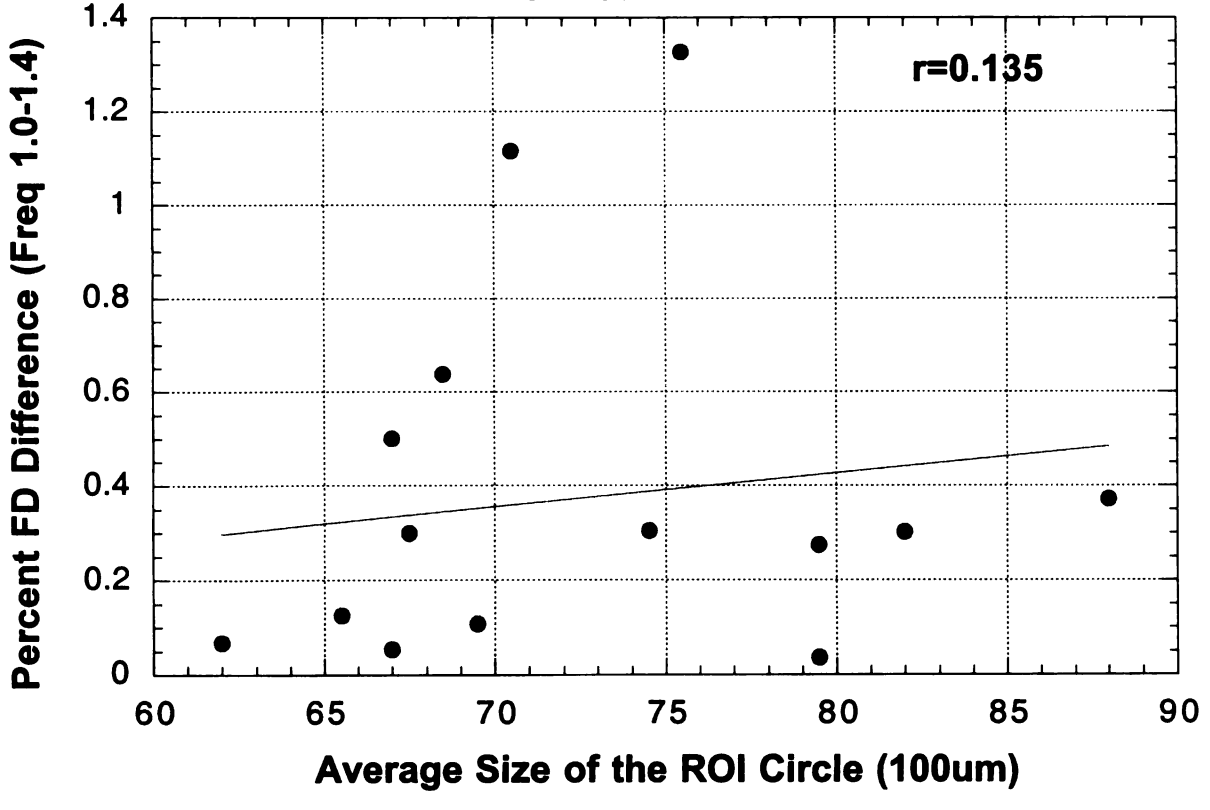

Figure 13k: Intraoperator FD Difference (Freq 1.2-1.4)
vs
the Average ROI Size
The Distal of Radius

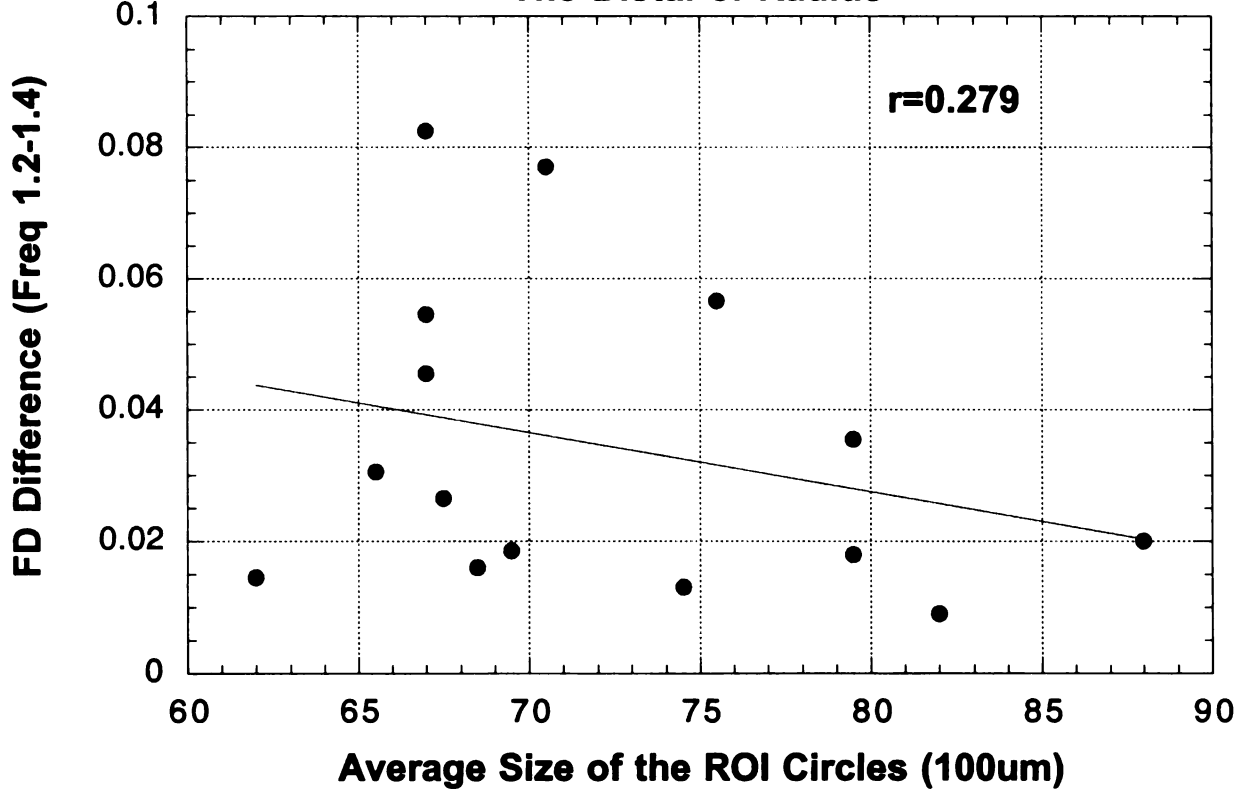

Figure 13l: Intraoperator Percent FD Difference (Freq 1.2-1.4) vs the Average ROI Size The Distal of Radius

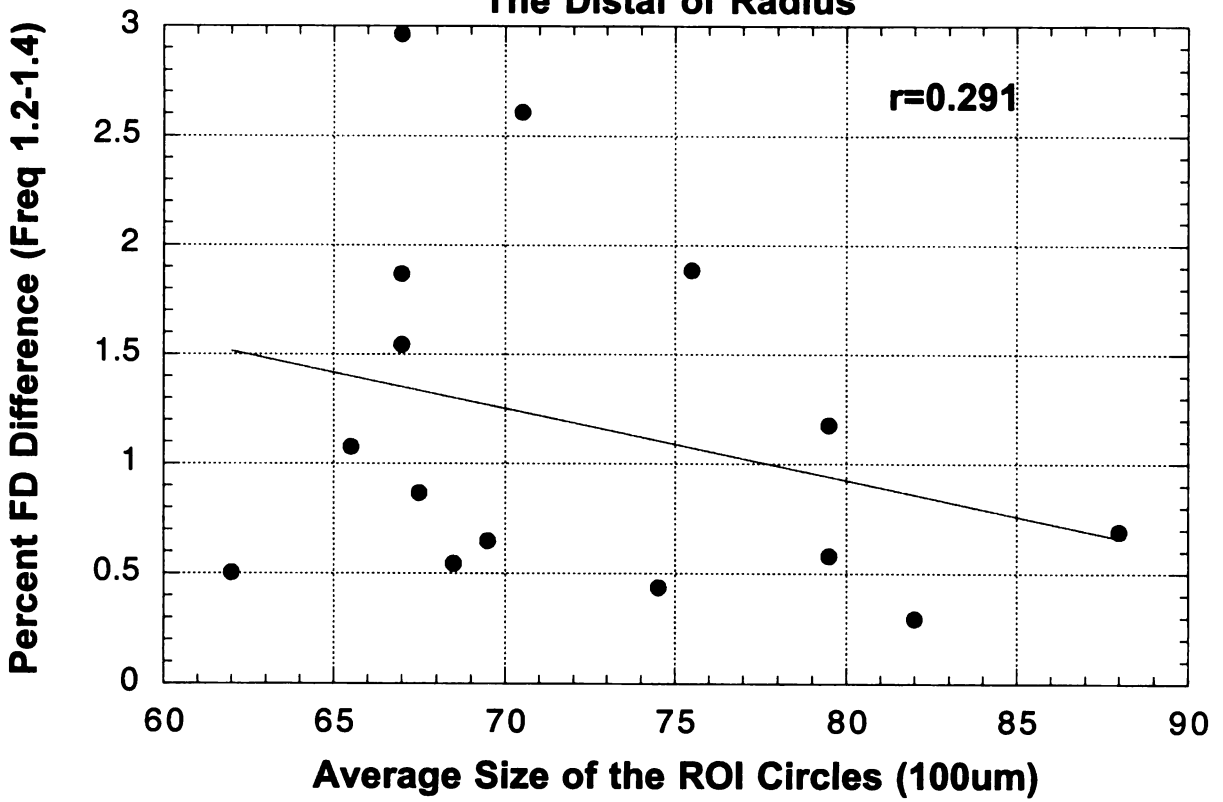

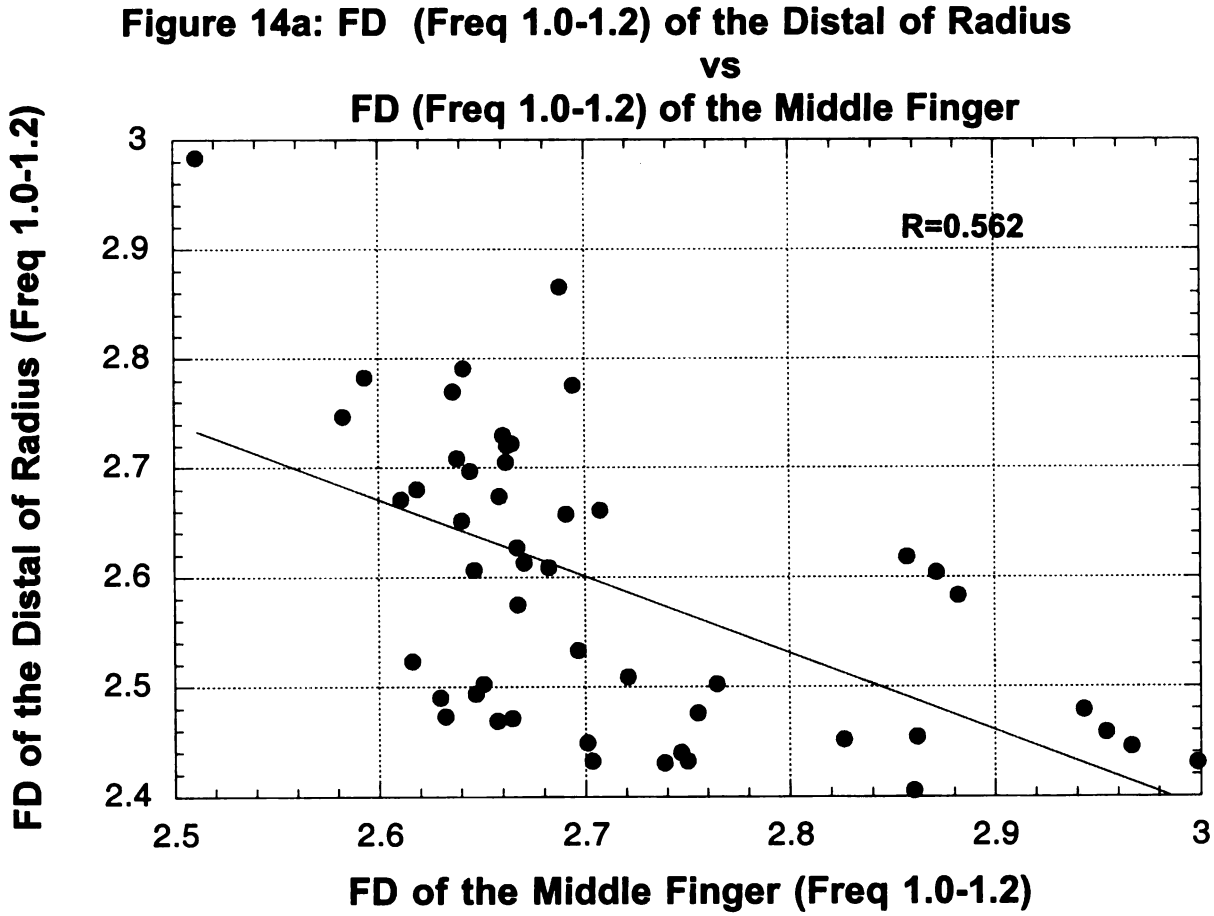

Figure 13: Correlations between the FD's of the two sites for the same frequency ranges

Figure 14b: FD (Freq 1.2-1.4) of the Distal of Radius vs FD (Freq 1.2-1.4) of the Middle Finger

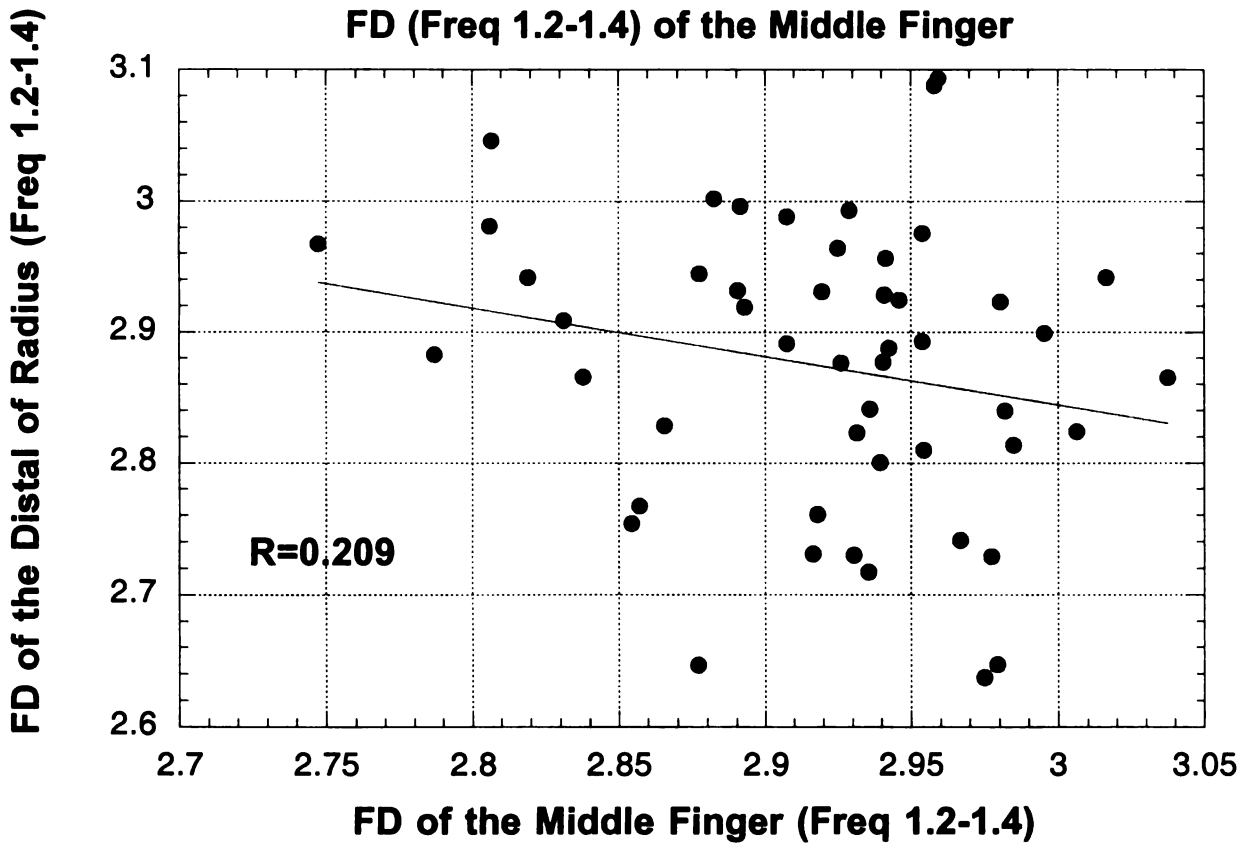

REFERENCES

1. Majumdar S, Weinstein RS, Prasad R. Application of fractal geometry techniques to the study of trabecular bone. Med Phys 1993, 20: 1611-1619.
2. Smith, RJ. Misuse of hand-wrist radiographs. Am J Orthod 1980, 77:75-78.
3. Bambha JK, Van Natta P. Longitudinal study of facial growth in relation to skeletal maturation during adolescence. Am J Ortho 1963, 49:481-493.
4. Hunter CJ. The correlation of facial growth with body height and skeletal maturation at adolescence. Angle Orthod 1966, 36:44-53.
5. Thompson GW, Popovich F. Relationship of craniofacial changes and skeletal age increments in females. Hum Biol 1973, 45:595-603.
6. Pileski RCA, Woodside DG, James G. Relationship of the ulnar sesamoid bone and maximum mandibular growth velocity. Angle Orthod 1973, 43:162-170.
7. Bjork A, Helm S. Prediction of the age of maximum pubetal growth in body height. Angle Orthod 1967, 37:134-143.
8. Shrout MK, Roberson B, Potter BJ, Mailhot JM, Hildebolt CF. A comparison of 2 patient populations using fractal analysis. Periodont 1998, 69:9-13.
9. Houston WJB, Miller JC, Tanner JM. Prediction of the timing of the adolescent growth spurt from ossification events in hand wrist film. Brit J Ortho 1979, 6:145-152.
10. Houston WJB. Relationships between skeletal maturity estimated from hand-wrist radiographs and the timing of the adolescent growth spurt. Eur J Ortho 1980, 2: 81-93.
11. Snyder W. Report of the Task Group on Reference Man. Pergamon Press, New York. 1975.

12. Forst HM. In *Bone Biodynamics,* H M Forst, Ed. Little Brown, Boston, 1964, pp. 315-334.

13. Fishman LS. Radiographic evaluation of skeletal maturation: A clinical oriented method based on hand-wrist films. Angle Orthod 1982, 52:88-112.

14. Marshall WA, Tanner JM. Variations in pattern of pubertal changes in girls. Arch Dis Child 1969, 44:291-303.

15. Grave KC, Brown T. Skeletal ossification and the adolescent growth spurt. Am J Ortho 1976, 69: 611-619.

16. Todd, TW. Atlas of Skeletal Maturation (Hand), CV Mosby Co., St. Louis, 1937.

17. Greulich WW, Pyle SI. Radiographic Atlas of Skeletal Development of the Hand and Wrist. Stanford University Press, Stanford, 1950.

18. Mandelbrot BB. The fractal geometry of nature. Freeman, New York, 1983.

19. Fazzalari NL, Parkinson IH. Fractal properties of subchondral cancellous bone in severe osteoarthritis of the hip. J Bone Min Res 1997, 12:632-640.

20. Smith TG, Marks WB, Lange GD, Shefiff Jr WH, Neale EA. A fractal analysis of cell images. J Neurosci Meth 1989, 27:173-180.

21. Bassingthwaighte JB, van Beek JHGM, King RB. Fractal branchings: The basis of myocardial flow heterogeneities? Ann NY Acad Sci 1990, 591:392-401.

22. Glenny RW, Robertson HT, Yamashiro S, Bassingthwaighte JB. Applications of fractal analysis to physiology. J Appl Physiol 1991, 70:2351-2367.

23. Keough KMW, Hyam P, Pink DA, Quinn B. Cell surfaces and fractal dimensions. J Microsc 1991, 163: 95-99.

24. Cross SS, Howat AJ, Stephenson TJ, Cotton DWK, Underwood JCE. Fractal geometric analysis of material from molar and non-molar pregnancies. J Pathol 1994, 173:11-118.

25. Cross SS, Bury JP, Silcocks PB, Stephenson TJ, Cotton DWK. Fractal geometric analysis of colorectal polyps. J Pathol 1994, 172:317-323.

26. Cox BL and Wang JSY. Fractal surfaces: Measurement and applications in the earth sciences. Fractal 1993, 1:87-115.

27. Ruttimann UE, Webber RL, Hazelrig JB. Fractal dimension from radiographs of peridental alveolar bone: A possible diagnostic indicator of osteoporosis. Oral Surg, Oral Med, Oral Path 1992, 74:98-110.

28. Khosrovi PM. Characterization of Trabecular Bone Structure from Radiographs Using Fractal Analysis. University of California, San Francisco, Masters Thesis, 1995.

29. Siffert R. Trabecular patterns in bone. Am J. Roentgenol, Radium Ther, Nucl Med 1967, 99:746-755.

30. Jansen M. On Bone Formation. Longmans, Green & Company, London, 1920.

31. Koch, JC. Laws of bone architecture. Am J Anat 1917, 21:179-298.

32. Robin, WJ. Internal architecture of femur and its clinical significance. J Bone & Joint Surg 1955, 37-A:57-72.

33. Schinz, HR, Baensch WE, Friedl E, Uehlinger E. Roentgen-Diagnostics. Vol. 1. Skeleton, Part I. Translated and edited by JT Case. Grune & Stratton, Inc., New York, 1951.

34. Townsley W. Architectural structure of upper end of femur in various pathological conditions. J Path. Bact 1944, 56:199-207.

35. Weinman JP, Sicher H. Bone and Bones: Fundamentals of Bone Biology. 2nd Ed. C.V. Mosby Company, St. Louis, 1955, p. 508.

36. Allison N, Brooks B. Bone atrophy: Experimental and clinical study of changes in bone which result from non-use. Surg Gynec Obst 1921, 33:250-260.

37. Tanner JM, Whitehouse RH, Cameron N, Marshall WA, Healy MJR, Goldstein H. Assessment of Skeletal Maturity and Prediction of Adult Height (TW2 Method). 2nd Ed. Academic Press, Harcourt Brace Jovanovich, New York, 1983.

38. Majumdar S, Link TM, Millard J, Lin JC, Augat P, Newitt D, Lane N, Genant HK. *In vivo* assessment of trabecular bone structure using the fractal dimension measured from distal radius radiographs. (Submitted to *Medical Physics*)

39. Deming J. Application of the Gompertz curve to the observed pattern of growth in length of 48 individual boys and girls during the adolescent cycle of growth. Hum Biol1957. 29:83.

40. Hagg U, Taranger J. Menarche and voice changes as indicators of the pubertal growth spurt. Acta Odontol Scand 1980, 38:179-186.

41. Stevenson F. Osteoporosis of immobilisation in recumbency. J Bone & Joint Surg 1952. 34-B:256-265.

42. Hamill PVV, Drizd TA, Johnson CL, Reed RB, Roche AF, Moore WM. Physical growth: National Center for Health Statistics Percentiles. Am J Clin Nutr 1979, 32:609-629.

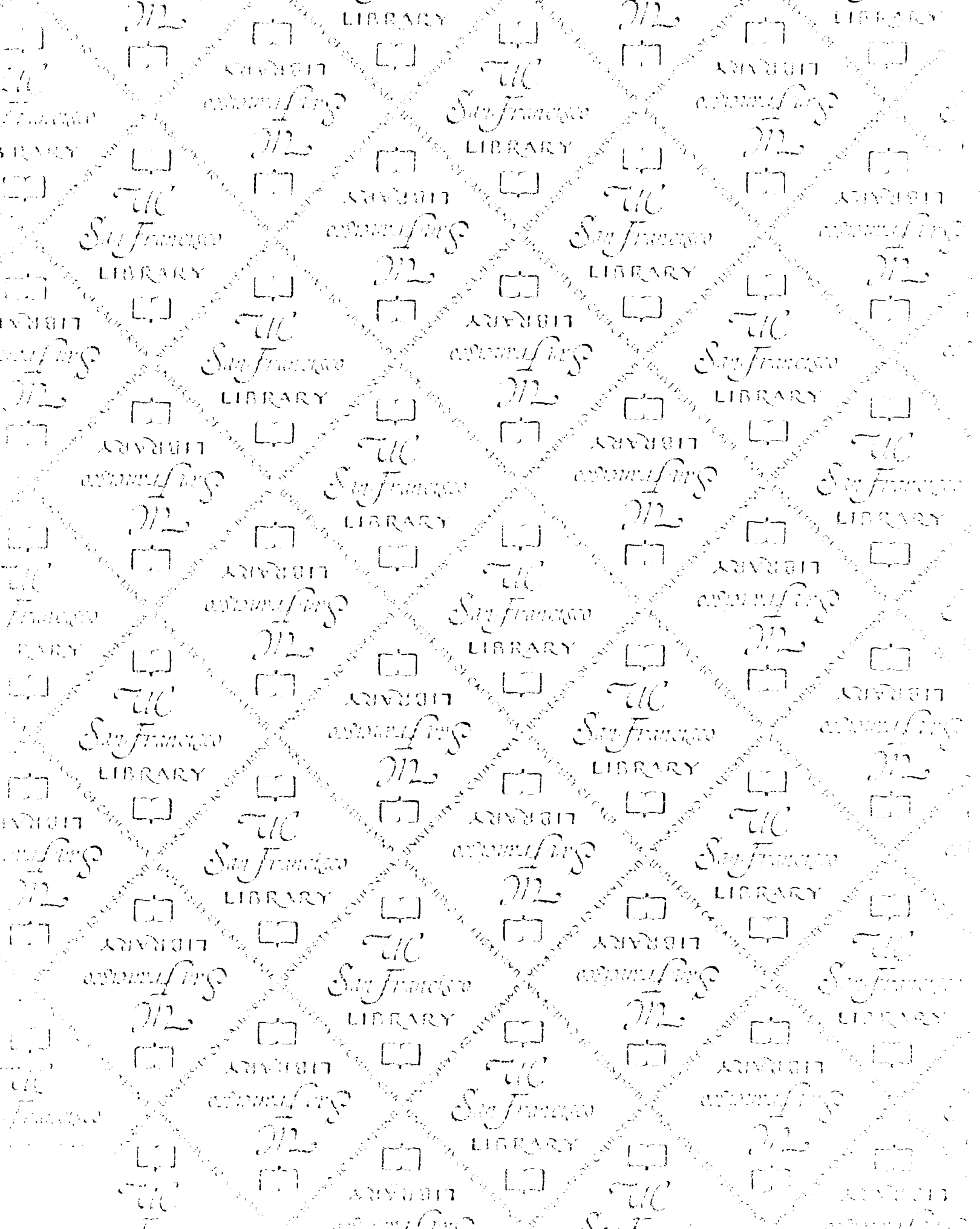
UC
San Francisco
LIBRARY